AD_____

Award Number: W81XWH-11-1-0587

TITLE: The Role of AR- and VDR-modulated miRNAs in sensitization of prostate cancer cells to therapy

PRINCIPAL INVESTIGATOR: Wei-Lin Winnie Wang

CONTRACTING ORGANIZATION: State University of New York at Albany,
Rensselaer, New York, 12144

REPORT DATE: October 2012

TYPE OF REPORT: Annual Summary

PREPARED FOR: U.S. Army Medical Research and Materiel Command
Fort Detrick, Maryland 21702-5012

REPORT DOCUMENTATION PAGE

Form Approved
OMB No. 0704-0188

1. REPORT DATE	2. REPORT TYPE	3. DATES COVERED
October 2012	Annual Summary	30 September 2011 – 29 September 2012

4. TITLE AND SUBTITLE
The Role of AR- and VDR-modulated miRNAs in sensitization of prostate cancer cells to therapy

5a. CONTRACT NUMBER

5b. GRANT NUMBER
W81XWH-11-1-0587

5c. PROGRAM ELEMENT NUMBER

6. AUTHOR(S)
Wei-Lin Winnie Wang B. Sc.

E-Mail: wwang3@albany.edu

5d. PROJECT NUMBER

5e. TASK NUMBER

5f. WORK UNIT NUMBER

7. PERFORMING ORGANIZATION NAME(S) AND ADDRESS(ES)
State University of New York at Albany
Rensselaer, New York, 12144

8. PERFORMING ORGANIZATION REPORT NUMBER

9. SPONSORING / MONITORING AGENCY NAME(S) AND ADDRESS(ES)
U.S. Army Medical Research and Materiel Command
Fort Detrick, Maryland 21702-5012

10. SPONSOR/MONITOR'S ACRONYM(S)

11. SPONSOR/MONITOR'S REPORT NUMBER(S)

12. DISTRIBUTION / AVAILABILITY STATEMENT
Approved for Public Release; Distribution Unlimited

13. SUPPLEMENTARY NOTES

14. ABSTRACT :
Epidemiological evidence has demonstrated an inverse association between serum vitamin D levels and sunlight exposure to prostate cancer incidence. In addition, serum androgen levels and biologically available testosterone decrease significantly in elder men while the incidence rate of prostate cancer increases. These findings lead to the hypothesis that androgen- and vitamin D-mediated signaling events may act together to inhibit prostate tumor initiation and/or development. Using concurrent microarray analyses, we demonstrated that testosterone and 1,25(OH)2D3 co-operate to regulate mRNA and miRNA expression, including some well-defined oncogenes and tumor suppressor genes. Pheno typically, this results in G0/G1 cell cycle arrest and increased neutral lipid accumulation in LNCaP cells, as a consequence of repression of various cell cycle regulators and the up-regulation of PPARα respectively. This suggests that the cross talk between T and 1,25(OH)2D3 induces cell cycle arrest and promotes cell differentiation in LNCaP cells. It is important ton ote that co-treatment of LNCaP cells with testosterone, 1,25(OH)2D3 and other standard therapeutics, including bicalutamide, docetaxel and TRAIL did not affect the potencies of these treatments, though there were no synergistic effects either. This suggests that androgen andvitamin D supplementation slow disease progression without affecting the efficacy of standard therapies for prostate cancer. Further analysis is still required to elucidate the underlying mechanisms of T and 1,25(OH)2D3 to modulate key mRNA and miRNA and their significance in prostate tumorigenesis and therapeutic interventions. expressions

15. SUBJECT TERMS
Prostate cancer, androgen, vitamin D

16. SECURITY CLASSIFICATION OF:			17. LIMITATION OF ABSTRACT	18. NUMBER OF PAGES	19a. NAME OF RESPONSIBLE PERSON
a. REPORT	b. ABSTRACT	c. THIS PAGE			USAMRMC
U	U	U	UU	96	19b. TELEPHONE NUMBER *(include area code)*

Table of Contents

INTRODUCTION

The development and progression of prostate adenocarcinoma is widely thought to be androgen dependent, since androgenic action is clearly required for normal prostate function. However, the age dependent incidence and associated mortality of the disease increase after serum testosterone levels start to decline significantly between 55 to 64 years of age at which point free testosterone has dropped more than 50% [1]. Similarly, prostate cancer incidence also exhibits an inverse correlation with vitamin D status in that more than 75% of men diagnosed with prostate cancer are vitamin D_3 deficient. Thus, most patients diagnosed with prostate cancer have declining serum testosterone and vitamin D levels, leading to the hypothesis that the two hormones interact to block prostate tumor initiation and/or progression. Though the cancer preventive property of vitamin D has been established in various solid tumors, its chemopreventive property in prostate cancer is still a matter of considerable debate, especially since clinical use of $1,25(OH)_2D_3$ or its less calcemic analogs have been disappointing [2-5]. While many studies have examined the individual effects of androgens and $1,25(OH)_2D_3$ on prostate cancer cells, very few studies have focused on the possible cross talk between the two signaling pathway and the downstream biological consequences. Our recent investigation on the combined effects of testosterone and $1,25(OH)_2D_3$ on AR+ prostate cancer cells using concurrent microarray analyses have revealed extensive interactions between the two pathways that affect gene and miRNA expression[6]. Many of the genes regulated by the two hormones are involved in cell cycle progression, calcium signaling, and lipid production and accumulation. In addition, some of the genes and miRNAs modulated by testosterone and $1,25(OH)_2D_3$ have well-defined role in tumorigenesis in other cancers. These include the synergistic down-regulation of MYC and miR-17/92 cluster, as well as up-regulation of miR-22. These data suggest that supplementation of vitamin D alone in androgen deplete disease patients may not be sufficient to achieve its full activity and probably requires adequate levels of androgens to do so. With the study proposed, we provide preclinical data regarding the combinatorial effect of androgen and vitamin D on prostate cancer therapy, particular in an adjuvant setting, as well as the underlying molecular changes that may contribute to the phenotype observed. **Aim 1:** *To investigate the combinatorial effects of VDR and AR signaling on cellular homeostasis, and sensitivity of prostate cancer cells to therapeutic agents*. **Aim 2:** *To identify of specific miRNAs/mRNAs responsible for the changes in cellular homeostasis and sensitivity of prostate cancer cells to therapy*.

BODY

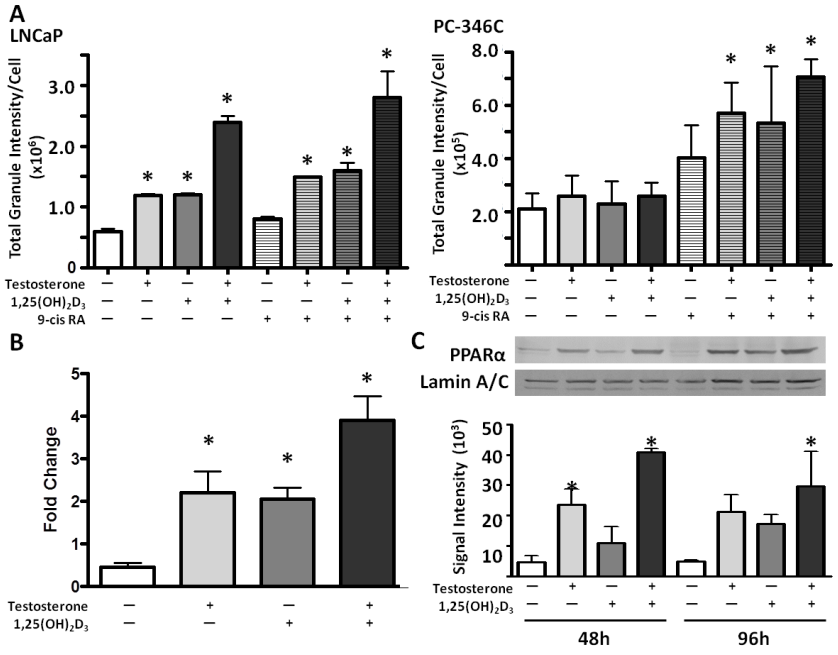

Figure 1: A) The effect of T, $1,25(OH)_2D_3$ and 9-cis RA on neutral lipid droplet accumulation in LNCaP and PC-346C cells. Neutral lipid accumulation was assessed by BODIPY neutral lipid staining and quantified using In Cell Analyzer after 120h of treatment. **B)** The effect of T and $1,25(OH)_2D_3$ on PPARA mRNA levels, measured by SYBR Green qPCR analysis. Data are tabulated using $2^{-\Delta\Delta C}{}_T$ method with GAPDH as the endogenous control. Results are represented as fold changes relative to 0h control (transformed so that a fold change of 0 is in 0h control cells). **C)** The effect of T and $1,25(OH)_2D_3$ on PPARα protein levels in LNCaP cells at 48h and 96h after treatment. Relative signal intensity is assessed by UN-SCAN-IT gel 6.1 with background correction, and normalized to nuclear Lamin A/C expression. All values are mean ± SD from three independent experiments. Statistical analysis was performed using one-way ANOVA with Tukey post-test. * P<0.05 compared to untreated controls.

The effect of T and 1,25(OH)$_2$D$_3$ alone and together on gene expression and associated gene ontologies in AR+ LNCaP cells have been documented (reportable outcome 4). In brief, T and 1,25(OH)$_2$D$_3$ together efficiently arrest LNCaP cells in G_1/G_0 phase. This is associated with synergistic down-regulation of many key cell cycle regulators, including cyclin A2, cyclin B2 and E2F1. We have also shown other important cellular processes, including calcium homeostasis, apoptosis, DNA repair mechanisms and lipid metabolism are modulated by T and 1,25(OH)$_2$D$_3$, which may influence prostate cancer development and progression. Recently, we have validated the effect of T and 1,25(OH)$_2$D$_3$ on lipid metabolism in LNCaP cells and PC-346C cells. We also established that the effects of T and 1,25(OH)$_2$D$_3$ was further enhanced by addition of 9-cis retinoic acid (9-cis RA), particularly in PC-346C cells. A concomitant increase in neutral lipid accumulation, measured by BODIPY staining was noted and further interrogated by qPCR and western blot analyses (Figure 1). Based on the genes we have identified from the microarray analysis and the follow up qPCR validation, the increases in lipogenesis is associated with T and 1,25(OH)$_2$D$_3$-mediated up-regulation of PPARα expression and its down-stream targets such as HMGCS1. We have also shown that changes in PPARα protein levels is greater than T- and 1,25(OH)$_2$D$_3$-induced PPARA mRNA levels, suggesting that post-transcriptional mechanism may play a role in T- and 1,25(OH)$_2$D$_3$-mediated lipogenesis in LNCaP cells. We hypothesized that T- and 1,25(OH)$_2$D$_3$ coordinately regulate PPARα expression via a two-step processes, including AR and VDR governed transcriptional control, as well as de-repression of miRNA-mediated PPARA degradation and/or translational repression (Wang et al., 2012, reportable outcome 5). We are intending to examine the effect of miRNA LNA inhibitors, particularly targeting the miR-17/92 cluster on PPARα expression and the associated lipogenesis in LNCaP cells once as part of Task 2. Additional to the induction of lipogenic genes, T and 1,25(OH)$_2$D$_3$ also inhibit the activity of AMPK by preventing β1 subunit phosphorylation. We have also examined nuclear SREBP-1 levels in LNCaP cells (Figure 2), however, no significant changes were detected, suggesting the role of SREBP-1 in T- and 1,25(OH)$_2$D$_3$-induced lipogenesis may not be as significant as we previously thought.

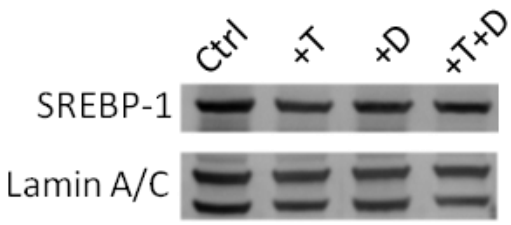

Figure 2: The effect of T and 1,25(OH)$_2$D$_3$ on nuclear SREBP-1 protein levels in LNCaP cells at 48h after treatment. Lamin A/C was used as loading control.

Similar phenotypic assessments were also performed in AR+ PC-346C and AR- PC-3 cells. Unlike LNCaP cells, T and 1,25(OH)$_2$D$_3$ has no significant effect on cell proliferation and cell cycle progression (Table 1), and neutral lipid accumulation was not induced by T and 1,25(OH)$_2$D$_3$ in PC-346C cells unless the medium is supplemented with 9-cis retinoic acid. Evaluation of lipogenic genes demonstrated that 9-cis RA is required in PC-346C cells for T- and 1,25(OH)$_2$D$_3$-induced lipogenic mRNA expression, though the fold-induction is not as significant as seen in LNCaP cells (Figure 3). As we have recently discovered in reviewing the literature, this cell line has lost both copies of chromosome 13 (Gaupel et al., reportable outcome 6). Differences in the karyotype of the two cell lines, particularly the loss of chromosome 13 in the PC-346C cells [7] may render the cells differentially sensitive to the anti-proliferative and lipogenic effects of T- and 1,25(OH)$_2$D$_3$, especially in the context of miR-17/92 cluster-mediated pathways. Further experiments using PC-346C cells will have to take the lack of the miR-17/92 cluster into account. As expected, PC-3 cells are not responsive to T and 1,25(OH)$_2$D$_3$ alone or together and no noticeable changes in neutral lipid content were observed, even in the presence of retinoic acid (Table 2). However, based on recent review on the current model

	Ctrl	T	D	Combo
G_0/G_1	74.6	67.8	74.2	67.4
S	5.7	11.7	4.9	10.3
G_2/M	18.9	19.7	20.3	21

Table 1: The effect of T and 1,25(OH)$_2$D$_3$ on cell cycle kinetics in PC-346C cells, measured by propidium iodide staining and flow cytometry.

	Ctrl	T	D	Combo
G_0/G_1	40.6	39.6	44.8	42.8
S	13.6	13.2	13.5	12.6
G_2/M	45.7	47.2	41.7	44.7

Table 2: The effect of T and 1,25(OH)$_2$D$_3$ on cell cycle kinetics in PC-3 cells, measured by propidium iodide staining and flow cytometry.

systems for prostate adenocarcinoma, PC-3 cells may not be an appropriate model system study prostate adenocarcinoma, instead it may represent the rare small-cell neuroendocrine carcinoma of prostate (Gaupel et al., in press, reportable outcome).

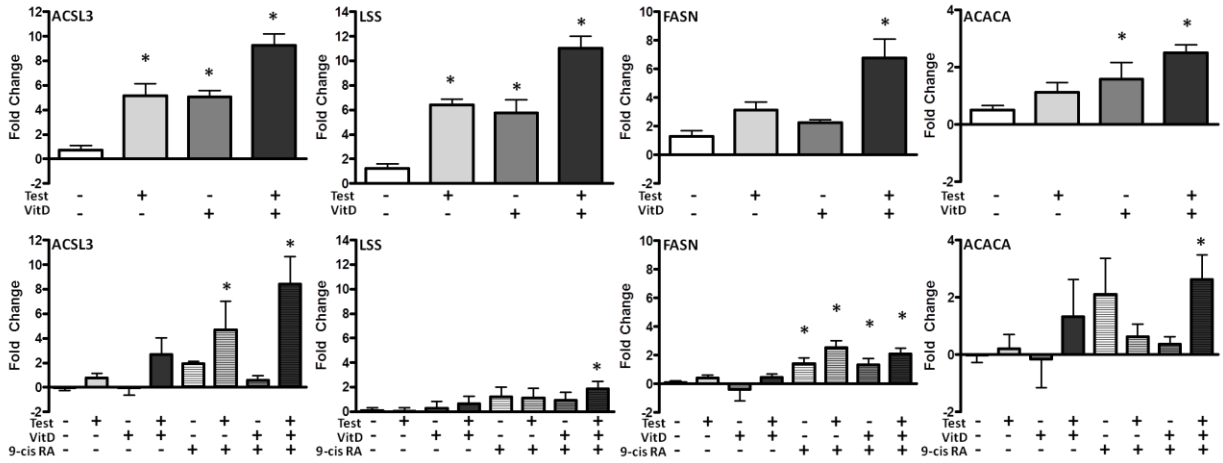

Figure 3: The effect of T and 1,25(OH)$_2$D$_3$ on ACSL3, LSS, FASN and ACACA mRNA levels at 48h in LNCaP (upper panel) and PC-346C (lower panel) cells. Relative gene expression was measured by SYBR Green qPCR analysis. Data are tabulated using $2^{-\Delta\Delta C}{}_T$ method with GAPDH as the endogenous control. Results are represented as fold changes relative to 0h control (transformed so that a fold change of 0 is in 0h control cells). Data are presented as mean ± SD from three independent experiments. Statistical analysis was performed using one-way ANOVA with Tukey post-test. * *P*<0.05 compared to untreated controls.

The combinatorial effect of T and 1,25(OH)$_2$D$_3$ on the efficacy of standard therapeutics, including bicalutamide (50μM), docetaxel (3nM) and TRAIL (100ng/mL) have been initiated in LNCaP cells. As shown in our preliminary data (Figure 4), addition of T and 1,25(OH)$_2$D$_3$ does not enhance nor hinder the effects of these agents to arrest or kill cancer cells at sub-optimal doses. We believe this is important in aiding the current paradigm of prostate cancer therapy, especially during the phases of "active surveillance" and "early stage" treatment that vitamin D supplementation in androgen replete patients may delay disease progression without affecting the subsequent efficacy of therapeutic for progressing tumors. On the other hand, treatment of T and 1,25(OH)$_2$D$_3$ may have protective function in LNCaP cells against doxorubicin at 1μM, an agent used as an alternative of ionizing radiation to induce DNA strand breakage in LNCaP cells. This may relate to the increased resident time at G_0/G_1 phase after exposure to T and 1,25(OH)$_2$D$_3$, essentially enough to repair DNA damage and lessen the toxicity of doxorubicin. It has been shown that excessive lipid production in ERBB2-positive breast cancer cells [8] sensitizes cancer cells to palmitate-induced toxicity. Hence, we are also interested to see if lipotoxicity can represent another strategy in prostate cancer treatment under adjuvant setting with androgen and vitamin D supplementation. We are also interested in examining if pre-exposure of prostate cancer cells to T and 1,25(OH)$_2$D$_3$, which models androgen and vitamin D replete disease patients, will sensitize them to standard therapeutics mentioned above. Assessment of current therapeutics in prostate cancer cell lines, along with androgen and vitamin D treatment will be completed during the second year of the award.

Examination of changes in intracellular calcium levels have been initiated, however, the protocol still needs to be optimized. We have had difficulties detecting Fura-2 signals using plate readers available at the facility. Currently, we are testing an alternative calcium indicator dye, Indo-1 to detect acute and chronic changes of intracellular calcium levels after treatment of T and $1,25(OH)_2D_3$ by flow cytometry. With the initial observation, only a small portion of LNCaP cells respond to external stimuli, including the positive control ionomycin while the majority of the cells maintained a balanced calcium levels. We are still in the process to determine if this is the conductive nature of LNCaP cells or an artifact due to uneven dye loading.

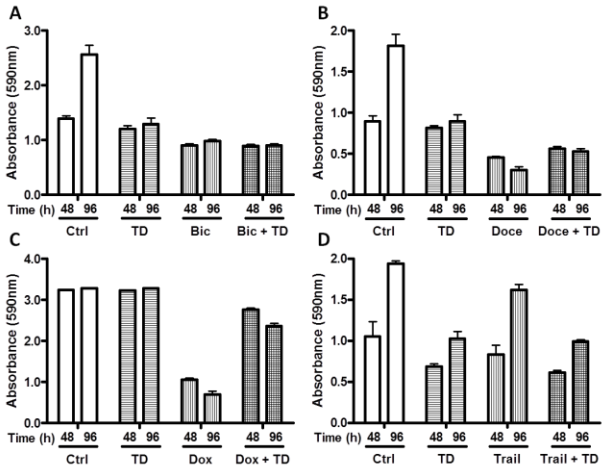

Figure 4: The combinatorial effect of T and $1,25(OH)_2D_3$ on the efficacy of therapeutics in LNCaP cells, measured by crystal violet assay at 48 and 96h after treatment A) Bicalutamide at 50μM, B) Docetaxel at 1nM, C) Doxorubicin at 1μM and D) Trail at 100ng/mL.

Summary of Progress:

Specific Aim 1: *To investigate the combinatorial effects of VDR and AR signaling on cellular homeostasis, and sensitivity of prostate cancer cells to therapeutic agents*. (~70% Completion)

Subaim 1: Documentation of the effects of T and $1,25(OH)_2D_3$ on miRNA, mRNA and cognate protein levels in three prostate cancer cell lines (Completed)

Subaim 2: Assess the impact of T and $1,25(OH)_2D_3$ on the sensitivity of prostate cancer cells to therapeutics (60% completion)

Specific Aim 2: *To identify of specific miRNAs/mRNAs responsible for the changes in cellular homeostasis and sensitivity of prostate cancer cells to therapy*. (will be initiated soon)

Subaim 1: Characterization of the roles of specific miRNAs in the regulation of calcium homeostasis, tumor progression and sensitivity to therapy (0% Completion)

Subaim 2: Investigate the mechanism of $1,25(OH)_2D_3$ and T in the modulation of miRNA expression (0% Completion)

KEY RESEARCH ACCOMPLISHMENTS

- We have established that testosterone and $1,25(OH)_2D_3$ cooperate to induce cell cycle arrest with concomitant increases of lipogenesis in LNCaP cells
- We have shown that accumulation of neutral lipid in LNCaP cells is associated with testosterone- and $1,25(OH)_2D_3$-induced lipogenic gene profiles, including PPARα, LSS, HMGCS1, ACSL1, FASN and ACACA
- Testosterone- and $1,25(OH)_2D_3$-mediated lipogenesis in PC-346C cells is dependent on the activity of 9-cis retinoic acid
- Testosterone and $1,25(OH)_2D_3$ alone or in combination does not affect the efficacy of commonly used therapeutics in prostate cancer therapy

REPORTABLE OUTCOMES

Poster Presentation:

1) Wang WLW, Welsh J & Tenniswood M. Vitamin D3 and testosterone coordinately mediate miRNA and mRNA expression in prostate cancer cells. Poster abstract presented at the Keystone Symposia of *Nuclear Receptor Matrix: Reloaded* held in Whistler, British Columbia on 04/15-04/20, 2012.
2) Wang WLW, Tenniswood M & Welsh J. Testosterone and Vitamin D3 coordinately modulate lipid metabolism via PPARa and AMPK activities in prostate cancer cells. Poster abstract presented at the Keystone Symposia of *Nuclear Receptor Matrix: Reloaded*, held in Whistler, British Columbia on 04/15-04/20, 2012.
3) Wang WLW, Welsh J & Tenniswood M. Testosterone and vitamin D3 coordinately modulate lipid metabolism via miRNA-mediated feed-forward loop in prostate cancer cells. Promoted abstract for oral presentation at the *15th Vitamin D Workshop*, held in Houston, Texas on 06/20-06/22, 2012.

Manuscripts:

4) Wang WLW, Chatterjee N, Chittur S, Welsh J & Tenniswood M. (2011) Effects of 1α,25 dihydroxyvitamin D3 and testosterone mediated signaling on miRNA and mRNA expression in LNCaP cells. Mol Cancer. 10:58 (7 Supplemental Figures & 2 Supplemental Tables)
5) Wang WLW*, Welsh J & Tenniswood T. (2012) Vitamin D3 modulates lipid metabolism in prostate cancer through miRNA mediated regulation of PPARa. J Steroid Biochem Mol Biol doi: 10.1016/j.jsbmb *Corresponding Author.
6) Gaupel AC[1], Wang WLW[1], Mordan-McCombs S, Lee ECY & Tenniswood M. Xenograft, transgenic and knockout models of prostate cancer. In: Conn M, ed. Animal models for the study of human disease, Elsevier Group. [1] Equal co-authors.

CONCLUSION

We have demonstrated that testosterone- and vitamin D-mediated pathways intersect in the AR+ LNCaP prostate cancer cell line and the combination of 5nM T and 100nM $1,25(OH)_2D_3$ leads to greater inhibition of cell proliferation with concomitant increases in lipid production and storage. This is associated with T- and $1,25(OH)_2D_3$-modulated gene expression, including key cell cycle regulators and many lipogenic genes. PPARα, in particular, is additively up-regulated by T and $1,25(OH)_2D_3$ via both transcriptional and post-transcriptional mechanisms, which we hypothesized is associated with miRNA-mediated mRNA degradation and translational repression. This is supported by the reduced potency of T and $1,25(OH)_2D_3$ to induce lipogenesis in PC-346C cells, which lacks chromosome 13 that encompasses the miR-17/92 cluster. In PC-346C cells, T and $1,25(OH)_2D_3$ only induces significant lipid accumulation, as well as lipogenic gene signatures when 9-cis retinoic acid is supplemented in the media. No significant phenotypic changes are observed in PC-3 cells, even in the presence of 9-cis RA. Using crystal violet assay, we have also shown that co-treatment of T and $1,25(OH)_2D_3$ does not affect the activity of standard therapeutics, including bicalutamide, docetaxel and TRAIL in LNCaP cells, however, T and $1,25(OH)_2D_3$ may exert protective effect against doxorubicin. We are currently interrogating the sensitivity of LNCaP cells to these therapeutics after pre-exposure to T and $1,25(OH)_2D_3$. Other possible therapeutic interventions, such as lipotoxicity, are being investigated as well. We are still in the process optimizing the protocol for measuring intracellular calcium levels after treatment with T and $1,25(OH)_2D_3$. Most sub aims in Task 1 have been initiated and nearly completed, and Task 2 will be initiated shortly.

REFERENCES

[1] J.M. Kaufman and A. Vermeulen, The decline of androgen levels in elderly men and its clinical and therapeutic implications, Endocr Rev 6 (2005) 833-876.

[2] T.M. Beer and A. Myrthue, Calcitriol in the treatment of prostate cancer, Anticancer Res 4A (2006) 2647-2651.

[3] S.Y. Park, R.V. Cooney, L.R. Wilkens, S.P. Murphy, B.E. Henderson, L.N. Kolonel, Plasma 25-hydroxyvitamin D and prostate cancer risk: The Multiethnic Cohort, Eur. J. Cancer(2010)

[4] H.V. Rhee, J.W. Coebergh, E.D. Vries, Sunlight, vitamin D and the prevention of cancer: a systematic review of epidemiological studies, Eur. J. Cancer Prev.(2009)

[5] S. Vijayakumar, R.R. Mehta, P.S. Boerner, S. Packianathan, R.G. Mehta, Clinical trials involving vitamin D analogs in prostate cancer, Cancer J. 5 (2005) 362-373.

[6] W.L. Wang, N. Chatterjee, S.V. Chittur, J. Welsh, M.P. Tenniswood, Effects of 1alpha,25 dihydroxyvitamin D3 and testosterone on miRNA and mRNA expression in LNCaP cells, Mol Cancer(2011) 58.

[7] A. van Bokhoven, A. Caires, M.D. Maria, A.P. Schulte, M.S. Lucia, S.K. Nordeen, G.J. Miller, M. Varella-Garcia, Spectral karyotype (SKY) analysis of human prostate carcinoma cell lines, Prostate 3 (2003) 226-244.

[8] A. Kourtidis, R. Srinivasaiah, R.D. Carkner, M.J. Brosnan, D.S. Conklin, Peroxisome proliferator-activated receptor-gamma protects ERBB2-positive breast cancer cells from palmitate toxicity, Breast Cancer Res 2 (2009) R16.

APPENDIX A

Copy of Abstract for Keystone Symposia of Nuclear Receptor Matrix: Reloaded

Androgens and Vitamin D_3 coordinately mediate miRNA and mRNA expression in prostate cancer cells

Wei-Lin Winnie Wang, JoEllen Welsh, Martin Tenniswood, Cancer Research Center, University at Albany, Rensselaer, NY 12144

While many studies suggest that prostate cancer is androgen responsive and dependent for its growth and development, the cancer incidence and mortality rates actually increase as serum testosterone (T) levels start to decline in older males. A similar association between sunlight exposure or serum 25-hydroxyvitamin D_3 levels with prostate tumor incidence and progression has been shown in several epidemiological studies. *In vitro*, 1,25-dihydroxyitamin D_3 ($1,25(OH)_2D_3$) has significant impact on cell proliferation and cell death. Since both T and vitamin D levels are often insufficient in most men after age 60, we hypothesize that the maintenance of these two hormones can slow cancer progression in patients with early stage disease. To assess the individual and combined effects of T and $1,25(OH)_2D_3$ on gene expression, we performed concurrent genome wide analysis of mRNA and miRNA in LNCaP cells. Significantly altered biological processes by T and $1,25(OH)_2D_3$ modulated mRNAs and miRNAs were assessed using gene ontology analysis (DAVID Bioinformatics Resources (NIAID)). Changes in the steady state mRNA and miRNA levels from several ontologies were validated by qPCR. Genes involved in cell cycle regulation and DNA strand break repair pathways are repressed by T and $1,25(OH)_2D_3$, either additively or synergistically. Many of these genes, including a key transcription factor E2F1, are targets of miRNAs concurrently evaluated by microarray, suggesting an important role of miRNAs in T- and $1,25(OH)_2D_3$-induced cell cycle arrest in prostate cancer cells. Transfac analysis of two of the modulated miRNA genes identifies 9 VDREs in promoter of miR-22, which is induced by T and $1,25(OH)_2D_3$, while c13orf25, the host gene of miR-17/92 cluster is enriched with AREs and two VDREs in close proximity to known E2F1 and Myc binding sites. Chromatin immunoprecipitation assays (ChIP) have shown that these binding sites are occupied by AR or VDR after treatment, suggesting that these miRNAs are regulated by nuclear receptor mediated transcription. Thus, in addition to their well characterized effects on transcription of target genes, T and $1,25(OH)_2D_3$ together also regulate mRNA stability by modulating miRNA levels, generating attenuation feed back and/or feed forward loops that have significant impact on the progression of prostate cancer.

APPENDIX B

Copy of Abstract for Keystone Symposia of Nuclear Receptor Matrix: Reloaded

Testosterone and Vitamin D_3 coordinately modulate lipid metabolism via PPARα and AMPK activities in prostate cancer cells

Wei-Lin Winnie Wang, Martin Tenniswood, JoEllen Welsh, Cancer Research Center, University at Albany, Rensselaer, NY 12144

Accumulated evidence has shown that androgens, including testosterone (T) can modulate prostate cancer metabolism leading to increased neutral lipid storages via regulation of SREBPs and lipogenic genes. This androgenic effect has been implicated in the development and progression of prostate cancer, though the direct association has not yet been established. Recent findings in our laboratory have shown that T and 1,25-dihydroxyvitamin D_3 ($1,25(OH)_2D_3$) co-operate to induce neutral lipid accumulation in LNCaP cells (measured by BODIPY staining), leading to a more differentiated phenotype with reduced cell proliferation. This correlates with well described role of the VDR in modulating fatty acid β-oxidation and lipolysis in adipocytes. In addition to the activity of SREBPs, the increase in T- and $1,25(OH)_2D_3$-induced lipid accumulation is correlated with the induction of PPARα mRNA in LNCaP cells as early as 48h, and T and $1,25(OH)_2D_3$ also affect PPARα expression post-transcriptionally, possibly through the regulation of miR-17/92 cluster. The effect of PPARα to induce genes involve in β-oxidation was not affected by T and $1,25(OH)_2D_3$ in LNCaP cells, as demonstrated by microarray analysis, suggesting a lipogenic role of PPARα in prostate cancer cells. In addition to the induction of genes in fatty acid synthesis, T and $1,25(OH)_2D_3$ also suppress the activity of the energy sensing kinase, AMPK via inhibition of β subunit phosphorylation in a time dependent manner. This leads to unhindered lipid synthesis in LNCaP cells after exposure to T and $1,25(OH)_2D_3$ relative to the regular proliferating cells with activated AMPK and reduced fatty acid synthesis. A similar phenotype has also been established in another AR positive prostate cancer cells, PC-346C. In this AR positive cell line, T- and $1,25(OH)_2D_3$-induced lipid deposition is also dependent on the presence of 9-cis retinoid acid. Collectively, we have demonstrated that T and $1,25(OH)_2D_3$ co-operate to modulate lipid metabolism and alter the sources for energy expenditure in prostate cancer cells.

Appendix C

Copy of Abstract for the 15th Vitamin D Workshop

TESTOSTERONE AND VITAMIN D_3 COORDINATELY MODULATE LIPID METABOLISM VIA MIRNA-MEDIATED FEED-FORWARD LOOP IN PROSTATE CANCER CELLS

Wei-Lin Winnie Wang, JoEllen Welsh, Martin Tenniswood, Cancer Research Center, University at Albany, Rensselaer, NY USA 12144

Many studies have suggested that prostate cancer is androgen responsive and dependent for its growth and development, partly through its lipogenic role in metabolism and its regulation of sterol regulatory element-binding protein (SREBP). However, such direct association has not yet been established and the cancer incidence and mortality rates actually increase as serum testosterone (T) levels start to decline in older males. A similar association between sunlight exposure or serum 25-hydroxyvitamin D_3 levels with prostate tumor incidence and progression has been shown in several epidemiological studies. Recent studies in our laboratory have shown that T and 1,25-dihydroxyvitamin D_3 ($1,25(OH)_2D_3$) co-operate to inhibit cancer cell proliferation and induce cell differentiation, marked by increases in neutral lipid accumulation (measured by BODIPY staining) in androgen-responsive prostate cancer cells (PC-347C and LNCaP cells). This correlates with the recent discovered role of vitamin D receptor (VDR) in fatty acid metabolism and lipogenesis in adipocytes. Furthermore, concurrent genome wide analysis of mRNA and miRNA in LNCaP cells reveals an extensive transcription regulatory network. This involves not only androgen receptor (AR)- and VDR-mediated transcription, but also transcription factors E2F1- and Myc-dependent transcription. Evidence suggests that changes in the activities of these factors may alter the steady state levels of miRNAs, particularly miR-22, leading to feed-forward loop that attenuates the expression of miR-17/92 (oncomir-1) cluster and alleviates their effect on the expression of peroxisome proliferator-activated receptor alpha (PPARα). This is supported by T- and $1,25(OH)_2D_3$-induced lipogenesis and suggests that T and $1,25(OH)_2D_3$ may exert cancer preventive properties by coordinately modulating lipid metabolism and altering the sources for energy expenditure in prostate cancer cells via miRNA-dependent mechanisms.

Wang et al. Molecular Cancer 2011, 10:58
http://www.molecular-cancer.com/content/10/1/58

MOLECULAR CANCER

RESEARCH Open Access

Effects of 1α,25 dihydroxyvitamin D3 and testosterone on miRNA and mRNA expression in LNCaP cells

Wei-Lin W Wang[1,2], Namita Chatterjee[1,2], Sridar V Chittur[1,2], JoEllen Welsh[2,3] and Martin P Tenniswood[1,2*]

Abstract

Background: There is evidence from epidemiological and *in vitro* studies that the biological effects of testosterone (T) on cell cycle and survival are modulated by 1,25-dihydroxyvitamin D_3 ($1,25(OH)_2D_3$) in prostate cancer. To investigate the cross talk between androgen- and vitamin D-mediated intracellular signaling pathways, the individual and combined effects of T and $1,25(OH)_2D_3$ on global gene expression in LNCaP prostate cancer cells were assessed.

Results: Stringent statistical analysis identifies a cohort of genes that lack one or both androgen response elements (AREs) or vitamin D response elements (VDREs) in their promoters, which are nevertheless differentially regulated by both steroids (either additively or synergistically). This suggests that mechanisms in addition to VDR- and AR-mediated transcription are responsible for the modulation of gene expression. Microarray analysis shows that fifteen miRNAs are also differentially regulated by $1,25(OH)_2D_3$ and T. Among these miR-22, miR-29ab, miR-134, miR-1207-5p and miR-371-5p are up regulated, while miR-17 and miR-20a, members of the miR-17/92 cluster are down regulated. A number of genes implicated in cell cycle progression, lipid synthesis and accumulation and calcium homeostasis are among the mRNA targets of these miRNAs. Thus, in addition to their well characterized effects on transcription, mediated by either or both cognate nuclear receptors, $1,25(OH)_2D_3$ and T regulate the steady state mRNA levels by modulating miRNA-mediated mRNA degradation, generating attenuation feedback loops that result in global changes in mRNA and protein levels. Changes in genes involved in calcium homeostasis may have specific clinical importance since the second messenger Ca^{2+} is known to modulate various cellular processes, including cell proliferation, cell death and cell motility, which affects prostate cancer tumor progression and responsiveness to therapy.

Conclusions: These data indicate that these two hormones combine to drive a differentiated phenotype, and reinforce the idea that the age dependent decline in both hormones results in the de-differentiation of prostate tumor cells, which results in increased proliferation, motility and invasion common to aggressive tumors. These studies also reinforce the potential importance of miRNAs in prostate cancer progression and therapeutic outcomes.

Background

Prostate cancer is the most commonly diagnosed non-cutaneous cancer in American males and is the second leading cause of cancer-related deaths in males in North America [1]. Androgens, including testosterone (T) and its active metabolite 5α-dihydrotestosterone (5α-DHT), are important for the development and growth of early stage prostate tumors and exert their effects via androgen receptor (AR) [2-4]. Androgen ablation has been one of the mainstays for the treatment of early stage, organ-confined prostate cancer along with surgery and radiation therapy.

Several epidemiological studies have suggested that adequate levels of vitamin D are critical for the prevention of various solid tumors, including breast, ovarian and colon cancers [5,6]. The risk of developing and

* Correspondence: mtenniswood@albany.edu
[1]Department of Biomedical Sciences, University at Albany, State University of New York, Albany, NY 12222, USA
Full list of author information is available at the end of the article

dying of these cancers appears to be inversely correlated with sun exposure, and/or vitamin D status, suggesting that vitamin D has chemopreventive properties [7]. Some studies have also suggested that vitamin D may play a role in prostate cancer prevention [8,9], but the data are less convincing than in other tumors and several recent meta-analyses have found weak or no associations between serum 25-hydroxyvitamin D_3 (25(OH)$_2D_3$) levels and tumor incidence and progression [10-13]. In addition, the effects of 1,25$(OH)_2D_3$ on tumor growth in the TRAMP, LPB-Tag transgenic and Nkx3.1;PTEN mutant mouse models of prostate cancer have produced conflicting results [14-16]. However, a variety of *in vitro* studies demonstrate that 1,25$(OH)_2D_3$ or its non-calcemic analogs (EB1089; CB 1093; Gemini analogs) induce apoptosis in a variety of prostate cancer cell lines including LNCaP, LNCaP C4-2, ALVA-3, LAPC-4, DU-145 and PC-3 [17-20]. These effects appear to occur through a combination of G_0/G_1 cell cycle arrest, apoptosis, differentiation and inhibition of angiogenesis [21-25]. In contrast, other studies have shown that 1,25$(OH)_2D_3$ induces cell cycle arrest but not apoptosis [26-28]. These disparate effects of 1,25$(OH)_2D_3$ on prostate tumor biology appear to be dictated predominantly by the androgen status of the mice [16] or the level of androgen in the culture medium [17,29], suggesting that in prostate cancer, there may be significant cross talk between androgen-mediated growth and vitamin D_3-mediated cell cycle arrest and differentiation which may influence tumor initiation and progression, and impact tumor growth and affect subsequent therapeutic intervention [17].

MicroRNAs (miRNAs) are a class of small non-coding, single-stranded RNAs that post-transcriptionally modulate the steady state levels of mRNA by targeting the 3' untranslated regions (3'UTR) of mRNAs. Recent studies have found that aberrant miRNA expression is closely associated with prostate cancer initiation and progression [30,31]. Several miRNAs that possess either oncogenic (miR-221/222, miR-21, miR-125b) [32-36] or tumor suppressor roles (miR-34 cluster, miR-146a, miR-200c) [37,38] have been identified in prostate cancer and some of these are associated with the castration resistant phenotype [34], or hormone-independent growth of prostate cancer [33]. Neither the effect of 1,25$(OH)_2D_3$ on miRNA levels in prostate cancer cell lines, nor the interaction with androgen signaling to modulate mRNA and miRNA transcription have been investigated. However, the importance of a regulatory loop involving miR-106b and p21 mRNA which is modulated by 1,25$(OH)_2D_3$ in non malignant prostate cells has recently been described [39]. The experiments described in this manuscript examine effects of testosterone and 1,25$(OH)_2D_3$, administered alone or in combination, on the mRNA and miRNA expression in LNCaP cells and demonstrate that cross talk between VDR- and AR-mediated signaling significantly influences the biology of prostate cancer cells. Using concurrent microarray analyses in LNCaP cells of both miRNA and mRNA, we have found that androgen-mediated transcription of both mRNA and miRNA is enhanced by 1,25$(OH)_2D_3$, either additively or synergistically, highlighting the extensive cross talk between the two receptors. Many of the gene targets of T and 1,25$(OH)_2D_3$ have significant clinical relevance. The data demonstrate that while androgens may play a central role in the development of prostate cancer, declining T levels common in older patients may play a significant role in tumor progression, particularly in patients who are also vitamin D deficient.

Results

Biological Response of LNCaP cells to T and 1,25$(OH)_2D_3$

1,25$(OH)_2D_3$ has variously been reported to induce G_0/G_1 cell cycle arrest or apoptosis in androgen-responsive LNCaP cells and other cell lines. In our hands, 100 nM 1,25$(OH)_2D_3$ and 5 nM T alone reduce growth of LNCaP cells as measured by crystal violet staining (Figure 1A). This correlates to the induction of G_0/G_1 cell cycle arrest in LNCaP cells (Figure 1B) with no evidence of apoptosis (Figure 1C). The combination of T and 1,25$(OH)_2D_3$ attenuates cell growth to a greater extent than either treatment alone (Figure 1A), which correlates to the nearly synchronous arrest of the cell populations in the G_0/G_1 phase of the cell cycle (Figure 1B). There was no evidence of cell death in LNCaP cells after treatment with 1,25$(OH)_2D_3$ alone or in combination with T, as monitored by changes in the sub G_0 population after staining with propidium iodide (not shown) or DNA fragmentation as measured by Apo-BrdU (Figure 1C). The lack of apoptosis in these cells is not due to defects in the apoptotic machinery, since bicalutamide induces apoptosis in LNCaP cells both in the absence and presence of T and 1,25$(OH)_2D_3$ (Figure 1C). The effects of T and 1,25$(OH)_2D_3$ on these parameters have been characterized at earlier and later time points with similar results (results not shown). These data demonstrate that AR- and VDR-mediated intracellular signaling pathways cooperate to modulate cell cycle kinetics in prostate cancer cells and attenuate their growth and proliferation without directly affecting apoptosis. They also demonstrate that the combination of T and 1,25$(OH)_2D_3$ does not block the sensitivity of the cells to bicalutamide.

Effect of T and 1,25$(OH)_2D_3$ on gene expression in LNCaP cells

Total RNA samples obtained from LNCaP cells treated for 48 h with 5 nM T and 100 nM 1,25$(OH)_2D_3$ alone

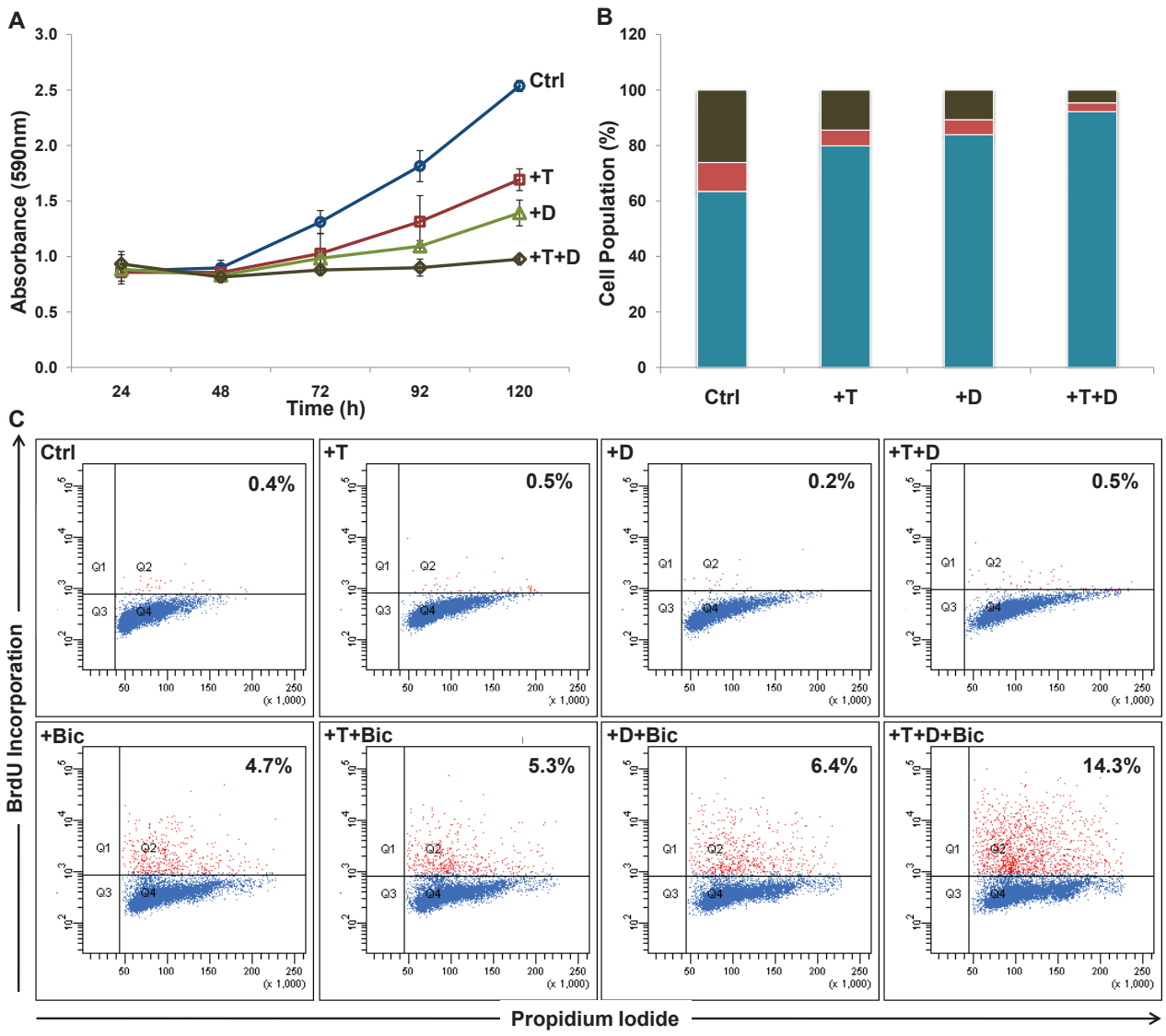

Figure 1 The effect of T and 1,25(OH)$_2$D$_3$ alone and in combination on LNCaP cells. LNCaP cells were plated as described in Material and Methods, and treated with 5 nM T and 100 nM 1,25(OH)$_2$D$_3$ alone or in combination for the indicated times (Panel A) or 48 h (panels B and C). *Panel A*: changes in cell number were measured by crystal violet; *Panel B*: cell cycle kinetics were measured by flow cytometry using propidium iodide staining (Blue:G_0/G_1 phase, Red: S phase; Black G_2/M); *Panel C*: Cell death was monitored by flow cytometry of Apo-BrdU incorporation as described in Experimental Procedures [(Apoptotic cells shown upper right quadrant (Q2)]. LNCaP cells were also treated with bicalutamide in the absence and presence of T and 1,25(OH)$_2$D$_3$ for 48 h.

or in combination were interrogated with Nimblegen-HG18-4plex whole genome microarrays. Gene expression profiles were clustered based on gene entities and treatment conditions. Treatment with T or 1,25(OH)$_2$D$_3$ alone and in combination shows distinct expression patterns that are tightly clustered by their treatment groups (Figure 2A). After filtering for the number of positive probes per gene, statistical analysis on the microarray array data with 1.5 fold cut-off generates a gene list that contains 1127 gene entities that are modulated by either T (326) or 1,25(OH)$_2$D$_3$ (825) or both additively (280) in LNCaP cells. Omnibus testing demonstrates that the effect of T and D on the expression of these genes is highly significant ($p < 0.0001$). Many of the 825 genes regulated by 1,25(OH)$_2$D$_3$, identified in this array have been identified as vitamin D responsive genes in other studies [40-42]. Approximately 65% of T modulated genes (202 of 326) has been previously reported to be responsive to androgens (T, 5α-dihydrotestosterone or R1881) in other *in vitro* systems (Androgen Responsive Gene Database: http://argdb.fudan.edu.cn). Thus, addition of exogenous T to the medium of LNCaP cells

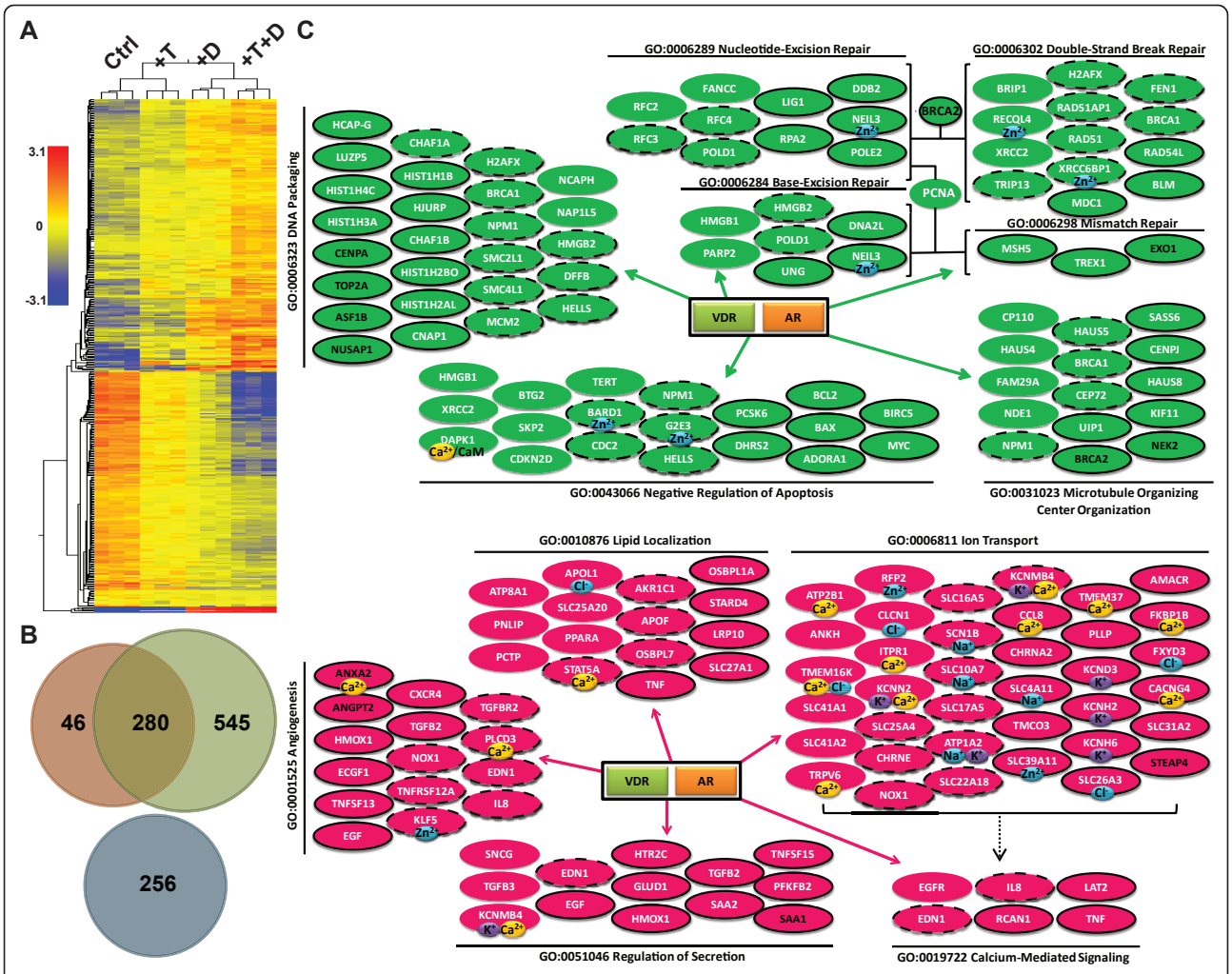

Figure 2 The effect of T and 1,25(OH)$_2$D$_3$ on mRNA expression in LNCaP cells. LNCaP cells were plated as described in Material and Methods, and treated with 5 nM T and 100 nM 1,25(OH)$_2$D$_3$ alone or in combination for 48 h. Total RNA was extracted and interrogated on Nimblegen-HG18-4plex arrays. Three independent replicates of each treatment were used for the analysis. *Panel A*: hierarchical clustering of the expression array data using the GeneSpring GX10 software. *Panel B*: Venn diagram analysis of the microarray data (Green: 1,25(OH)$_2$D$_3$-moduated, Orange: T-modulated, Blue: synergistically modulated genes by T and 1,25(OH)$_2$D$_3$. *Panel C*: Analysis of Selected Gene Ontologies Modulated by T and 1,25(OH)$_2$D$_3$ in LNCaP Cells. Functional annotation of each gene was assigned based on DAVID Bioinformatics Resources 2008 (NIAID). Magenta: gene up regulated by treatment; Green: down regulated by treatment; No shape outline: genes modulated by either T or 1,25(OH)$_2$D$_3$; dashed outline with white text: 1,25(OH)$_2$D$_3$ or T modulation is enhanced by the presence of T or 1,25(OH)$_2$D$_3$ respectively (synergy); solid outline with white text: additive effect of T and 1,25(OH)$_2$D$_3$ on mRNA levels; solid outline with black text: synergistic effect of T and 1,25(OH)$_2$D$_3$ on mRNA levels. Genes reported to be ion binding or ion channels are indicated (Ca^{2+}: yellow, Cl^-; blue, K^+: purple, Na^+: blue, Zn^{2+}: blue).

identifies a significant new cohort of 124 mRNAs that are androgen responsive. Furthermore, T and 1,25(OH)$_2$D$_3$ also synergistically modulate 256 genes that are not significantly regulated by either hormone alone, and thus form a nonintersecting dataset (Figure 2B). These data suggest AR and VDR share many common gene targets and cooperate to regulate cellular processes in LNCaP cells.

Gene Set Enrichment Analysis using Pathways Studio and Gene Ontology analysis from DAVID Bioinformatics Resources (NIAID) were used to assess the significance of the interactions between T and 1,25(OH)$_2$D$_3$ in LNCaP cells. As shown in Table 1, T alone significantly affects processes associated with cell division (particularly mitosis), microtubule based movement, chromosome segregation and progression through anaphase in LNCaP cells. 1,25(OH)$_2$D$_3$ alone also significantly affects the expression of genes associated with these cellular processes, in addition to those involved in calcium ion homeostasis and phosphoinositide-mediated signaling. Treatment with T and 1,25(OH)$_2$D$_3$ enhances the response of genes associated with these ontologies,

Table 1 Gene Set Enrichment Analysis of representative gene sets identified as significantly enriched after 1,25(OH)$_2$D$_3$ treatment in the presence of androgen in LNCaP cells.

Biological Process	Testosterone		1,25(OH)$_2$D$_3$		T & D	
	Median Change	p-value	Median Change	p-value	Median Change	p-value
Mitosis	-1.54	3.51E-10	-1.98	3.63E-07	-3.63	1.27E-15
Microtubule-based movement	-1.62	2.54E-05	-2.11	1.17E-04	-4.19	5.78E-07
Chromosome segregation	-1.61	1.11E-03	-1.99	2.13E-03	-3.44	1.12E-04
Anaphase-promoting complex-dependent proteasomal ubiquitin-dependent protein catabolic process	-1.47	5.90E-03	n/a	n/a	-3.63	2.10E-03
DNA repair	n/a	n/a	-1.77	1.08E-02	-2.55	2.24E-03
DNA recombination	n/a	n/a	-2.02	4.30E-02	-3.42	1.41E-02
Phosphoinositide-mediated signaling	n/a	n/a	-1.73	4.97E-02	-2.40	1.60E-02
Elevation of cytosolic calcium ion concentration	n/a	n/a	2.02	1.76E-02	3.43	2.95E-02

(False Discovery Rate <5%)

and, as revealed by comparing Figure 2C and additional files 1 and 2, the combination of the two hormones also additively or synergistically modulates a significantly greater number of genes than either hormone alone. It is evident that T and 1,25(OH)$_2$D$_3$ individually modulate the expression of many of the genes in these ontologies while the combination of the two hormones modulates a significant number of additional genes.

qPCR Validation of Microarray Analyses

Validation of the microarray data of selected genes associated with the gene sets was performed in LNCaP cells after treatment with T and 1,25(OH)$_2$D$_3$ over a 72 h time course. The effects of these treatments on the expression of AR and VDR, as well as two well characterized androgen responsive genes, prostate specific antigen (PSA) and TMPRSS2, and CYP24A1, the classical VDR target gene are shown in Figure 3. Neither the AR nor VDR transcripts are significantly induced in LNCaP cells by T. However, 1,25(OH)$_2$D$_3$ alone or in combination with T increases the steady state level of AR mRNA at 48 and 72 h. This corresponds to a consistent increase in the level of the androgen receptor in the nucleus after treatment with 1,25(OH)$_2$D$_3$ in the absence or presence of T (additional file 3). Both hormones increase the transcript levels of PSA and

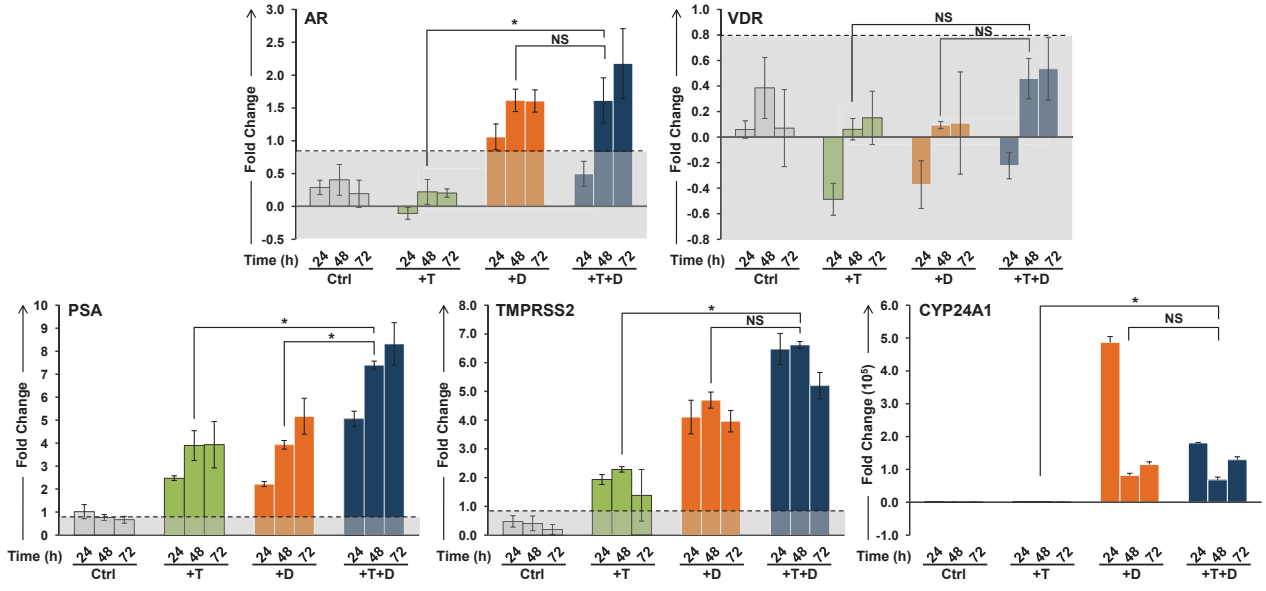

Figure 3 Validation of changes in the mRNA levels of AR, VDR, PSA, TMPRSS2 and CYP24A1. LNCaP cells were treated with 5 nM T and 100 nM 1,25(OH)$_2$D$_3$ alone and in combination and transcript levels were measured by Real Time-PCR over a 72 h time course. Fold changes greater than 0.8 are statistically significant; values within the shaded areas in each graph are not significantly modulated (0.8 or below after transformation). Comparisons between different treatment groups were analyzed using one-way ANOVA; differences were considered significant if $p < 0.05$ (*), NS: not significant. Significant changes ($p < 0.05$) in at least two out of three time points were required for the changes to be considered biologically relevant. Note: Scales on the ordinate axis vary from transcript to transcript.

TMPRSS2, and the effect of the two hormones together is additive. The classic VDR target gene CYP24A1 is strongly induced by 1,25$(OH)_2D_3$, however T alone has little or no effect on its expression. These data demonstrate that the two intracellular signaling pathways are active in LNCaP cells and that the VDR-mediated signaling significantly affects the response of both androgen responsive PSA and TMPRSS2 genes. Representative qPCR validation data, grouped by GO classification, are shown in Figure 4 (cell cycle) and Figure 5 (ion homeostasis), and the changes in the expression of genes associated with other ontologies are shown in additional file 4 (cell survival and cell death), and additional file 5 (lipid metabolism, angiogenesis, DNA repair). It is clear from these data that a number of genes are modulated by the combination of the two steroids either additively (CYP2U1, HPGD, CXCR4, CACNG4, KCNMB4, GMNN) or synergistically (CCNA2, CDC20, CCNB2, Survivin/BIRC5, GADD45G, E2F1, ITPR1, BRCA1). Genes that are known to modulate the cell cycle (CCNA2, CDC20, CCNB2) are down regulated by T and 1,25$(OH)_2D_3$ in a similar manner, reaching a nadir at 48 h after treatment (Figure 4). T and 1,25$(OH)_2D_3$ also display prolonged effects on the steady state levels of the transcripts when administered together and the transcript levels of the genes involved in prostaglandin and lipid metabolism (CYP2U1 and HPGD), and calcium homeostasis (TRPV6, ITPR1, and KCNMB4) show time-dependent increases throughout the 72 h time course (Figure 5).

It is well established that ligand-activated AR and VDR bind to cognate response elements (ARE and VDRE respectively) to modulate gene transcription and thus the coordination between T and 1,25$(OH)_2D_3$ may be the consequence of receptor mediated transcription by both AR and VDR. While *in silico* searches for ARE and VDREs within 10 kb upstream or downstream of the structural genes shown to be modulated by T or 1,25 $(OH)_2D_3$ or both, demonstrate that many of the genes have canonical response elements in their promoters

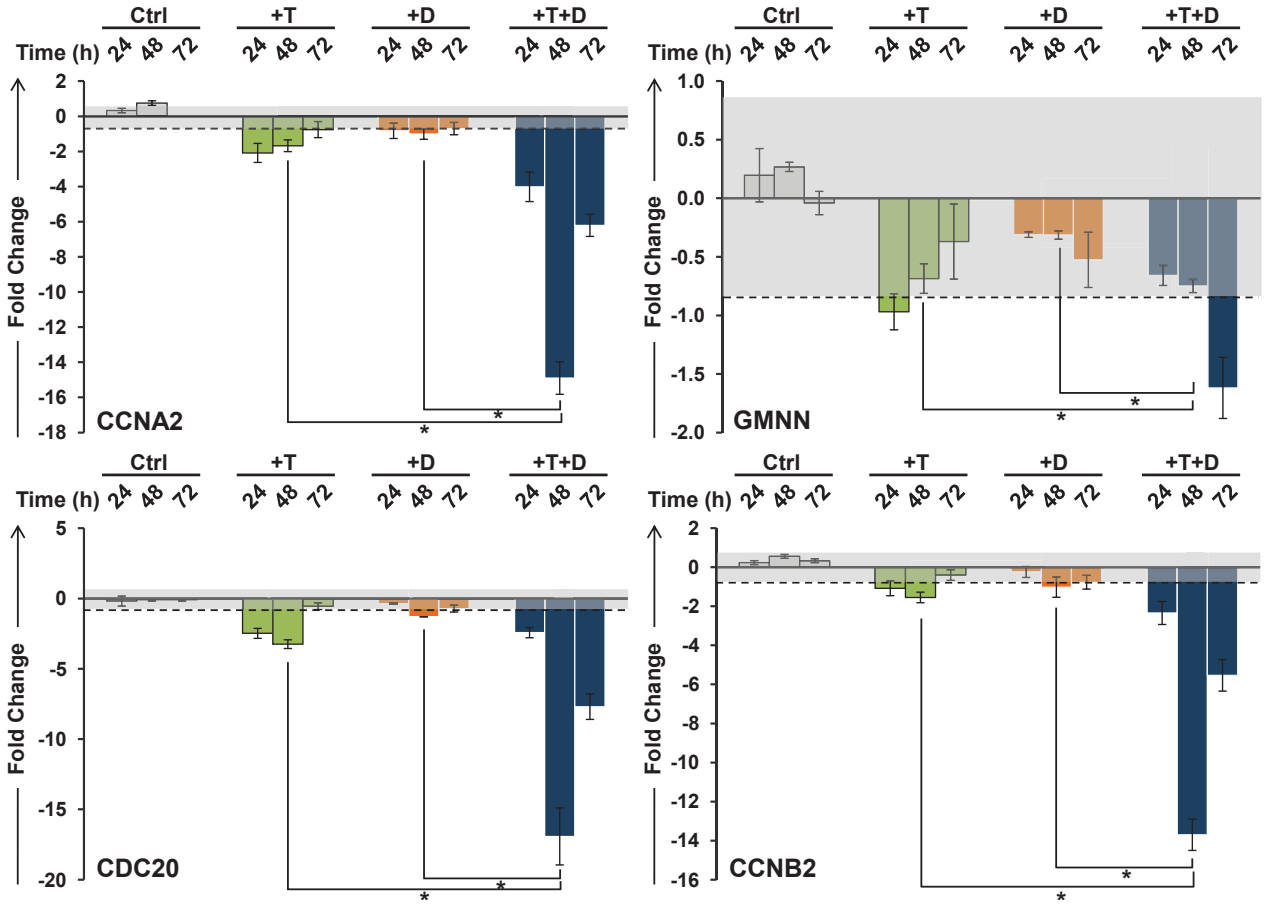

Figure 4 Validation of changes in the mRNA levels of cell cycle regulators. CCNA2, GMNN, CDC20 and CCNB2 transcript levels were measured over a 72 h time course in LNCaP cells after treatment with 5 nM T and 100 nM 1,25$(OH)_2D_3$ alone and in combination. Other details as shown in Figure 3.

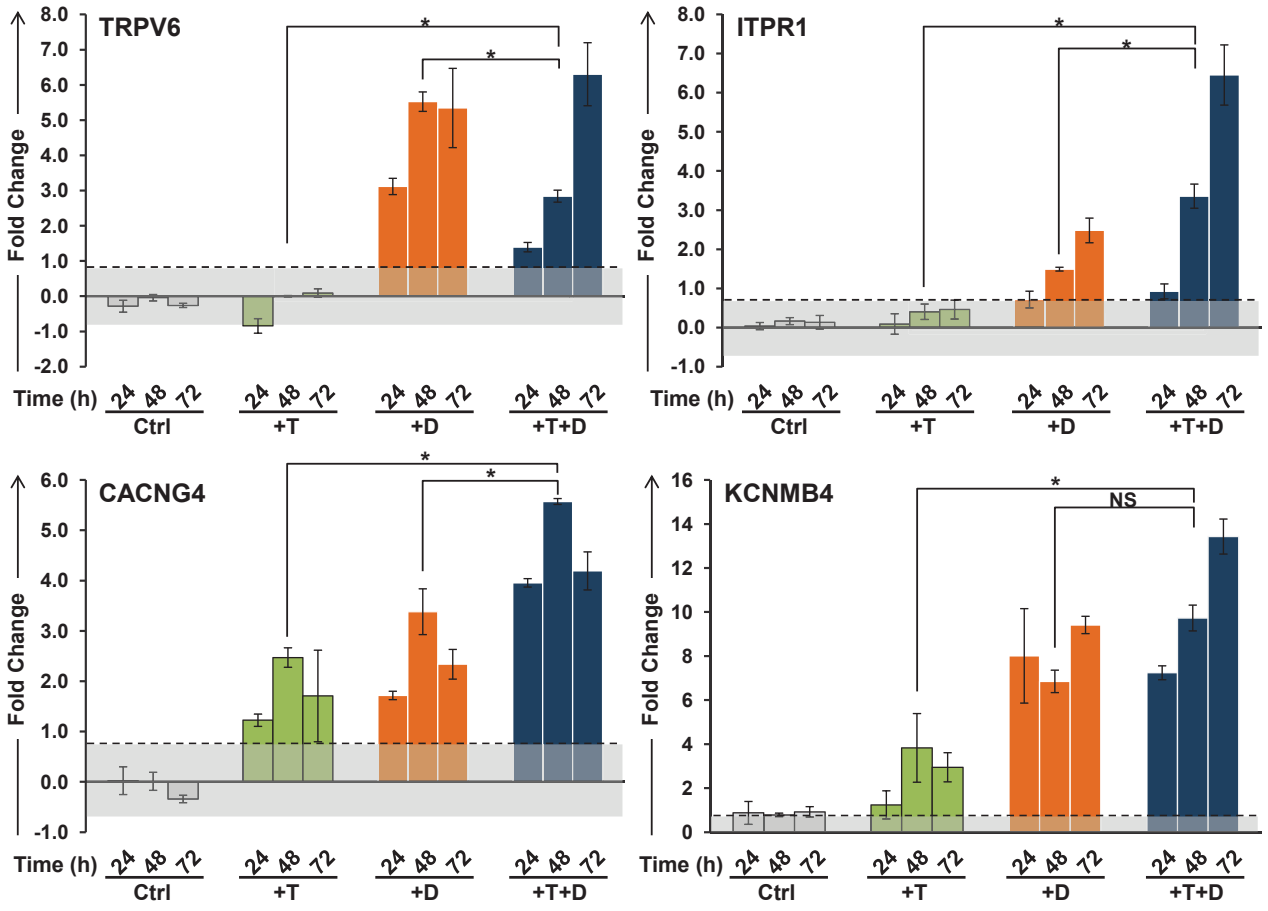

Figure 5 Validation of changes in the mRNA levels of genes involved in the calcium ion homeostasis. TRPV6, ITPR1, CACNG4 and KCNMB4 transcript levels were measured over a 72 h time course in LNCaP cells after treatment with 5 nM T and 100 nM $1,25(OH)_2D_3$ alone and in combination. Other details as shown in Figure 3.

(additional file 6), nearly 50% of the genes identified in the expression microarray analysis appear to lack functional hormone response elements (either ARE or VDRE or both) in their promoters (additional file 6). For instance, genes that have previously been documented to be only $1,25(OH)_2D_3$ inducible and/or contain VDRE at their promoters (KCNMB4, CXCR4) are also modulated by T (Figures 5 and additional file 4). Furthermore, genes such as CDC20 that lack both VDREs and AREs are down regulated by $1,25(OH)_2D_3$ and T together while neither steroid alone has significant effects on gene expression (Figures 4 and additional file 5). These data demonstrate that $1,25(OH)_2D_3$ has distinct effects on the regulation of transcript levels and that for a significant proportion the genes, the effects of $1,25(OH)_2D_3$ require the presence of T for maximal effect. Furthermore, it appears that in addition to modulating transcription of the responsive genes, T and $1,25(OH)_2D_3$ modulate the stability of the transcripts via modulation of miRNA expression.

Effect of T and $1,25(OH)_2D_3$ on miRNA expression

To examine the effect of T and $1,25(OH)_2D_3$ on miRNA expression, total RNA prepared from LNCaP cells 48 h after treatment using the same experimental paradigm outlined above was analyzed on the Agilent Human miRNA microarray v3, which contains 866 human miRNAs from the Sanger database v12.0. The miRNA expression profiles in LNCaP cells after treatment cluster to the different treatment groups are shown in Figure 6A. Statistical analysis with a stringent cut-off of 2.0 fold, identifies 15 miRNAs that are significantly modulated by T and $1,25(OH)_2D_3$ (Table 2). The majority of miRNAs identified are up regulated by T and $1,25(OH)_2D_3$ additively, including miR-29ab and miR-371/373 clusters. In contrast, two miRNAs, including miR-17 and miR-20a, members of the miR-17/92 cluster, are down regulated by T and $1,25(OH)_2D_3$ synergistically. Bioinformatic analysis using the available miRNA target prediction databases (TargetScan Human v5.1) identifies approximately 8500 putative mRNA targets of these

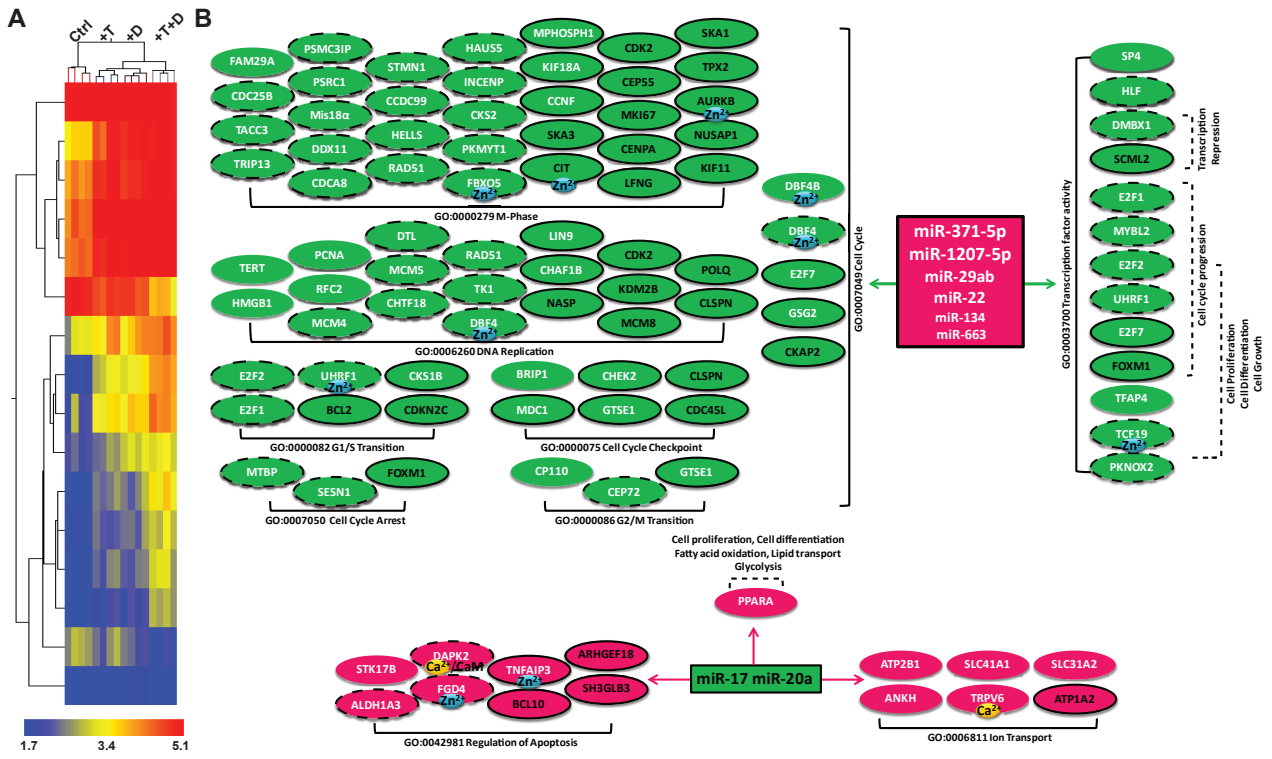

Figure 6 The effect of T and 1,25(OH)$_2$D$_3$ on miRNA expression in LNCaP cells. Cells were plated as described in Material and Methods, and treated with 5 nM T and 100 nM 1,25(OH)$_2$D$_3$ alone or in combination for 48 h. Total RNA was extracted and interrogated on Agilent Human miRNA v3 arrays. Three independent replicates were used for the analysis. *Panel A*: hierarchical clustering of the miRNA array data using the GeneSpring GX10 software. *Panel B*: Gene Ontology analysis of mRNA targets of miRNAs, predominantly focused on those that are targeted at the 3'UTR and affect the transcript stability. The inverse correlations of miRNAs targeted mRNAs and their associated Gene Ontology grouping are summarized and color coded. Magenta: gene up regulated by treatment; Green: down regulated by treatment; No shape outline: genes modulated by either T or 1,25(OH)$_2$D$_3$; dashed outline with white text: 1,25(OH)$_2$D$_3$ or T modulation is enhanced by the presence of T or 1,25 (OH)$_2$D$_3$ respectively (synergy); solid outline with white text: additive effect of T and 1,25(OH)$_2$D$_3$ on mRNA levels; solid outline with black text: synergistic effect of T and 1,25(OH)$_2$D$_3$ on mRNA levels. Genes reported to be ion binding or ion channels are indicated (Ca^{2+}: yellow, Zn^{2+}: blue). Different font size of miRNAs ranks the effect of miRNAs by the number of concordant mRNA targets in LNCaP cells.

Table 2 miRNAs differentially modulated by 1,25(OH)$_2$D$_3$ and T alone or in combination in LNCaP cells, identified by Agilent Human miRNA microarray v3.

miRNA	Seed	Testosterone	1,25(OH)$_2$D$_3$	T + 1,25(OH)$_2$D$_3$
hsa-miR-17	aaagug	-1.237	-1.255	-2.337
hsa-miR-20a	aaagug	-1.220	-1.287	-2.318
hsa-miR-20b	aaagug	-1.174	-1.391	-2.273
hsa-miR-542-5p	cgggga	-1.232	2.304	1.197
hsa-miR-29b	agcacc	1.317	1.911	2.081
hsa-miR-1207-5p	ggcagg	1.756	1.637	2.242
hsa-miR-22	agcugc	1.691	1.745	2.312
hsa-miR-1915	cccagg	2.005	2.044	3.007
hsa-miR-29a	agcacc	2.122	2.577	3.108
hsa-miR-371-5p	cucaaa	1.918	2.163	3.197
has-miR-663	ggcggg	2.293	2.561	3.685
hsa-miR-134	gugacu	2.995	2.923	4.597
hsa-miR-135a*	auaggg	2.609	2.773	4.818
hsa-miR-1181	cgucgc	3.003	3.454	5.775
hsa-miR-629*	uucucc	3.143	3.263	6.160

The seed sequence corresponds to individual miRNAs is indicated.

miRNAs. However, most of these targets are not expressed in the prostate and are not identified as differentially regulated by T and $1,25(OH)_2D_3$ by microarray. In total, 264 target transcripts are responsive to T and $1,25(OH)_2D_3$ in LNCaP cells and show an inverse association with the targeting miRNA(s) (Figure 6B). This corresponds to approximately 23% of the genes modulated by T and $1,25(OH)_2D_3$ in LNCaP cells. However this is at best a rough estimate since many of the targets of the modulated miRNAs identified by Target Scan have not yet been validated in LNCaP cells. A complete list of the miRNAs and their mRNA targets is provided in additional file 7.

The effects of T and $1,25(OH)_2D_3$ on the steady state levels of selected miRNAs were further assessed in LNCaP cells by TaqMan® qPCR to validate microarray data. T and $1,25(OH)_2D_3$ alone showed time-dependent induction of miR-29a, miR-29b, miR-21, miR-22 and miR-134 expression in LNCaP cells while the combination of the two have a more rapid additive effects on these miRNAs (Figure 7). In contrast, neither steroid alone down regulates miR-17 and miR-20a of the miR-17/92 cluster, however the combination of T and $1,25(OH)_2D_3$ significantly down regulates miR-17 and miR-20a, demonstrating the synergistic ability of T and $1,25(OH)_2D_3$ to modulate miRNA levels (Figure 8). We have also assessed the changes of miR-18a, another member of the miR-17/92 cluster. Changes in miR-18a transcript levels showed a similar pattern as that of miR-17 and 20a, suggesting that T and $1,25(OH)_2D_3$ together modulate all members of the miR-17/92 cluster rather than selectively down regulating individual members of the cluster.

In addition to the miRNAs identified from the microarray analysis, we have also assessed the effect of T and $1,25(OH)_2D_3$ on miRNAs that have been reported to be deregulated in prostate cancer. The oncogenic miR-221, which has been reported to contribute to androgen-resistance phenotype is slightly down regulated by T and $1,25(OH)_2D_3$ at 48 h, though the fold change is not statistically significant (additional file 8). Changes in the AR-inducible [35] and VDR-inducible [43] miR-125b are also not significant in LNCaP cells in this experimental paradigm (additional file 8). However, as already shown, the steady state levels of miR-21 are up regulated by T and $1,25(OH)_2D_3$ in LNCaP cells with the highest fold-induction at 72 h in the presence of both hormones (Figure 7). This implies that the expression of miR-21 targets, such as PDCD4, may also be modulated by AR and VDR in LNCaP cells.

Discussion

The data presented here demonstrate that both T and $1,25(OH)_2D_3$ modulate the mRNA and miRNA profiles in LNCaP cells, and that the combination of the two hormones modulates a significantly larger cohort of transcripts than either hormone alone. In most cases, the effects of the two hormones are additive or synergistic. Since the predicted changes in the cohort of proteins present in the cells would be expected to influence the

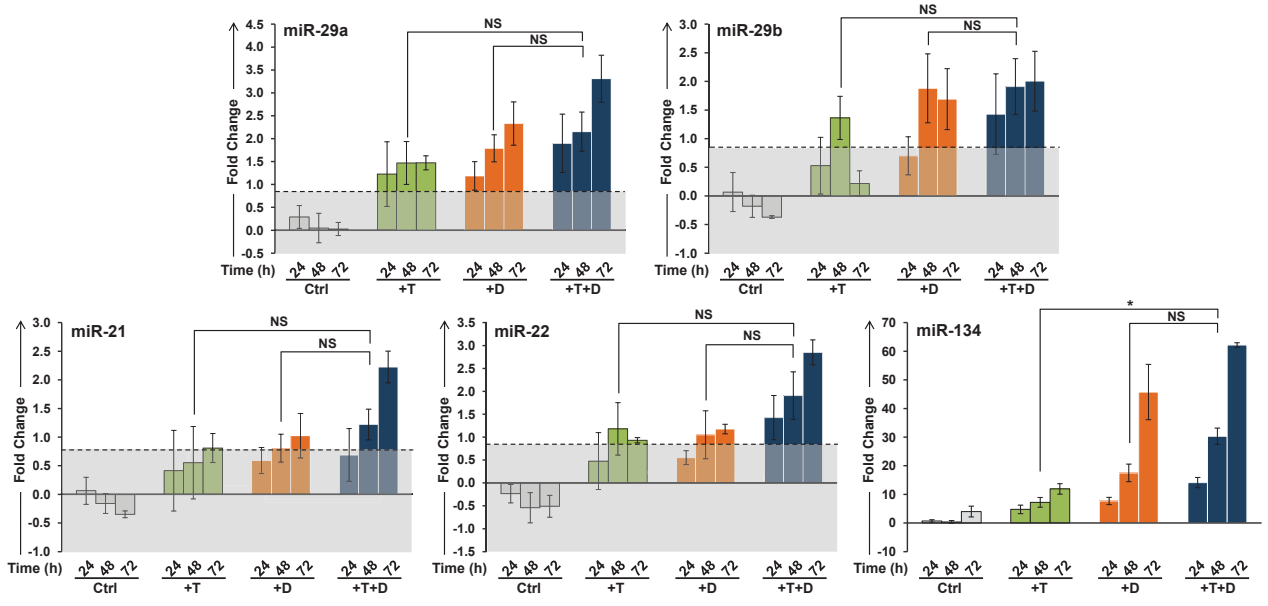

Figure 7 Validation of induction of steady state levels of miR-29a, miR-29b, miR-21, miR-22, and miR-134. LNCaP cells were treated with 5 nM T and 100 nM $1,25(OH)_2D_3$ alone and in combination and transcript levels were measured by TaqMan® qPCR over a 72 h time course. Other details as shown in Figure 3.

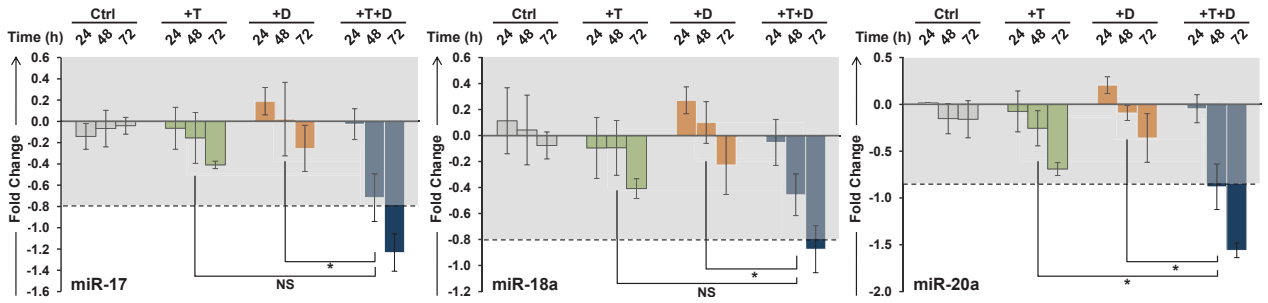

Figure 8 Validation of the down regulation of steady state levels of members of the miR-17/92 cluster. LNCaP cells were treated with 5 nM T and 100 nM $1,25(OH)_2D_3$ alone and in combination and transcript levels were measured by TaqMan® qPCR over a 72 h time course. Other details as shown in Figure 3.

response to therapeutic agents, this raises questions regarding the interpretation of previous *in vitro* data describing the responsiveness of prostate cancer cell lines grown in the absence of these hormones.

The time frame we have chosen for the initial microarray experiments (48 h) and the times chosen for qPCR validation (24, 48 and 72 h) were selected based on previous experiments examining the induction of apoptosis in LNCaP cells by diverse agents including bicalutamide and Iejimalide [44]. These time points will not discriminate between primary effects of T and $1,25(OH)_2D_3$ on transcription and secondary effects which may be due to either the modulation of miRNA, and subsequent degradation of target mRNAs or cascading regulation of transcription of other genes. However, this time frame is appropriate to examine the effects of induced miRNAs on transcript stability.

Bioinformatic analysis demonstrates that T and $1,25(OH)_2D_3$ alter the expression of genes associated with several relevant gene ontologies that clearly have the potential to significantly influence the biology of the tumor cells, their interaction with the tumor microenvironment and their response to therapeutic intervention. Perhaps the most important of these changes relate to the regulation of calcium ion homeostasis and cell cycle progression. One of the primary physiological roles of $1,25(OH)_2D_3$ is to regulate calcium and phosphorus metabolism in bone. However, $1,25(OH)_2D_3$ also plays an important role in cell cycle regulation in many cancers, including breast, ovarian and colon cancer, through its interaction with the VDR [6,45-48]. In LNCaP cells, $1,25(OH)_2D_3$ induces the expression of both voltage-gated (CACNG4) and non-voltage-gated (TRPV6) Ca^{2+} channels located on the plasma membrane. Though TRPV6 is primarily modulated by VDR, the full induction of ITPR1, annexin AII (ANXA2) and S100A10, major components of the TRPV6 auxiliary protein complex, requires the presence of both hormones, as does the induction of the highly Ca^{2+} sensitive PLC-δ3 (PLCD3). There is also a concurrent increase in ITPR1 in response to T and $1,25(OH)_2D_3$ which has been shown to lead to increased signaling through the PI3K/AKT pathway [49]. This suggests that in response to T and $1,25(OH)_2D_3$, the production of IP3 will increase, triggering the release of Ca^{2+} from endoplasmic reticulum (ER) stores via ITPR1, leading to the activation of TRPV6 through S100A10, resulting in an influx of Ca^{2+} and augmenting intracellular Ca^{2+} levels. In addition, diacylglycerol, produced by PLC mediated cleavage of PIP2, may activate PKC, to further increase the activity of TRPV6 via phosphorylation [50]. Together, these data suggest that the combination of T and $1,25(OH)_2D_3$ elevates the intracellular Ca^{2+} level to establish a new homeostatic set point without inducing cell death. Since the induction of the execution phase of apoptosis in prostate cancer cells requires the elevation of intracellular free Ca^{2+} into the micromolar range [51], resetting the intracellular Ca^{2+} concentration closer to this threshold may render tumor cells more sensitive to apoptosis-inducing agents including doxorubicin, bicalutamide and radiation. It is well known that uncontrolled release of Ca^{2+} stores from the ER, for example in response to thapsigargin, initiates apoptosis via the activation of Ca^{2+}-dependent caspases accompanied by release of cytochrome c through the mitochondrial permeability transition pore [52]. It is therefore likely that a fine-tuned Ca^{2+} balance within the cellular compartments in prostate cancer cells occurs after treatment with $1,25(OH)_2D_3$ and thus prevents Ca^{2+} overload in the mitochondria and maintains other Ca^{2+}-dependent signaling, which may include the modulation of miRNA expression [53]. Importantly, both T and $1,25(OH)_2D_3$ appear to be required to establish the elevated homeostatic calcium levels. In this regard, the capacitative Ca^{2+} entry that has been shown to block the development of the apoptosis resistance phenotype such as that seen in Bcl-2 over-expressing LNCaP cells [54,55] may be equivalent to the elevated homeostatic Ca^{2+} level

induced by T and 1,25$(OH)_2D_3$, suggesting that adequate levels of the two hormones should also prevent the development of the apoptosis-resistant, or castration resistant, phenotype in prostate cancer.

Many of the changes in the steady state mRNA levels can be attributed to changes in transcriptional activity due to the presence of functional AREs and/or VDREs in the promoters of target genes. However, *in silico* searches suggests that the promoters of nearly 40% of the affected genes do not contain either response element. Both T and 1,25$(OH)_2D_3$ have been shown to induce rapid Ca^{2+} influx via store-operated Ca^{2+} (SOC) channels whose activities are mediated by membrane receptors (mVDR & mAR) and are related to the non-genomic action of AR and VDR [56-58]. In addition, the ligand-activated VDR can modulate transcription of some target genes through Sp-1 sites [59-61]. Therefore, it is likely that additional mechanisms are responsible for the extensive modulation seen in response to the two hormones.

As demonstrated here, T and 1,25$(OH)_2D_3$ cooperatively modulate a circumscribed group of miRNAs, which mediate mRNA degradation depending on the complementarity of the miRNA seed sequence to sequences within the 3'UTR of the transcript. While alterations in individual miRNAs are not as profound as those seen in the mRNA profiles, many of the miRNAs share identical seed sequences, which results in a cumulative effect on the target transcripts. In LNCaP cells, most of the miRNAs identified in this study are up regulated in response to T and 1,25$(OH)_2D_3$, including miR-21, miR-22, miR-29ab, miR-134 and miR-371-5p and miR-1207-5p. Both miR-21 and miR-29b have previously been shown to be induced by R1881 in LNCaP and LAPC-4 prostate cancer cells [62]. Induction of these miRNAs results in substantial down regulation of several large cohorts of genes classified by GO. Thus, in addition to down regulating transcription through their cognate hormone response elements, T and 1,25$(OH)_2D_3$ can profoundly affect the stability of the transcripts encoding proteins that function in cell cycle control, cytoskeleton organization, and DNA damage repair among others. In this context, MYCBP, a positive regulator of c-Myc activity and a validated miR-22 target should be repressed by T and 1,25$(OH)_2D_3$, thus inhibiting c-Myc mediated transcription of E-box containing genes [63]. In breast cancer cells, this correlates with suppressed cell proliferation and anchorage-independent growth suggesting that increased expression of miR-22 at 48 h in prostate tumor cells by T and 1,25$(OH)_2D_3$ may be partially responsible for cell cycle arrest and the prevention of tumor progression. In LNCaP cells miR-134 is very significantly up regulated by 1,25$(OH)_2D_3$ in the absence and presence of T. The role of miR-134 in prostate cancer has not been previously described, however the steady state level of miR-134 is modulated by members of the p53/p73/p63 family as part of a miRNA-tumor suppressor network [64]. Thus, increased expression of miR-134 may further contribute to the activity of T and 1,25$(OH)_2D_3$ to suppress tumor growth.

While miR-21 was not identified in the microarray as a T and/or 1,25$(OH)_2D_3$ regulated miRNA, it was identified in the more informative qPCR analysis as a target of T and 1,25$(OH)_2D_3$, and the increases in the steady state level of miR-21 are significant after 48 h of treatment. Previous studies in breast and pancreatic cancer cell lines have suggested that over expression of miR-21 may lead to increased cell proliferation and decreased apoptosis through the targeted degradation of tumor suppressor protein PDCD4 [62,65]. In prostate cancer cells, these effects would be anticipated to counteract the anti-proliferative effects of 1,25$(OH)_2D_3$, suggesting that not all interactions between AR- and VDR-mediated signaling are beneficial. Interestingly, neither of the other miRNAs that have been implicated in prostate tumor progression (miR-221 or miR-125b) is modulated by T nor 1,25$(OH)_2D_3$ in this *in vitro* model system. In addition to up regulating miRNAs that encode cell cycle regulatory proteins and calcium ion homeostasis, T and 1,25$(OH)_2D_3$ down regulate the expression of the oncomiR cluster, miR-17/92. These data suggest that miRNAs may play important roles in T- and 1,25$(OH)_2D_3$-induced cell cycle arrest in prostate cancer cells. The concurrent analysis of mRNA and miRNA expression has demonstrated that many of the combined effects of T and 1,25$(OH)_2D_3$ are modulated by a small cohort of 15 miRNAs that are additively or synergistically regulated by the two hormones. Since the majority of men diagnosed with prostate cancer are likely to be vitamin D insufficient [66], these data may have a profound impact on our understanding of the molecular mechanisms underlying the chemopreventive and chemotherapeutic effects of vitamin D_3. Based on the data presented here, vitamin D deficiency is likely to render tumor cells more aggressive and less sensitive to chemotherapy. Given the trend toward "active surveillance" for men diagnosed with early stage prostate cancer, understanding the cross talk between the androgen- and vitamin D-mediated cellular effects may have a significant impact on the care of men in the period between diagnosis and the initiation of treatment. If these two signaling pathways interact in tumor tissue as demonstrated here, individual variations in dietary vitamin D and/or sun exposure, as well as differences in circulating T levels, may greatly influence the rate of prostate tumor growth and the sensitivity of prostate cancer to hormone and other chemotherapies. In this

context, the age related decline in serum testosterone may also contribute to the progression of prostate cancer. Thus, maintaining serum testosterone and combined with supplementation of vitamin D may substantially slow disease progression for men diagnosed with very early stage cancer, extending the time between diagnosis and treatment.

Methods

Cell Culture

LNCaP human prostate cancer cells, obtained from American Type Culture Collection (Rockville, MD), were grown in RPMI-1640 medium (Invitrogen, Carlsbad, CA) supplemented with 10% FBS (Sigma-Aldrich, St Louis, MO), 100 U/mL penicillin and 100 μg/mL streptomycin. Cells were maintained at 37°C in a humidified atmosphere of 95% air/5% CO_2. For all the experiments performed in this study, with the exception of crystal violet assays, LNCaP cells were plated at a density of 1×10^6 cells per 150 cm^2 dish for 48 h prior to treatment with 5 nM T (Sigma-Aldrich) and 100 nM $1,25(OH)_2D_3$ (Sigma-Aldrich) alone or in combination. The steroids were dissolved in ethanol, and control cells were treated with the same volume of vehicle.

Crystal Violet Assay

LNCaP cells were seeded at 20,000 cells/well in 24 well plates for 24 h prior to treatment with 5 nM T and 100 nM $1,25(OH)_2D_3$ alone or in combination. Cells were fixed with 2% glutaraldehyde in PBS for 20 min at room temperature followed by staining with 0.1% crystal violet (Sigma-Aldrich) for 30 min. The crystal violet stain was solubilized in 0.2% Triton X-100 in ddH_2O for 30 min and the absorbance was read with Victor^{3}V 1420 Multilabel Counter (PerkinElmer Inc, Waltham MA) at 590 nm. Three independent biological replicates were analyzed in triplicate.

Flow Cytometry

LNCaP cells were treated with 5 nM T and 100 nM $1,25(OH)_2D_3$ as described above. Cells treated with either vehicle (EtOH) or 100 μM bicalutamide serve as the negative and positive control, respectively. For cell cycle analysis, the cells were treated for 24, 48 and 72 h and harvested by trypsinization, followed by 90% ethanol permeabilization overnight at -20°C. Permeabilized cells were stained with 5 μg/mL propidium iodide (Sigma-Aldrich) in the presence of 0.015 U/mL RNase (Roche Applied Science, Indianapolis, IN) in PBS for 20 min at room temperature. Samples were analyzed within 3 h of labeling on BD™ LSR II Flow Cytometer (BD Biosciences, San Jose, CA). A minimum of 10,000 events were analyzed for each experimental condition. Three independent biological replicates for each treatment group were analyzed.

Apoptosis was analyzed using Apo-BrdU staining. Cells were harvested by trypsinization and fixed with 4% formaldehyde in PBS for 30 min on ice, followed by 70% ethanol permeabilization overnight at -20°C. Samples were enzymatically labeled with bromodeoxyuridine triphosphate in TdT reaction buffer (Br-dUTP, 2.5 mM cobalt chloride, and terminal transferase 24,000 U) for 1 h at 37°C to label the 3'-OH ends of fragmented DNA (Roche). DNA strand breaks were counterlabeled with FITC-conjugated anti-BrdU monoclonal antibody according to the manufacturer's directions (Phoenix Flow Systems, San Diego, CA). Cells were counterstained with 5 μg/mL propidium iodide for 30 min at room temperature. Samples were analyzed on BD™ LSR II Flow Cytometer (BD Biosciences) within 3 h of labeling and a minimum of 10,000 events were analyzed for each experimental condition. Three independent biological replicates for each treatment group were analyzed.

mRNA Microarray Analysis

Total RNA isolated from LNCaP cells was processed using standard protocols for Nimblegen arrays. Briefly 10 μg of total RNA was reverse transcribed to cDNA using oligo-dT primers and Superscript II (Invitrogen), converted to double stranded cDNA and Klenow labeled with Cy3-labeled random 9-mers before hybridization to Nimblegen-Human-HG18 4 × 72 microarrays at 42°C for 16 h using a Nimblegen Hybridization system. The arrays were washed and scanned on a Genepix 4000B scanner following which the data was extracted using NimbleScan software. Further data analysis was performed using GeneSpring GX10. The raw dataset is available as a curated dataset at GEO (SuperSeries GSE23815, SubSeries GSE17461). Three independent biological replicates for each treatment group were analyzed.

miRNA Microarray Analysis

Total RNA was processed and hybridized to Agilent Human miRNA microarrays using standard protocols. 100 ng of total RNA was dephosphorylated with calf intestinal phosphatase and end-labeled with Cy3-pCp by T4 RNA ligase prior to an overnight hybridization at 55° C onto Agilent Human miRNA v3 (Sanger release 12.0) microarrays. The arrays were washed and scanned on a high resolution GC2565CA Agilent Scanner using the manufacturer's recommended settings. The raw data was extracted using Agilent Feature Extraction software v10.1.1 and imported into GeneSpring GX10 for further analysis. The raw data is available as a curated dataset at GEO (SuperSeries GSE23815, SubSeries GSE23814).

qPCR Validation of Microarray Data

Changes in mRNA and miRNA identified by microarray were validated in independent biological replicates. LNCaP cells were plated and treated as previously described for 24, 48 and 72 h. Cells were harvested by trypsinization and total RNA (both mRNA and miRNA) was extracted using miRNeasy mini kit (Qiagen, Valencia, CA). Reverse transcription PCR reactions were performed with 1.5 μg total RNA using Taqman® Reverse Transcription Reagents (Applied Biosystems, Carlsbad, CA) to synthesize cDNA for mRNA expression analysis. The reaction mixture was incubated for 10 min at 25°C, 1 h at 37°C and 5 min at 95°C and kept at -20°C until further analysis. qPCR probes for each gene were designed using Primer-Blast (National Center for Biotechnology Information) with default settings and synthesized by Integrated DNA Technologies (Coralville, IA). The list of primers for each gene is available in additional file 9. SYBR Green reactions with SYBR® Green PCR Master Mix (Applied Biosystems) were analyzed using the ABI 7900HT Fast Real-Time PCR System (Applied Biosystems): 50°C for 2 min, 95°C for 10 min, 95°C for 15 sec and 60°C for 1 min, repeated for 40 cycles. Relative expression levels of each gene in real time were analyzed using the $2^{-\Delta\Delta C}{}_T$ method [67] and presented as ratio relative to the expression of the housekeeping gene GAPDH. For miRNA expression analysis, 10 ng total RNA were used to make cDNA with TaqMan® MicroRNA Reverse Transcription Reagents (Applied Biosystems). The reaction mixture was incubated for 30 min at 16°C, 30 min at 42°C and 5 min at 85°C and kept at -20°C until further analysis. TaqMan® MicroRNA Assays were used to evaluate miRNA expression according to manufacturer's protocol. TaqMan reactions were analyzed using the ABI 7900HT Fast Real-Time PCR System: 95°C for 10 min, 95°C for 15 sec and 60°C for 60 sec repeated for 40 cycles. Relative expression levels of each miRNA in real time were analyzed using the $2^{-\Delta\Delta C}$T method with U6 snRNA as the reference control. Each sample was replicated twice from three independent sets of RNA preparations. Results are tabulated as mean ± SD and presented as fold change after transformation to show divergence from no effect (zero fold change).

Statistical Analysis of Microarray Data

For mRNA microarray analysis in GeneSpring GX10, the gene list was filtered to exclude entities which showed low signal values across all samples (i.e bottom 20th percentile). Statistically significant genes from each expression profile were selected using one-way ANOVA ($p \leq 0.05$). The multiple testing correction Benjamini and Hochberg false discovery rate (FDR) (p-value <0.05) was integrated within each test. A fold change cut-off at 1.5 fold was implemented to generate the final list of differentially expressed genes. Genes passing the statistical tests were further assigned into their gene ontology (GO) grouping using DAVID Bioinformatics Resources v6.7 (NIAID) with the default setting, essentially as previously described [68]. Significantly regulated and enriched GO groups were selected for qPCR analysis.

For miRNA microarray analysis, the raw data was imported into GeneSpring GX10, log2 transformed, normalized to the 75th percentile following which the entity list was filtered to exclude probes that showed low signal values across all treatment groups (i.e. bottom 20th percentile). This list was further filtered to only include entities that were marked "present;' or "marginal" in all 3 replicates for at least one of the 4 treatment groups. Entities with fold changes greater than 2.0 were considered significant when $p < 0.05$ using one-way ANOVA with Benjamini-Hochberg FDR post-test. Targets of miRNAs that passed the statistical test were identified using TargetScan Human v5.1 from Whitehead Institute for Biomedical Research. Gene targets whose mRNA expression levels were inversely proportional to the corresponding miRNA expression levels were considered concordant and were further analyzed for their enrichment in Gene Ontology grouping.

Additional material

Additional file 1: Analysis of Selected Gene Ontologies Modulated by T in LNCaP Cells. Functional annotation of each gene was assigned based on DAVID Bioinformatics Resources 2008 (NIAID). Magenta: gene up regulated by treatment; Green: down regulated by treatment; No shape outline: genes modulated by either T or $1,25(OH)_2D_3$; dashed outline with white text: $1,25(OH)_2D_3$ or T modulation is enhanced by the presence of T or $1,25(OH)_2D_3$ respectively (synergy); solid outline with white text: additive effect of T and $1,25(OH)_2D_3$ on mRNA levels; solid outline with black text: synergistic effect of T and $1,25(OH)_2D_3$ on mRNA levels. Genes reported to be ion binding or ion channels are indicated (Ca^{2+}: yellow, Zn^{2+}: blue)

Additional file 2: Analysis of Selected Gene Ontologies Modulated by $1,25(OH)_2D_3$ in LNCaP Cells. Functional annotation of each gene was assigned based on DAVID Bioinformatics Resources 2008 (NIAID). Magenta: gene up regulated by treatment; Green: down regulated by treatment; No shape outline: genes modulated by either T or $1,25(OH)_2D_3$; dashed outline with white text: $1,25(OH)_2D_3$ or T modulation is enhanced by the presence of T or $1,25(OH)_2D_3$ respectively (synergy); solid outline with white text: additive effect of T and $1,25(OH)_2D_3$ on mRNA levels; solid outline with black text: synergistic effect of T and $1,25(OH)_2D_3$ on mRNA levels. Genes reported to be ion binding or ion channels are indicated (Ca^{2+}: yellow, Zn^{2+}: blue)

Additional file 3: Immunoblotting analysis of 5 nM T and 100 nM $1,25(OH)_2D_3$ on nuclear AR and VDR expression. LNCaP cells were treated with 5 nM T and 100 nM $1,25(OH)_2D_3$ alone and in combination for 48 h. Nuclear proteins were extracted and ran on 10% SDS-PAGE and transferred to PVDF membrane. Antibodies against AR (Millipore) and VDR (Santa Cruz) were used to detect the protein levels of AR and VDR in the nucleus. Lamin A/C was used as the loading control.

Additional file 4: Validation on changes in the mRNA levels of genes involved in cell death. GADD45G, STK17B, E2F1 and Survivin/BIRC5 transcript levels were measured over a 72 h time course in LNCaP

cells after treatment with 5 nM T and 100 nM $1,25(OH)_2D_3$ alone and in combination. Other details as shown in Figure 3.

Additional file 5: Validation on changes in the mRNA levels of selected genes involved in lipid metabolism, angiogenesis, calcium induced signaling and DNA repair. CYP2U1, HPGD, CXCR4, ANXA2, EGFR and BRCA1 transcripts were measured over a 72 h time course in LNCaP cells after treatment with 5 nM T and 100 nM $1,25(OH)_2D_3$. Fold changes greater than 0.8 are statistically significant; values within the shaded areas in each graph are not significantly modulated (0.8 or below after transformation). Comparisons between different treatment groups were analyzed using one-way ANOVA; differences were considered significant if $p < 0.05$ (*), NS: not significant. Significant changes ($p < 0.05$) in at least two out of three time points were required for the changes to be considered biologically relevant. Note: Scales on the ordinate axis vary from transcript to transcript.

Additional file 6: Differentially regulated mRNAs by T and $1,25(OH)_2D_3$ in LNCaP cells after 48 h of treatment. Down regulated mRNAs are shaded in green and up regulated mRNAs are shaded in red. The presence (1) or absence (0) of hormone response elements are indicated based on the *in silico* searches for androgen response elements (AREs) and/or vitamin D response elements (VDREs) in the promoters of T and $1,25(OH)_2D_3$ responsive genes identified from microarray analysis.

Additional file 7: miRNA targeted that are differentially regulated by T and $1,25(OH)_2D_3$ in LNCaP cells after 48 h of treatment. Down regulated mRNAs/miRNAs are shaded in green and up regulated mRNAs/miRNAs are shaded in red.

Additional file 8: Effects of T and $1,25(OH)_2D_3$ on the expression of miR-125b and miR-221 in LNCaP cells. LNCaP cells were treated with 5 nM T and 100 nM $1,25(OH)_2D_3$ alone and in combination and transcript levels were measured by TaqMan® qPCR over a 72 h time course. Other details as shown in Figure S4.

Additional file 9: Sequence of Primers used for qPCR.

Acknowledgements
The research presented in this manuscript was supported by an operating grant from the USPHS (RO1 CA101114-04). The authors would like to thank David Frank and Marcy Kuentzel for excellent technical help with the microarray experiments; and Dr. Andrew Reilly for his help and insights into the analysis of the microarray data.

Author details
[1]Department of Biomedical Sciences, University at Albany, State University of New York, Albany, NY 12222, USA. [2]Cancer Research Center, University at Albany, Rensselaer, NY 12144, USA. [3]Department of Environmental Health Sciences, University at Albany, State University of New York, Albany, NY 12222, USA.

Authors' contributions
WWW was responsible for execution of the experiments described in this manuscript and the analysis of the data. She also wrote the first draft of the manuscript. NC assisted with the analysis of the microarray data and SVC performed the microarray experiments and the initial bioinformatic analyses. JW was responsible for experimental design and editing the manuscript. MT was responsible for experimental design and editing the manuscript. All authors read and approved the final manuscript.

Competing interests
The authors declare that they have no competing interests.

Received: 8 March 2011 Accepted: 18 May 2011 Published: 18 May 2011

References

1. Surveillance Epidemiology and End Results Web. [http://seer.cancer.gov].
2. Lamont KR, Tindall DJ: **Androgen regulation of gene expression.** *Adv Cancer Res* 2010, **107**:137-162.
3. Vis AN, Schroder FH: **Key targets of hormonal treatment of prostate cancer. Part 1: the androgen receptor and steroidogenic pathways.** *BJU Int* 2009, **104**:438-448.
4. Vis AN, Schroder FH: **Key targets of hormonal treatment of prostate cancer. Part 2: the androgen receptor and 5alpha-reductase.** *BJU Int* 2009, **104**:1191-1197.
5. Giovannucci E: **Expanding roles of vitamin D.** *J Clin Endocrinol Metab* 2009, **94**:418-420.
6. Thorne J, Campbell MJ: **The vitamin D receptor in cancer.** *Proc Nutr Soc* 2008, **67**:115-127.
7. Garland CF, Gorham ED, Mohr SB, Garland FC: **Vitamin D for cancer prevention: global perspective.** *Ann Epidemiol* 2009, **19**:468-483.
8. Schwartz GG, Skinner HG: **Vitamin D status and cancer: new insights.** *Curr Opin Clin Nutr Metab Care* 2007, **10**:6-11.
9. Tseng M, Breslow RA, DeVellis RF, Ziegler RG: **Dietary patterns and prostate cancer risk in the National Health and Nutrition Examination Survey Epidemiological Follow-up Study cohort.** *Cancer Epidemiol Biomarkers Prev* 2004, **13**:71-77.
10. Barnett CM, Nielson CM, Shannon J, Chan JM, Shikany JM, Bauer DC, *et al*: **Serum 25-OH vitamin D levels and risk of developing prostate cancer in older men.** *Cancer Causes Control* 2010, **21**:1297-1303.
11. Park SY, Cooney RV, Wilkens LR, Murphy SP, Henderson BE, Kolonel LN: **Plasma 25-hydroxyvitamin D and prostate cancer risk: the multiethnic cohort.** *Eur J Cancer* 2010, **46**:932-936.
12. Rhee HV, Coebergh JW, Vries ED: **Sunlight, vitamin D and the prevention of cancer: a systematic review of epidemiological studies.** *Eur J Cancer Prev* 2009.
13. Yin L, Raum E, Haug U, Arndt V, Brenner H: **Meta-analysis of longitudinal studies: Serum vitamin D and prostate cancer risk.** *Cancer Epidemiol* 2009, **33**:435-445.
14. Alagbala AA, Moser MT, Johnson CS, Trump DL, Foster BA: **Characterization of Vitamin D insensitive prostate cancer cells.** *J Steroid Biochem Mol Biol* 2007, **103**:712-716.
15. Banach-Petrosky W, Ouyang X, Gao H, Nader K, Ji Y, Suh N, *et al*: **Vitamin D inhibits the formation of prostatic intraepithelial neoplasia in Nkx3.1; Pten mutant mice.** *Clin Cancer Res* 2006, **12**:5895-5901.
16. Mordan-McCombs S, Brown T, Wang WL, Gaupel AC, Welsh J, Tenniswood M: **Tumor progression in the LPB-Tag transgenic model of prostate cancer is altered by vitamin D receptor and serum testosterone status.** *J Steroid Biochem Mol Biol* 2010, **121**:368-371.
17. Murthy S, Agoulnik IU, Weigel NL: **Androgen receptor signaling and vitamin D receptor action in prostate cancer cells.** *Prostate* 2005, **64**:362-372.
18. Oades GM, Dredge K, Kirby RS, Colston KW: **Vitamin D receptor-dependent antitumour effects of 1,25-dihydroxyvitamin D3 and two synthetic analogues in three in vivo models of prostate cancer.** *BJU Int* 2002, **90**:607-616.
19. Saito T, Okamoto R, Haritunians T, O'Kelly J, Uskokovic M, Maehr H, *et al*: **Novel Gemini vitamin D(3) analogs have potent antitumor activity.** *J Steroid Biochem Mol Biol* 2008, **112**:151-156.
20. Washington MN, Kim JS, Weigel NL: **1alpha,25-dihydroxyvitamin D(3) inhibits C4-2 prostate cancer cell growth via a retinoblastoma protein (Rb)-independent G(1) arrest.** *Prostate* 2010.
21. Bao BY, Yao J, Lee YF: **1alpha, 25-dihydroxyvitamin D3 suppresses interleukin-8-mediated prostate cancer cell angiogenesis.** *Carcinogenesis* 2006, **27**:1883-1893.
22. Ben Shoshan M, Amir S, Dang DT, Dang LH, Weisman Y, Mabjeesh NJ: **1alpha,25-dihydroxyvitamin D3 (Calcitriol) inhibits hypoxia-inducible factor-1/vascular endothelial growth factor pathway in human cancer cells.** *Mol Cancer Ther* 2007, **6**:1433-1439.
23. Jiang F, Bao J, Li P, Nicosia SV, Bai W: **Induction of ovarian cancer cell apoptosis by 1,25-dihydroxyvitamin D3 through the down-regulation of telomerase.** *J Biol Chem* 2004, **279**:53213-53221.
24. Kizildag S, Ates H, Kizildag S: **Treatment of K562 cells with 1,25-dihydroxyvitamin D(3) induces distinct alterations in the expression of apoptosis-related genes BCL2, BAX, BCL(XL), and p21.** *Ann Hematol* 2009.
25. Mantell DJ, Owens PE, Bundred NJ, Mawer EB, Canfield AE: **1 alpha,25-dihydroxyvitamin D(3) inhibits angiogenesis in vitro and in vivo.** *Circ Res* 2000, **87**:214-220.
26. Campbell MJ, Koeffler HP: **Toward therapeutic intervention of cancer by vitamin D compounds.** *J Natl Cancer Inst* 1997, **89**:182-185.

27. Miller GJ, Stapleton GE, Hedlund TE, Moffat KA: **Vitamin D receptor expression, 24-hydroxylase activity, and inhibition of growth by 1alpha,25-dihydroxyvitamin D3 in seven human prostatic carcinoma cell lines.** *Clin Cancer Res* 1995, **1**:997-1003.
28. Zhuang SH, Burnstein KL: **Antiproliferative effect of 1alpha,25-dihydroxyvitamin D3 in human prostate cancer cell line LNCaP involves reduction of cyclin-dependent kinase 2 activity and persistent G1 accumulation.** *Endocrinology* 1998, **139**:1197-1207.
29. Weigel NL: **Interactions between vitamin D and androgen receptor signaling in prostate cancer cells.** *Nutr Rev* 2007, **65**:S116-S117.
30. Ambs S, Prueitt RL, Yi M, Hudson RS, Howe TM, Petrocca F, *et al*: **Genomic profiling of microRNA and messenger RNA reveals deregulated microRNA expression in prostate cancer.** *Cancer Res* 2008, **68**:6162-6170.
31. Porkka KP, Pfeiffer MJ, Waltering KK, Vessella RL, Tammela TL, Visakorpi T: **MicroRNA expression profiling in prostate cancer.** *Cancer Res* 2007, **67**:6130-6135.
32. Li T, Li D, Sha J, Sun P, Huang Y: **MicroRNA-21 directly targets MARCKS and promotes apoptosis resistance and invasion in prostate cancer cells.** *Biochem Biophys Res Commun* 2009, **383**:280-285.
33. Ribas J, Ni X, Haffner M, Wentzel EA, Salmasi AH, Chowdhury WH, *et al*: **miR-21: an androgen receptor-regulated microRNA that promotes hormone-dependent and hormone-independent prostate cancer growth.** *Cancer Res* 2009, **69**:7165-7169.
34. Sun T, Yang M, Kantoff P, Lee GS: **Role of microRNA-221/-222 in cancer development and progression.** *Cell Cycle* 2009, **8**:2315-2316.
35. Shi XB, Xue L, Yang J, Ma AH, Zhao J, Xu M, *et al*: **An androgen-regulated miRNA suppresses Bak1 expression and induces androgen-independent growth of prostate cancer cells.** *Proc Natl Acad Sci USA* 2007, **104**:19983-19988.
36. Shi XB, Xue L, Ma AH, Tepper CG, Kung HJ, White RW: **miR-125b promotes growth of prostate cancer xenograft tumor through targeting pro-apoptotic genes.** *Prostate* 2011, **71**:538-549.
37. Lin SL, Chiang A, Chang D, Ying SY: **Loss of mir-146a function in hormone-refractory prostate cancer.** *RNA* 2008, **14**:417-424.
38. Rokhlin OW, Scheinker VS, Taghiyev AF, Bumcrot D, Glover RA, Cohen MB: **MicroRNA-34 mediates AR-dependent p53-induced apoptosis in prostate cancer.** *Cancer Biol Ther* 2008, **7**:1288-1296.
39. Thorne JL, Maguire O, Doig CL, Battaglia S, Fehr L, Sucheston LE, *et al*: **Epigenetic control of a VDR-governed feed-forward loop that regulates p21(waf1/cip1) expression and function in non-malignant prostate cells.** *Nucleic Acids Res* 2011, **39**:2045-2056.
40. Krishnan AV, Shinghal R, Raghavachari N, Brooks JD, Peehl DM, Feldman D: **Analysis of vitamin D-regulated gene expression in LNCaP human prostate cancer cells using cDNA microarrays.** *Prostate* 2004, **59**:243-251.
41. Peehl DM, Shinghal R, Nonn L, Seto E, Krishnan AV, Brooks JD, *et al*: **Molecular activity of 1,25-dihydroxyvitamin D3 in primary cultures of human prostatic epithelial cells revealed by cDNA microarray analysis.** *J Steroid Biochem Mol Biol* 2004, **92**:131-141.
42. Wang TT, Tavera-Mendoza LE, Laperriere D, Libby E, MacLeod NB, Nagai Y, *et al*: **Large-scale in silico and microarray-based identification of direct 1,25-dihydroxyvitamin D3 target genes.** *Mol Endocrinol* 2005, **19**:2685-2695.
43. Mohri T, Nakajima M, Takagi S, Komagata S, Yokoi T: **MicroRNA regulates human vitamin D receptor.** *Int J Cancer* 2009, **125**:1328-1333.
44. Wang WL, McHenry P, Jeffrey R, Schweitzer D, Helquist P, Tenniswood M: **Effects of Iejimalide B, a marine macrolide, on growth and apoptosis in prostate cancer cell lines.** *J Cell Biochem* 2008, **105**:998-1007.
45. Colston KW, Hansen CM: **Mechanisms implicated in the growth regulatory effects of vitamin D in breast cancer.** *Endocr Relat Cancer* 2002, **9**:45-59.
46. Harris DM, Go VL: **Vitamin D and colon carcinogenesis.** *J Nutr* 2004, **134**:3463S-3471S.
47. Welsh J, Wietzke JA, Zinser GM, Smyczek S, Romu S, Tribble E, *et al*: **Impact of the Vitamin D3 receptor on growth-regulatory pathways in mammary gland and breast cancer.** *J Steroid Biochem Mol Biol* 2002, **83**:85-92.
48. Zhang X, Nicosia SV, Bai W: **Vitamin D receptor is a novel drug target for ovarian cancer treatment.** *Curr Cancer Drug Targets* 2006, **6**:229-244.
49. Khan MT, Wagner L, Yule DI, Bhanumathy C, Joseph SK: **Akt kinase phosphorylation of inositol 1,4,5-trisphosphate receptors.** *J Biol Chem* 2006, **281**:3731-3737.
50. Al Ansary D, Bogeski I, Disteldorf BM, Becherer U, Niemeyer BA: **ATP modulates Ca2+ uptake by TRPV6 and is counteracted by isoform-specific phosphorylation.** *FASEB J* 2010, **24**:425-435.
51. Tombal B, Denmeade SR, Gillis JM, Isaacs JT: **A supramicromolar elevation of intracellular free calcium ([Ca(2+)](i)) is consistently required to induce the execution phase of apoptosis.** *Cell Death Differ* 2002, **9**:561-573.
52. Szabadkai G, Duchen MR: **Mitochondria: the hub of cellular Ca2+ signaling.** *Physiology (Bethesda)* 2008, **23**:84-94.
53. Sonkoly E, Wei T, Pavez LE, Suzuki H, Kato M, Torma H, *et al*: **Protein kinase C-dependent upregulation of miR-203 induces the differentiation of human keratinocytes.** *J Invest Dermatol* 2010, **130**:124-134.
54. Vanden Abeele F, Skryma R, Shuba Y, Van Coppenolle F, Slomianny C, Roudbaraki M, *et al*: **Bcl-2-dependent modulation of Ca(2+) homeostasis and store-operated channels in prostate cancer cells.** *Cancer Cell* 2002, **1**:169-179.
55. Flourakis M, Prevarskaya N: **Insights into Ca2+ homeostasis of advanced prostate cancer cells.** *Biochim Biophys Acta* 2009, **1793**:1105-1109.
56. Foradori CD, Weiser MJ, Handa RJ: **Non-genomic actions of androgens.** *Front Neuroendocrinol* 2008, **29**:169-181.
57. Nakagawa K, Tsugawa N, Okamoto T, Kishi T, Ono T, Kubodera N, *et al*: **Rapid control of transmembrane calcium influx by 1alpha,25-dihydroxyvitamin D3 and its analogues in rat osteoblast-like cells.** *Biol Pharm Bull* 1999, **22**:1058-1063.
58. Steinsapir J, Socci R, Reinach P: **Effects of androgen on intracellular calcium of LNCaP cells.** *Biochem Biophys Res Commun* 1991, **179**:90-96.
59. Cheng HT, Chen JY, Huang YC, Chang HC, Hung WC: **Functional role of VDR in the activation of p27Kip1 by the VDR/Sp1 complex.** *J Cell Biochem* 2006, **98**:1450-1456.
60. Huang YC, Hung WC: **1,25-dihydroxyvitamin D3 transcriptionally represses p45Skp2 expression via the Sp1 sites in human prostate cancer cells.** *J Cell Physiol* 2006, **209**:363-369.
61. McGaffin KR, Chrysogelos SA: **Identification and characterization of a response element in the EGFR promoter that mediates transcriptional repression by 1,25-dihydroxyvitamin D3 in breast cancer cells.** *J Mol Endocrinol* 2005, **35**:117-133.
62. Ribas J, Ni X, Haffner M, Wentzel EA, Salmasi AH, Chowdhury WH, *et al*: **miR-21: an androgen receptor-regulated microRNA that promotes hormone-dependent and hormone-independent prostate cancer growth.** *Cancer Res* 2009, **69**:7165-7169.
63. Xiong J, Du Q, Liang Z: **Tumor-suppressive microRNA-22 inhibits the transcription of E-box-containing c-Myc target genes by silencing c-Myc binding protein.** *Oncogene* 2010, **29**:4980-4988.
64. Boominathan L: **The tumor suppressors p53, p63, and p73 are regulators of microRNA processing complex.** *PLoS One* 2010, **5**:e10615.
65. Frankel LB, Christoffersen NR, Jacobsen A, Lindow M, Krogh A, Lund AH: **Programmed cell death 4 (PDCD4) is an important functional target of the microRNA miR-21 in breast cancer cells.** *J Biol Chem* 2008, **283**:1026-1033.
66. Trump DL, Chadha MK, Sunga AY, Fakih MG, Ashraf U, Silliman CG, *et al*: **Vitamin D deficiency and insufficiency among patients with prostate cancer.** *BJU Int* 2009, **104**:909-914.
67. Livak KJ, Schmittgen TD: **Analysis of relative gene expression data using real-time quantitative PCR and the 2(-Delta Delta C(T)) Method.** *Methods* 2001, **25**:402-408.
68. Huang dW, Sherman BT, Lempicki RA: **Systematic and integrative analysis of large gene lists using DAVID bioinformatics resources.** *Nat Protoc* 2009, **4**:44-57.

doi:10.1186/1476-4598-10-58
Cite this article as: Wang *et al.*: Effects of 1α,25 dihydroxyvitamin D3 and testosterone on miRNA and mRNA expression in LNCaP cells. *Molecular Cancer* 2011 **10**:58.

Journal of Steroid Biochemistry & Molecular Biology xxx (2012) xxx–xxx

Contents lists available at SciVerse ScienceDirect

Journal of Steroid Biochemistry and Molecular Biology

journal homepage: www.elsevier.com/locate/jsbmb

Review

1,25-Dihydroxyvitamin D_3 modulates lipid metabolism in prostate cancer cells through miRNA mediated regulation of PPARA

Wei-Lin Winnie Wang[a,c,*], JoEllen Welsh[b,c], Martin Tenniswood[a,c]

[a] Department of Biomedical Sciences, University at Albany, State University of New York, Albany, NY 12222, United States
[b] Department of Environmental Health Sciences, University at Albany, State University of New York, Albany, NY 12222, United States
[c] Cancer Research Center, University at Albany State University of New York, 1 Discovery Drive, Rensselaer, NY 12144, United States

ARTICLE INFO

Article history:
Received 10 July 2012
Received in revised form
26 September 2012
Accepted 30 September 2012

Keywords:
Androgen
Vitamin D
miRNA
PPARA
Lipogenesis
Prostate cancer

ABSTRACT

Previous studies from our laboratory have shown that testosterone (T) and 1,25-dihydroxyvitamin D_3 ($1,25(OH)_2D_3$) co-operate to inhibit cell proliferation and induce significant changes in gene expression and differentiation in LNCaP cells. The data presented here demonstrate that the two agents alter fatty acid metabolism, and accumulation of neutral lipid. Concurrent genome wide analysis of mRNA and miRNA in LNCaP cells reveals an extensive transcription regulatory network modulated by T and $1,25(OH)_2D_3$. This involves not only androgen receptor (AR)- and vitamin D receptor (VDR)-mediated transcription, but also transcription factors E2F1- and c-Myc-dependent transcription. Changes in the activities of these transcription factors alter the steady state levels of several miRNAs, including the miR-17/92 cluster. These changes correlate with the up-regulation of the mRNA encoding peroxisome proliferator-activated receptor alpha (PPARA) and its downstream targets, leading to increased lipogenesis. These data suggest that the coordinated effect of T and $1,25(OH)_2D_3$ in prostate cancer cells increases lipogenesis, diverting energy away from Warburg-based tumor energy metabolism, which slows or halts cell growth and tumor progression.

This article is part of a Special Issue entitled 'Vitamin D Workshop'.

Contents

1. Introduction

Epidemiological evidence suggests that maintaining adequate serum 25-hydoxyvitamin D_3 (D_3) is important in preventing prostate cancer (PCa) [1], and more than 75% of men diagnosed with PCa are D_3 deficient [2]. The cancer preventive property of D_3 has been demonstrated in various solid tumors [3,4], and it is associated with a number of biological processes, including cell cycle arrest, apoptosis, differentiation and inhibition of angiogenesis [5–7]. $1,25(OH)_2D_3$ modulates transcription after binding to the vitamin D receptor (VDR) which heterodimerizes with retinoid X receptor (RXR) and engages vitamin D response elements (VDREs) to regulate the transcription of target genes [8]. While PCa is generally thought of as an androgen-dependent disease since aberrant androgen signaling is associated with malignant transformation and disease progression [9], androgens exert a biphasic response in cell culture systems, stimulating proliferation at low doses while inhibiting cell division and inducing cell differentiation at high

* Corresponding author at: Cancer Research Center, One Discovery Drive, Rensselaer, NY 12144, United States. Tel.: +1 518 591 7231; fax: +1 518 591 7201.
E-mail addresses: wwang3@albany.edu (W.-L.W. Wang), jwelsh@albany.edu (J. Welsh), mtenniswood@albany.edu (M. Tenniswood).

0960-0760/$ – see front matter © 2012 Published by Elsevier Ltd.
http://dx.doi.org/10.1016/j.jsbmb.2012.09.033

doses [10,11]. Also, the age dependent incidence of the disease (and associated mortality) increases after serum testosterone (T) levels have decreased significantly [12]. The incidence of PCa first increases between 55 and 64 years of age, when the average serum testosterone levels drop below 20 nM/L and the free testosterone has decreased by 50% [13]. Thus, at the time of diagnosis of PCa, the majority of men have declining serum T and low D_3 levels, leading to the hypothesis that the two hormones may interact to block prostate tumor initiation and/or progression. This hypothesis predicts that D_3 plays a much more prominent role in PCa tumor progression than previously realized.

Investigation of the molecular mechanisms underlying this phenomenon using genome wide expression studies in androgen receptor (AR) positive LNCaP cells, has established that a cohort of T and $1,25(OH)_2D_3$-modulated genes are critical for PCa tumor progression [7]. These genes cover a spectrum of ontologies, including cell cycle regulation, lipid localization and transport, and cholesterol metabolic processes. In particular, microRNAs (miRNAs), a class of small non-coding, single-stranded RNAs that post-transcriptionally modulate the steady state levels of mRNAs by targeting the 3′ untranslated regions (3′UTR) are differentially regulated by T and $1,25(OH)_2D_3$ and some of these miRNAs are associated with prostate cancer initiation and progression [14,15]. Changes in the miR-17/92 cluster in particular and the effect of these miRNAs on PPARA levels and energy metabolism are highlighted in this manuscript.

2. Materials and methods

2.1. Cell culture

LNCaP cells, obtained from American Type Culture Collection (Rockville, MD), were grown in RPMI-1640 medium (Invitrogen, Carlsbad, CA) (Sigma–Aldrich, St. Louis, MO) respectively, supplemented with 10% fetal bovine serum (Sigma–Aldrich), 100 U/mL penicillin and 100 μg/mL streptomycin. Cells were maintained at 37 °C in a humidified atmosphere of 95% air/5% CO_2.

2.2. Gene expression analysis

The relative mRNA and miRNA expression after treatment of 5 nM T and 100 nM $1,25(OH)_2D_3$ alone or in combination at 48 h were assessed by Nimblegen-Human-HG18 4×72 and Agilent Human miRNA v3 microarrays, respectively. Analysis was performed as described by Wang et al. [7]. The miR-17/92 cluster targeting sites of the 3′UTR of PPARA transcript was identified using TargetScan Human v6.1 tool.

2.3. Oil red O staining

LNCaP cells were seeded at 20,000 cells/well in 24 well plates (Corning, Corning, NY) for 48 h prior to treatment with 5 nM T and 100 nM $1,25(OH)_2D_3$ alone or in combination. Cells were fixed with 4% formaldehyde in PBS for 30 min at room temperature, followed by Oil Red O staining for 30 min at room temperature. Excess stain was removed via washing with tap water. Cells were imaged by Carl Zeiss Axiovert 25 CFL immediately after staining.

3. Results

Crosstalk between T- and $1,25(OH)_2D_3$-mediated signaling pathways leads to additive and/or synergistic effects on coding and non-coding RNA expression [7]. Analysis of miRNA microarray data demonstrates that 5 nM testosterone and 100 nM $1,25(OH)_2D_3$ together down-regulate the miR-17/92 cluster in LNCaP cells by 48 h while either agent alone has minimal effect on the transcript levels of these miRNAs (Table 1). While it might be expected that miRNAs in this cluster are modulated identically since they are processed from the same primary transcript transcribed from C13orf25, the differences in the relative levels probably reflect the influence of pri-miRNA structure, which affects Drosha- and Dicer-mediated processing [16].

Table 1
The effect of 5 nM T and 100 nM $1,25(OH)_2D_3$ alone or in combination on miR-17/92 cluster and PPARA transcript levels at 48 h after treatment.

	Testosterone	$1,25(OH)_2D_3$	Combo
miR-17	−1.24	−1.25	−2.34
miR-18a	−1.43	−1.16	−1.89
miR-19a	−1.24	−1.04	−1.73
miR-20a	−1.22	−1.29	−2.32
miR-19b	−1.07	−1.07	−1.64
miR-92a	−1.13	−1.14	−1.61
PPARA	1.16	1.81	2.07

Relative expression between treatments is measured by microarray analysis using Nimblegen-Human-HG18 4×72 and Agilent Human miRNA v3, essentially as described by Wang et al. [7].

TargetScan Human analysis v6.1, which predicts microRNA targets based on the complimentarity between 3′UTR and miRNA seed sequences shows that with the exception of miR-92a, each of the miRNAs in the miR-17/92 cluster targets the 3′UTR of PPARA, with a total of 9 sites identified (Fig. 1). Analysis of mRNA microarray data demonstrates an up-regulation of PPARA mRNA levels by T and $1,25(OH)_2D_3$ (Table 1), indicating that PPARA is likely a target of the miR-17/92 cluster. We have not examined the effect of individual miRNA binding sites in PPARA 3′UTR on transcript stability and translational efficiency, however, it is likely that occupation of different sites by miR-17/92 cluster impacts both miRNA-mediated RNA degradation and translational repression. This suggests that T and $1,25(OH)_2D_3$ cooperate to increase PPARA transcript stability, as well as alleviate miRNA-mediated translation repression by down-regulating the miR-17/92 cluster.

Since PPARA is known to modulate lipid metabolism, particularly fatty acid β-oxidation in hepatocytes, the effect of T and $1,25(OH)_2D_3$ on lipid content in LNCaP cells was also examined using Oil Red O staining. In LNCaP cells, it is evident that T and $1,25(OH)_2D_3$ alone induce moderate levels of lipid accumulation while the combination of the two has a greater impact on neutral lipid content in cells within 72 h (data not shown) and becomes more evident with prolonged exposure, up to 6 days (Fig. 2). Furthermore, the degree of lipogenesis in LNCaP cells after T and $1,25(OH)_2D_3$ stimulation also correlates with the ability of T and $1,25(OH)_2D_3$ to induce cell cycle arrest and inhibit cell proliferation [7]. This suggests that T and $1,25(OH)_2D_3$ modulate triglyceride synthesis in LNCaP cells, essentially directing energy metabolism to neutral lipid production and storage rather than pro-proliferation phospholipid synthesis as the cells fully differentiate.

4. Discussion

Previous miRNA microarray analysis has demonstrated that T and $1,25(OH)_2D_3$ coordinately regulate the expression of the miR-17/92 cluster in LNCaP cells and may thus contribute to the cancer preventive properties of vitamin D_3 in prostate cancer [7]. The miR-17/92 cluster, also known as oncomir-1, has been implicated in embryonic development and tumor progression. In mice, deletion of miR-17/92 cluster leads to perinatal death with various developmental defects, which is associated with the function of miR-17/92 in cell death and cell fate decision [17,18]. Aberrant expression of

Please cite this article in press as: W.-L.W. Wang, et al., 1,25-Dihydroxyvitamin D_3 modulates lipid metabolism in prostate cancer cells through miRNA mediated regulation of PPARA, J. Steroid Biochem. Mol. Biol. (2012), http://dx.doi.org/10.1016/j.jsbmb.2012.09.033

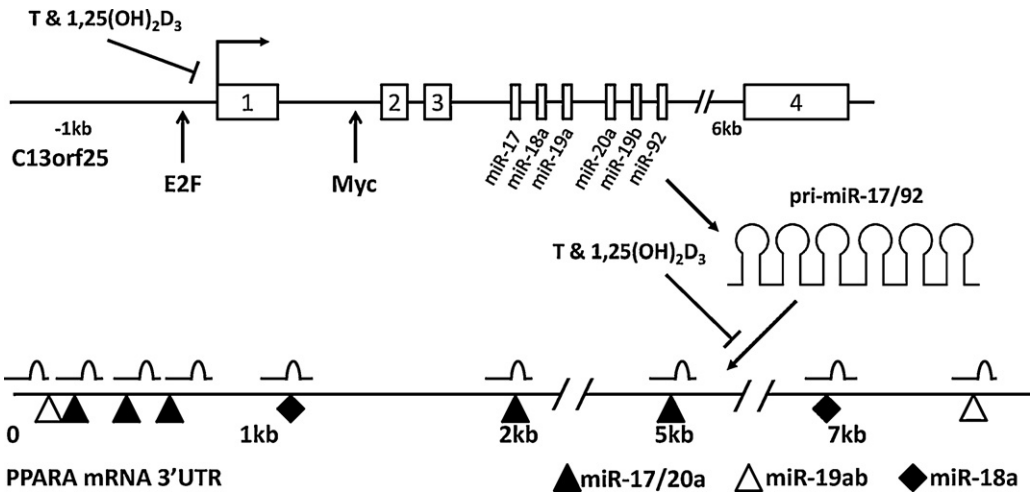

Fig. 1. Proposed model of modulation of the miR-17/92 cluster and PPARA by T and $1,25(OH)_2D_3$. T and $1,25(OH)_2D_3$ inhibits c-MYC- and E2Fs-dependent transcription of miR-17/92 cluster, alleviating negative effect of miR-17/92 on the stability and translatability of PPARA transcript. The 3′UTR of PPARA transcript and the relative positioning of miRNA predicted target sites by different members of miR-17/92 cluster using TargetScan Human v6.1 tool are indicated.

miR-17/92 cluster, including gene amplification, has been linked to malignant transformation of human cancers by promoting cell proliferation and inhibiting apoptosis through the repressive effects of individual members of the cluster on p21, Bim and PTEN [19,20]. In particular, miR-17 and 20a are up-regulated in clinical samples of prostate cancer [21] and their anti-apoptotic and oncogenic properties have been demonstrated in AR null PC-3 cells [22]. Given the importance of miR-17/92 cluster in tumor progression, the ability of T and $1,25(OH)_2D_3$ to repress this cluster may thus prevent PCa progression by enhancing the mRNA stability of p21 transcript, which is also a direct target of $1,25(OH)_2D_3$ [23]. Modulation of miRNA steady state levels by $1,25(OH)_2D_3$ has been reported previously in several systems, including human myeloid leukemia cells in which miR-32 and miR-181a influence the expression of Bim and p27Kip1; and non-malignant prostate cells RWPE-1 in which miR-106b regulates p21(waf1/Cip1) levels [24–26]. In addition to the expression of p21, T and $1,25(OH)_2D_3$ together also control energy metabolism in LNCaP cells through regulation of PPARA. Using TargetScan analysis, 9 predicted targeting sites, specific for members of the miR-17/92 cluster, are present in the 3′UTR of PPARA. Recent studies have demonstrated the validity of miRNA target prediction programs, including Pictar, TargetScan and Miranda to

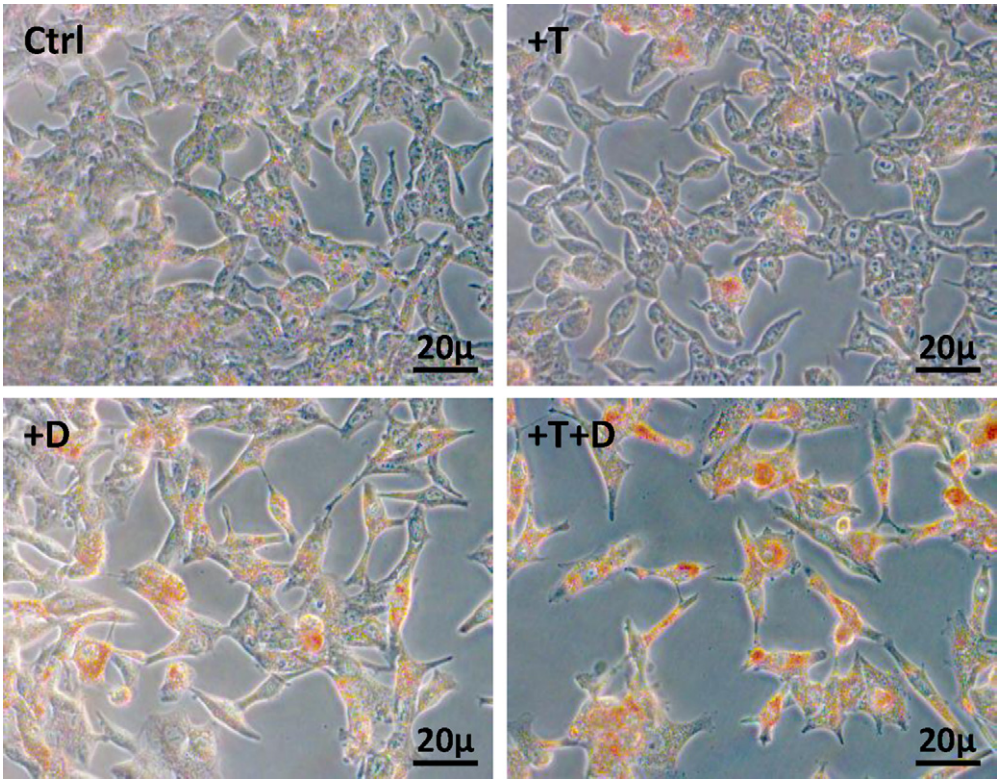

Fig. 2. The effect of T and $1,25(OH)_2D_3$ on neutral lipid accumulation in LNCaP cells. LNCaP cells were treated with 5 nM T and 100 nM $1,25(OH)_2D_3$ alone or in combination for 6 days. Neutral lipid content was assessed by Oil Red O staining, as described in Section 2.

Please cite this article in press as: W.-L.W. Wang, et al., 1,25-Dihydroxyvitamin D_3 modulates lipid metabolism in prostate cancer cells through miRNA mediated regulation of PPARA, J. Steroid Biochem. Mol. Biol. (2012), http://dx.doi.org/10.1016/j.jsbmb.2012.09.033

predict miRNA targets via a proteomic approach [27]. In addition, both expression microarray and western blot analysis confirms the up-regulation of PPARA transcript and protein levels, supporting the post-transcriptional control of PPARA mRNA by miR-17/92 cluster (Wang et al., submitted for publication). The increase in PPARA expression appears to be associated with significant accumulation of neutral lipid in LNCaP cells, implicating an anabolic function of PPARA following stimulation by T and $1,25(OH)_2D_3$. The lipogenic effects of androgen are known to be mediated by SREBP-1/2 and the downstream effectors in AR positive models of PCa [28]. In comparison, $1,25(OH)_2D_3$ has been shown to increase lipid content in T47D breast cancer cells in association with cell differentiation [6]. Though increases in lipogenesis are sometimes associated with metabolic switch, enhanced cell proliferation and cancer progression [29], the observed phenotype and the miRNA signature in LNCaP cells treated with T and $1,25(OH)_2D_3$ is indicative of a more differentiated cell fate with enhanced de novo lipogenesis.

Testosterone and $1,25(OH)_2D_3$ are known to transactivate gene expression through the activity of their cognate nuclear receptors, AR and VDR. The role of AR and VDR in modulating transcription of protein-coding genes has been studied extensively [30,31]. However, their role in the transcription regulation of miRNAs is not as well understood. AR has been shown to bind to the promoter region of miR-125b-2 upon ligand induction to drive its expression [32]. Similarly, ERβ mediates miR-30a repression through binding at proximal sites and thus inhibiting pri-miRNA transcription [33]. It has also been demonstrated that ERβ antagonizes the inhibitory effect of ERα on miRNA maturation by binding to the genomic loci of miRNA clusters [33]. ERα and GR have been found to induce or repress miR-17/92 cluster expression respectively, as well as to affect the maturation process of miRNAs through interaction with Drosha complex [34–36]. Based on these studies, we suggest that AR and VDR regulate the expression of the miR-17/92 cluster through the binding to canonical AREs and VDREs located in the C13orf25 promoter (Wang, unpublished data). In addition, both c-Myc and E2F1-3 bind to this region of the miR-17/92 cluster [22,37,38], and $1,25(OH)_2D_3$ is known to repress c-Myc and E2F1 mediated pathways in prostate cancer cells [39,40]. These data suggest that T and $1,25(OH)_2D_3$ may down-regulate c-Myc- and E2F1-3-dependent transcription of miR-17/92 cluster in LNCaP cells through their direct transcriptional effects on c-Myc- and E2F1-3 expression, or by squelching the stimulation of miR-17/92 transcription through competition with c-Myc binding site in the promoter of the C13orf25 gene.

We propose that T and $1,25(OH)_2D_3$ coordinately regulate miR-17/92 cluster expression in LNCaP cells through AR-, VDR-, c-Myc- and E2Fs-mediated mechanisms. The data suggest that down-regulation of miR-17/92 alleviates the inhibitory effect of miRNAs on transcript stability and translatability of PPARA mRNA (Fig. 1), leading to increases in PPARA protein expression, which in turn promotes neutral lipid synthesis and energy storage. This is critical for energy homeostasis since it switches metabolism from lipolysis and energy production to lipogenesis and energy storage. Elevated expression of PPARA protein, as well as other miR-17/92 targeted genes, such as Bim and p21 also works in concert to facilitate T and vitamin D_3-induced cell differentiation and growth inhibition. In this context, the cancer preventive property of vitamin D_3 in prostate cancer can be partly attributed to the effects on miR-17/92 cluster and the subsequent PPARA expression. The ability of $1,25(OH)_2D_3$ to slow disease progression is also augmented by androgen action in androgen responsive PCa. These findings offer a mechanistic explanation for the epidemiological data linking T and vitamin D_3, and suggest that maintenance of serum T and critically, vitamin D_3 levels in older men may be sufficient to render many prostate cancer cases indolent.

Acknowledgements

This work was supported by RO1 CA101114-04 to JW and MT. WLWW would like to acknowledge the DAMD for Pre-doctoral support (W81XWH-11-1-0587). The authors declare no conflict of interest.

References

[1] E. Giovannucci, Strengths and limitations of current epidemiologic studies: vitamin D as a modifier of colon and prostate cancer risk, Nutrition Reviews 2 (8 Pt) (2007) S77–S79.
[2] D.L. Trump, M.K. Chadha, A.Y. Sunga, M.G. Fakih, U. Ashraf, C.G. Silliman, B.W. Hollis, M.K. Nesline, L. Tian, W. Tan, C.S. Johnson, Vitamin D deficiency and insufficiency among patients with prostate cancer, British Journal of Urology International 7 (2009) 909–914.
[3] E. Giovannucci, Expanding roles of vitamin D, The Journal of Clinical Endocrinology & Metabolism 2 (2009) 418–420.
[4] J. Thorne, M.J. Campbell, The vitamin D receptor in cancer, Proceedings of the Nutrition Society 2 (2008) 115–127.
[5] F. Jiang, J. Bao, P. Li, S.V. Nicosia, W. Bai, Induction of ovarian cancer cell apoptosis by 1,25-dihydroxyvitamin D3 through the down-regulation of telomerase, Journal of Biological Chemistry 51 (2004) 53213–53221.
[6] G. Lazzaro, A. Agadir, W. Qing, M. Poria, R.R. Mehta, R.M. Moriarty, T.K. Das Gupta, X.K. Zhang, R.G. Mehta, Induction of differentiation by 1alpha-hydroxyvitamin D(5) in T47D human breast cancer cells and its interaction with vitamin D receptors, European Journal of Cancer 6 (2000) 780–786.
[7] W.L. Wang, N. Chatterjee, S.V. Chittur, J. Welsh, M.P. Tenniswood, Effects of 1alpha, 25 dihydroxyvitamin D3 and testosterone on miRNA and mRNA expression in LNCaP cells, Molecular Cancer (2011) 58. Q4
[8] M.R. Haussler, C.A. Haussler, P.W. Jurutka, P.D. Thompson, J.C. Hsieh, L.S. Remus, S.H. Selznick, G.K. Whitfield, The vitamin D hormone and its nuclear receptor: molecular actions and disease states, Journal of Endocrinology (1997) S57–S73. Q5
[9] K.R. Lamont, D.J. Tindall, Androgen regulation of gene expression, Advances in Cancer Research (2010) 137–162.
[10] K. Hofman, J.V. Swinnen, G. Verhoeven, W. Heyns, E2F activity is biphasically regulated by androgens in LNCaP cells, Biochemical and Biophysical Research Communications 1 (2001) 97–101.
[11] K.E. Knudsen, K.C. Arden, W.K. Cavenee, Multiple G1 regulatory elements control the androgen-dependent proliferation of prostatic carcinoma cells, Journal of Biological Chemistry 32 (1998) 20213–20222.
[12] S.F. Altekruse, C.L. Kosary, M. Krapcho, N. Neyman, R. Aminou, W. Waldron, J. Ruhl, N. Howlader, Z. Tatalovich, H. Cho, A. Mariotto, M.P. Eisner, D.R. Lewis, K. Cronin, H.S. Chen, E.J. Feuer, D.G. Stinchcomb, in: B.K. Edwards (Ed.), SEER Cancer Statistics Review, National Cancer Institute, 1975–2007, http://seer.cancer.gov/csr/1975_2007/ Q6
[13] A. Vermeulen, Declining androgens with age: an overview, in: A. Vermeulen, B.J. Oddens (Eds.), Androgens and the Aging Males, Parthenon Publishing, New York, 1996, pp. 3–14.
[14] S. Ambs, R.L. Prueitt, M. Yi, R.S. Hudson, T.M. Howe, F. Petrocca, T.A. Wallace, C.G. Liu, S. Volinia, G.A. Calin, H.G. Yfantis, R.M. Stephens, C.M. Croce, Genomic profiling of microRNA and messenger RNA reveals deregulated microRNA expression in prostate cancer, Cancer Research 15 (2008) 6162–6170.
[15] K.P. Porkka, M.J. Pfeiffer, K.K. Waltering, R.L. Vessella, T.L. Tammela, T. Visakorpi, MicroRNA expression profiling in prostate cancer, Cancer Research 13 (2007) 6130–6135.
[16] S.G. Chaulk, G.L. Thede, O.A. Kent, Z. Xu, E.M. Gesner, R.A. Veldhoen, S.K. Khanna, I.S. Goping, A.M. MacMillan, J.T. Mendell, H.S. Young, R.P. Fahlman, J.N. Glover, Role of pri-miRNA tertiary structure in miR-17–92 miRNA biogenesis, RNA Biology 6 (2011) 1105–1114.
[17] L. de Pontual, E. Yao, P. Callier, L. Faivre, V. Drouin, S. Cariou, A. Van Haeringen, D. Genevieve, A. Goldenberg, M. Oufadem, S. Manouvrier, A. Munnich, J.A. Vidigal, M. Vekemans, S. Lyonnet, A. Henrion-Caude, A. Ventura, J. Amiel, Germline deletion of the miR-17 approximately 92 cluster causes skeletal and growth defects in humans, Nature Genetics 10 (2011) 1026–1030.
[18] Y. Lu, J.M. Thomson, H.Y. Wong, S.M. Hammond, B.L. Hogan, Transgenic over-expression of the microRNA miR-17–92 cluster promotes proliferation and inhibits differentiation of lung epithelial progenitor cells, Developmental Biology 2 (2007) 442–453.
[19] I. Ivanovska, A.S. Ball, R.L. Diaz, J.F. Magnus, M. Kibukawa, J.M. Schelter, S.V. Kobayashi, L. Lim, J. Burchard, A.L. Jackson, P.S. Linsley, M.A. Cleary, MicroRNAs in the miR-106b family regulate p21/CDKN1A and promote cell cycle progression, Molecular and Cellular Biology 7 (2008) 2167–2174.
[20] C. Xiao, L. Srinivasan, D.P. Calado, H.C. Patterson, B. Zhang, J. Wang, J.M. Henderson, J.L. Kutok, K. Rajewsky, Lymphoproliferative disease and autoimmunity in mice with increased miR-17–92 expression in lymphocytes, Nature Immunology 4 (2008) 405–414.
[21] S. Volinia, G.A. Calin, C.G. Liu, S. Ambs, A. Cimmino, F. Petrocca, R. Visone, M. Iorio, C. Roldo, M. Ferracin, R.L. Prueitt, N. Yanaihara, G. Lanza, A. Scarpa, A. Vecchione, M. Negrini, C.C. Harris, C.M. Croce, A microRNA expression signature of human solid tumors defines cancer gene targets, Proceedings of the National Academy of Sciences 7 (2006) 2257–2261.

Please cite this article in press as: W.-L.W. Wang, et al., 1,25-Dihydroxyvitamin D_3 modulates lipid metabolism in prostate cancer cells through miRNA mediated regulation of PPARA, J. Steroid Biochem. Mol. Biol. (2012), http://dx.doi.org/10.1016/j.jsbmb.2012.09.033

[22] Y. Sylvestre, G.V. De, E. Querido, U.K. Mukhopadhyay, V. Bourdeau, F. Major, G. Ferbeyre, P. Chartrand, An E2F/miR-20a autoregulatory feedback loop, Journal of Biological Chemistry 4 (2007) 2135–2143.
[23] M. Liu, M.H. Lee, M. Cohen, M. Bommakanti, L.P. Freedman, Transcriptional activation of the Cdk inhibitor p21 by vitamin D3 leads to the induced differentiation of the myelomonocytic cell line U937, Genes and Development 2 (1996) 142–153.
[24] E. Gocek, X. Wang, X. Liu, C.G. Liu, G.P. Studzinski, MicroRNA-32 upregulation by 1,25-dihydroxyvitamin D3 in human myeloid leukemia cells leads to Bim targeting and inhibition of AraC-induced apoptosis, Cancer Research 19 (2011) 6230–6239.
[25] J.L. Thorne, O. Maguire, C.L. Doig, S. Battaglia, L. Fehr, L.E. Sucheston, M. Heinaniemi, L.P. O'Neill, C.J. McCabe, B.M. Turner, C. Carlberg, M.J. Campbell, Epigenetic control of a VDR-governed feed-forward loop that regulates p21(waf1/cip1) expression and function in non-malignant prostate cells, Nucleic Acids Research 6 (2011) 2045–2056.
[26] X. Wang, E. Gocek, C.G. Liu, G.P. Studzinski, MicroRNAs181 regulate the expression of p27Kip1 in human myeloid leukemia cells induced to differentiate by 1,25-dihydroxyvitamin D3, Cell Cycle 5 (2009) 736–741.
[27] H. Kanzaki, S. Ito, H. Hanafusa, Y. Jitsumori, S. Tamaru, K. Shimizu, M. Ouchida, Identification of direct targets for the miR-17–92 cluster by proteomic analysis, Proteomics 17 (2011) 3531–3539.
[28] J.V. Swinnen, W. Ulrix, W. Heyns, G. Verhoeven, Coordinate regulation of lipogenic gene expression by androgens: evidence for a cascade mechanism involving sterol regulatory element binding proteins, Proceedings of the National Academy of Sciences 24 (1997) 12975–12980.
[29] W.C. Huang, X. Li, J. Liu, J. Lin, L.W. Chung, Activation of androgen receptor, lipogenesis, and oxidative stress converged by SREBP-1 is responsible for regulating growth and progression of prostate cancer cells, Molecular Cancer Research 1 (2012) 133–142.
[30] P.S. Nelson, N. Clegg, H. Arnold, C. Ferguson, M. Bonham, J. White, L. Hood, B. Lin, The program of androgen-responsive genes in neoplastic prostate epithelium, Proceedings of the National Academy of Sciences 18 (2002) 11890–11895.
[31] T.T. Wang, L.E. Tavera-Mendoza, D. Laperriere, E. Libby, N.B. MacLeod, Y. Nagai, V. Bourdeau, A. Konstorum, B. Lallemant, R. Zhang, S. Mader, J.H. White, Large-scale in silico and microarray-based identification of direct 1,25-dihydroxyvitamin D3 target genes, Molecular Endocrinology 11 (2005) 2685–2695.
[32] X.B. Shi, L. Xue, J. Yang, A.H. Ma, J. Zhao, M. Xu, C.G. Tepper, C.P. Evans, H.J. Kung, R.W. deVere White, An androgen-regulated miRNA suppresses Bak1 expression and induces androgen-independent growth of prostate cancer cells, Proceedings of the National Academy of Sciences 50 (2007) 19983–19988.
[33] O. Paris, L. Ferraro, O.M. Grober, M. Ravo, M.R. De Filippo, G. Giurato, G. Nassa, R. Tarallo, C. Cantarella, F. Rizzo, A. Di Benedetto, M. Mottolese, V. Benes, C. Ambrosino, E. Nola, A. Weisz, Direct regulation of microRNA biogenesis and expression by estrogen receptor beta in hormone-responsive breast cancer, Oncogene (2012).
[34] L. Castellano, G. Giamas, J. Jacob, R.C. Coombes, W. Lucchesi, P. Thiruchelvam, G. Barton, L.R. Jiao, R. Wait, J. Waxman, G.J. Hannon, J. Stebbing, The estrogen receptor-alpha-induced microRNA signature regulates itself and its transcriptional response, Proceedings of the National Academy of Sciences 37 (2009) 15732–15737.
[35] L.K. Smith, R.R. Shah, J.A. Cidlowski, Glucocorticoids modulate microRNA expression and processing during lymphocyte apoptosis, Journal of Biological Chemistry 47 (2010) 36698–36708.
[36] K. Yamagata, S. Fujiyama, S. Ito, T. Ueda, T. Murata, M. Naitou, K. Takeyama, Y. Minami, B.W. O'Malley, S. Kato, Maturation of microRNA is hormonally regulated by a nuclear receptor, Molecular Cell 2 (2009) 340–347.
[37] K.A. O'Donnell, E.A. Wentzel, K.I. Zeller, C.V. Dang, J.T. Mendell, c-Myc-regulated microRNAs modulate E2F1 expression, Nature 7043 (2005) 839–843.
[38] K. Woods, J.M. Thomson, S.M. Hammond, Direct regulation of an oncogenic micro-RNA cluster by E2F transcription factors, Journal of Biological Chemistry 4 (2007) 2130–2134.
[39] M.N. Washington, J.S. Kim, N.L. Weigel, 1alpha, 25-dihydroxyvitamin D3 inhibits C4-2 prostate cancer cell growth via a retinoblastoma protein (Rb)-independent G1 arrest, Prostate 1 (2011) 98–110.
[40] S. Toropainen, S. Vaisanen, S. Heikkinen, C. Carlberg, The down-regulation of the human MYC gene by the nuclear hormone 1alpha, 25-dihydroxyvitamin D3 is associated with cycling of corepressors and histone deacetylases, Journal of Molecular Biology 3 (2010) 284–294.

Please cite this article in press as: W.-L.W. Wang, et al., 1,25-Dihydroxyvitamin D_3 modulates lipid metabolism in prostate cancer cells through miRNA mediated regulation of PPARA, J. Steroid Biochem. Mol. Biol. (2012), http://dx.doi.org/10.1016/j.jsbmb.2012.09.033

Appendix F

Copy of Book Chapter entitled "Xenograft, transgenic and knockout models of prostate cancer" in Animal models for the study of human disease.

Xenograft, Transgenic and Knockout Models of Prostate Cancer

Ann-Christin Gaupel[1]*, Wei-Lin Winnie Wang[1*], Sarah Mordan-McCombs[2],

Edmund Chun Yu Lee[3] and Martin Tenniswood[1]

[1]Department of Biomedical Sciences, School of Public Health and Cancer Research Center, University at Albany, 1 Discovery Drive, Rensselaer, NY 12144

[2]Department of Biology, Franklin College, Franklin, IN 46131

[3]Discovery Oncology, Roche Pharmaceuticals, Nutley NJ 07110

*These authors contributed equally to this chapter

Running Title: Animal models of prostate cancer

Summary:

In humans, the natural history of prostate cancer spans 30-40 years, which makes it a difficult disease to model in rodents. Furthermore the molecular pathology of prostate cancer responsible for tumor initiation and progression is complex and often redundant. The sequential changes in oncogene and tumor suppressor gene expression during prostate cancer progression have not been fully delineated. Despite these issues, there are model systems including carefully designed orthotopic xenograft models that provide robust platforms for drug evaluation and studying the effects of diet and environmental stress on prostate carcinogenesis. Comprehensive transgenic and knockout models have also been developed that recapitulate individual steps in tumor initiation and metastatic progression and highlight the importance of the tumor microenvironment. While very few of the transgenic and knockout systems recapitulate the entire natural history of prostate cancer, individual model systems provide valuable genetic insight into the biological consequences of disrupting prostate homeostasis.

Keywords:

Oncogene, Tumor Suppressor Gene, androgens, adenocarcinoma, neuroendocrine tumors, castration resistance prostate cancer, microenvironment, prostatic intraepithelial neoplasia

1. Introduction

According to the NCI-SEER database prostate cancer is the most commonly diagnosed non-cutaneous cancer and is the second leading cause of cancer-related deaths in males in North America (1). The prostate is an androgen-dependent tissue, and prostate cancer is generally thought of as an androgen-dependent disease. However it is paradoxical that the age-dependent incidence of the disease, and its associated mortality, increase after serum testosterone levels have decreased significantly. Prostate cancer is predominantly a disease of older men, and the incidence increases significantly in men over the age of 65. Thus while androgens, including testosterone and its active metabolite 5α-dihydrotestosterone (5α-DHT), are clearly important for the development and growth of early stage prostate tumors and exert their effects via androgen receptor (AR) (2), it is less clear how critical they are in the natural history of prostate cancer. Autopsy studies have shown that there is clear evidence of prostatic adenocarcinoma and an "active epithelium" (now referred to as prostatic intraepithelial neoplasia (PIN)) in many men in their early and mid-thirties, establishing that prostate adenocarcinoma is a slow growing tumor, with a very low mitotic index and a long natural history (3). The low mitotic rate accounts for the difficulty in developing a Spectral Karyotyping (SKY) analysis of tumor progression since this methodology requires metaphase spreads. It has also been established that prostate cancer is largely restricted to the peripheral zone of the prostate while benign prostatic hyperplasia (BPH) is commonly localized to the central zone, confirming that BPH is not a precursor of prostate cancer (4).

The natural history of prostate cancer is outlined in Figure 1, along with the relevant changes in the molecular pathology associated with tumor progression. As mentioned above, the progression from normal prostate to PIN to localized adenocarcinoma occurs over many years.

Progression to advanced, locally invasive prostate cancer and metastatic disease appears to be a relatively late process, but it is difficult to treat once initiated. Castration-resistant prostate cancer (CRPC) arises after initial hormonal ablation therapy fails, and there are currently no effective treatments.

As a result of comprehensive screening strategies based on the Prostate Specific Antigen (PSA) test, most prostate cancers are now diagnosed as early stage, localized disease, and 70% of men identified with prostate cancer at this stage have indolent disease that does not require therapeutic intervention. The remaining 30% of men will develop locally invasive disease and aggressive prostate cancer that metastasizes to the bones, lungs and liver. One of the pressing issues related to the treatment of prostate cancer is the need to distinguish between indolent and aggressive disease. Unlike colorectal cancer, which has well-defined molecular markers of tumor progression, an equivalent diagnostic molecular signature of prostate adenocarcinoma progression has not been developed. There are several molecular events involved in tumor progression that have been used to develop transgenic models for prostate cancer, including deletions of Nkx3.1 in early stage and PTEN (phosphatase and tensin homologue) in late stage prostate cancer (5, 6). The homeobox transcription factor Nkx3.1 is an androgen-regulated haploinsufficient tumor suppressor, which maps to chromosome 8p21.2, a region that frequently undergoes loss of heterozygosity (LOH) in prostate cancer (7). Nkx3.1 loss has been associated with tumor progression in human biopsy material (8). PTEN is a tumor suppressor gene, located on chromosome 10q23, a region frequently deleted in a variety of human cancers, including prostate, brain (glioblastomas) and breast (9-11). The protein encoded by this gene preferentially dephosphorylates phosphoinositides, particularly phosphatidylinositol-3,4,5-trisphosphate, and functions as a tumor suppressor by negatively regulating the Akt/PKB signaling pathway. PTEN

deletion/loss of expression is predominantly associated with high-grade primary or metastatic prostate cancer, although there is evidence of mutational heterogeneity at different metastatic sites in the same patient (12, 13). These results indicate that PTEN loss is an event occurring in the later stages of prostate cancer. In contrast to many other tumors, mutations in p53 and Rb (retinoblastoma protein) are late events, and most prostate cancers do not harbor mutations in these genes. Mutations in AR also appear to be late events in the progression and arise predominantly after castration or hormone ablation therapies utilizing anti-androgens such as flutamide or bicalutamide (14). Most of these mutations appear to be located in the ligand binding domain of the AR (15), and frequently alter the specificity of the receptor, resulting in promiscuous activation of the receptor by other ligands including adrenal androgens and even some anti-androgens including flutamide (15-17). Two other common events include the significant up-regulation of PCA3, a prostate-specific non-coding RNA that is overexpressed in prostate cancer (18), although the expression levels in urine do not appear to correlate to adverse pathology, Gleason score, or extraprostatic extension (19).

Gene expression profiling and immunohistochemistry have identified the consistent overexpression of hepsin, a transmembrane serine protease in PIN and prostate carcinoma (20, 21). The strongest hepsin protein expression was detected in PIN (20). However, since hepsin mRNA (22, 23) and protein (24, 25) expression increases with disease progression, it is not clear whether the protein plays a role in initiation or progression of prostate cancer or both.

Fusion between the androgen regulated TMPRSS2 gene and ERG, a member of the ETS family of transcription factors, has been identified in approximately 50-80% of patients with prostate cancer. The fusion between the two genes, both of which are localized on chromosome 21 appears to be associated with locally recurrent CRPC rather than metastatic disease (26). A

second TMPRSS2 fusion with ETV1 (located on 7p21.2) has also been identified in prostate cancer (27). The biological importance of these gene fusions has not yet been established and a large prospective cohort study has recently shown that while TMPRSS2:ERG fusion is associated with tumor stage, the presence of the gene fusion is not predictive of recurrence or mortality among men treated with radical prostatectomy (28). Thus, while the androgen regulated expression of the TMPRSS:ERG fusion protein is thought to contribute to more aggressive disease, the underlying cell and molecular biology is still unclear (29).

Fibroblast growth factors (FGF) and their receptors (FGFR) are expressed at elevated levels in prostate cancer. FGF1 was found to be highly expressed in 80% of prostate cancers and expression is correlated with Gleason score (30). FGF signaling has an impact on the epithelial and stromal compartment affecting proliferation, angiogenesis and metastasis as well as resistance to cell death (30).

2. Xenograft Models of Prostate Cancer

As with other animal models for human disease, there are advantages and disadvantages when using xenograft model systems that utilize immune-compromised athymic nude (nu/nu) or severe combined immunodeficiency (SCID) mice. Xenograft models of prostate cancer make it possible to examine the effects of therapies on human tumor cells, eliminating many of the species-specific challenges of modeling. While subcutaneous injection of tumor cells does not provide an appropriate microenvironment or vascularization for tumor growth, it is useful for the rapid assessment of therapeutic efficacy in the screening of new drugs. Orthotopic models, while surgically more challenging, provide a more “prostate specific context” and an appropriate

microenvironment and vasculature for the mechanistic analysis of drug action. The microenvironment provided by the prostatic stroma in these studies is derived from the murine prostate. In addition, since these mouse strains cannot generate mature T lymphocytes, they do not have the ability to mount or sustain an immune response. Thus, while the use of immune-compromised mice for xenograft studies facilitates the examination of the effects of novel chemo-therapies and dietary intervention on human prostate cancer cells, interactions between the tumor and stromal cells and the immune system is difficult to recapitulate in these hosts.

There is a further complication when using the athymic nude mouse model. Homozygous nude (*Foxn1*^{nu}/*Foxn1*^{nu}) mice are athymic and hairless as a result of the recessive *nu* mutation, however they also have seminiferous tubule dysgenesis, a decrease in Leydig cell number, and defective androgen synthesis (31). As a result, many male athymic nude mice often have low circulating androgen levels, and it is important to supplement these animals with exogenous testosterone to ensure androgen-dependent tumor growth (32).

There are additional caveats to consider when initiating xenograft studies. First, the human prostate cell lines typically used for xenograft studies are frequently aneuploid, which may have contributed to their ability to grow in cell culture. However, since many of the cell lines were developed 20-30 years ago and have been maintained in culture since then, it is likely that additional mutations, chromosomal rearrangements, additions and deletions have accumulated in culture since they were established. Most xenograft cell lines have copy number alterations that are reminiscent of advanced prostate cancer. Secondly, a significant number of prostate cancer cell lines have been inadvertently cross-contaminated by two commonly used androgen-independent cell lines (PC3 and DU145) (33). The provenance of cell lines used for xenograft studies needs to be carefully validated before embarking on these kinds of expensive

animal studies. Thirdly, cell lines used in xenograft studies should be tested to ensure they are free of known human and murine viruses. This is best illustrated by the recent identification of replication competent gamma retroviruses in several prostate cancer cell lines. Xenotropic murine-leukemia-virus related virus (XMRV) was first identified in the 22Rv1 cell line (34, 35), and was shown to be the result of the recombination of two murine leukemia virus genomes during passage of the CWR22 xenografts in nude mice (36). Similar viruses have since been found in the VCAP and LAPC4 cell lines as well as others (37). Testing can be done using commercial services that provide health monitoring and diagnostic screening for human and murine viruses. If specific viral pathogens are found in the cell line to be used, the xenograft studies must be performed under quarantine containment conditions to ensure that other colonies in the facility are not inadvertently infected.

a. Cell Lines Derived from LNCaP

The LNCaP cell line was developed from a needle aspiration tissue biopsy of a supraclavicular lymph node lesion in a 50-year-old Caucasian male, diagnosed with stage D_1 prostate cancer one year prior to admission (38). The patient sequentially failed hormone therapies (oral estrogen with subsequent orchiectomy) and chemotherapies (methyl CCNU and estramustine) and developed bone metastases. In comparison to other models discussed in this chapter, the patient was relatively young and presented with a rapidly progressing prostate adenocarcinoma that failed to respond to hormone ablation and other therapies. Tumor tissue obtained from needle biopsy was adapted in culture to establish the LNCaP cell line. Electron microscopic analysis reveals desmosome structures and confirms the epithelial origin of LNCaP

cells (39). Subcutaneous injection of LNCaP cells into athymic male nude mice leads to development of tumors that are fast growing, highly vascularized and poorly differentiated. Tumor take in castrated nude mice is significantly reduced, but not eliminated, and the take rate can be restored by testosterone supplementation. Some subcutaneous tumors show regional invasion with no evidence of distant metastases. Subcutaneous LNCaP tumor xenografts are androgen-responsive and the tumors can grow in androgen-independent fashion, recapitulating many of the properties of the original tumor. However, LNCaP cells do not appear to be particularly invasive *in vitro* which is somewhat surprising considering their origin.

Orthotopic injection of LNCaP cells into the dorsal prostate of athymic nude male mice leads to a tumor take rate between 55-70% (40-42). In comparison, orthotopic injection of LNCaP cells into the dorsal lobes of the prostate in SCID mice has a tumor take rate closer to 90% (42), a difference which is likely attributed to circulating androgen levels in the two host strains. Orthotopic implantation of LNCaP cells into the prostatic ventral lobe of testosterone-supplemented athymic nude mice also improves the tumor take rate and development, up to 90%, and can be increased to nearly 100% if Matrigel™ or other types of scaffold matrix are mixed with the inoculated cells (43, 44). Matrigel™ forms a semi-solid plug at body temperature, preventing the leakage of cells from the prostate capsule. This reduces one of the potential technical errors associated with orthotopic injection - leakage of the cells into the peritoneal cavity - which can lead to spurious "peritoneal metastases" (45). Matrigel™ also provides a growth factor-enriched environment for the initial growth of the tumor cells which enhances the take rate. The most important aspect of orthotopic xenografts of LNCaP cells is their ability to develop metastatic lesions, which are rare when the cells are injected subcutaneously. Between 50-60% of tumor-bearing athymic nude mice develop regional lymph node metastases as well as

lung and liver metastases; all tumor-bearing SCID mice display lymph node metastases, and 40% of the SCID mice also develop pulmonary lesions (42). This more closely recapitulates the biology of primary prostate cancer as compared to subcutaneous implantation. However, even when implanted orthotopically, these tumors do not metastasize to the bone in mice and thus do not fully mirror human disease. Higher tumor incidence and metastasis in SCID mice has been attributed to higher degrees of immuno-compromisation, due to a deficiency in both B and T lymphocytes relative to athymic nude mice (46), however SCID mice also have significantly higher serum testosterone levels which may facilitate metastatic tumor growth. Both primary and metastatic lesions formed by LNCaP cells are poorly differentiated with only occasional glandular structures, but express AR and secrete PSA. In SCID mice, castration suppresses LNCaP orthotopic tumor formation. In tumor-bearing SCID mice, PSA mRNA levels drop below 90% within one week after castration and return to normal or even higher levels within 2-3 weeks, recapitulating the PSA response seen in patients after castration or hormone ablation therapy (40, 42, 47).

LNCaP cells are aneuploid with a modal chromosome number ranging from 76 to 91. They are cytokeratin 8 and 18 positive and negative for basal cell and neuroendocrine cell markers, confirming a luminal epithelial origin. The cells express wild type p53, PSA mRNA and protein, and PCA3 (48). However, there is a T877A mutation in the ligand binding domain of AR, rendering the receptor promiscuous to progesterone, estradiol and anti-androgens, (49, 50) which may contribute to androgen-independent tumor growth. Though the tumors express the estrogen receptor, 17β-estradiol supplementation has no significant effect on tumor development in male or female nude mice (39). LNCaP cells also contain a frameshift mutation at codon 6 of one *PTEN* allele that leads to premature termination at codon 9 and, together with

the loss of the other allele, renders LNCaP cells null for PTEN expression (10, 11). Cytogenetic analysis reveals one particular genetic rearrangement, a cryptic insertion of the entire *ETV1* locus (7p21) into a prostate-specific region on the long arm of chromosome 14 (14q13.3-14q21.1). This is clinically relevant as it results in aberrant *ETV1* overexpression and has been shown to promote the development of prostatic intraepithelial neoplasia in mice (51). Based on the genetic features, including the common AR mutation, *ETV1* overexpression and *PTEN* deletion, LNCaP cells and xenografts serve as a good model system to examine late stage prostate cancer with metastatic potential into the lymph nodes and lungs.

Various sublines of LNCaP cells have been established with conventional selection strategies, including androgen deprivation, transfection, serial propagation of metastatic lesions in mice, high passage number from long-term culture, and a more novel approach via co-injection or co-culture with other cell types. With conventional methods, various lymph node-selected (LN series), prostate-selected (Pro series), continuous *in vitro* passaging (C series) and androgen-independent (AI, 104 series, abl, CL1-GFP and CS10) lines have been developed and exhibit increased tumorigenicity and metastatic potential, though as with the original LNCaP cells, they rarely metastasize to the bone (40, 52, 53).

The C4 and C5 lines were derived from LNCaP cells after subcutaneous co-inoculation with MS bone stromal cells into intact athymic nude mice. Co-inoculation resulted in tumor formation after 4 to 5 weeks (54). Subsequent castration suppressed tumor growth initially, but the growth rate was restored approximately 4 weeks post-castration. Two sublines were established four (C4) or five weeks (C5) after castration. Subcutaneous co-inoculation of the C4 cells with MS bone stromal cells into castrated hosts generated the C4-2 subline, which routinely yields bone metastases. The C4-2 subline has a similar, but not identical, cytogenetic signature as

the parental LNCaP cells. C4-2 cells show a loss of the Y chromosome and the acquisition of an additional marker chromosome, designated *ml*. Though the C4 and C5 sublines are weakly responsive to 5α-DHT-induced cell growth in culture, androgens are required for tumor formation unless co-inoculated with MS cells. In contrast, the C4-2 subline is not responsive to 5α-DHT in culture and forms subcutaneous tumors in both intact (75%) and castrated (50%) male athymic nude mice. It is also the only subline that produces tumors without co-injection of MS cells into castrated males, thus demonstrating its independence from both androgen and inductive fibroblasts for tumor formation. These tumors are highly vascularized with connective tissues interspersed between cancer cells. Molecular analysis shows positive PSA staining for all LNCaP sublines, though decreases in AR mRNA and protein levels are noted in the C4-2 subline.

C4-2 tumors are more tumorigenic when injected orthotopically rather than subcutaneously. Intraprostatic injection of C4-2 cells resulted in highly vascularized prostate tumor development with equal propensity (100%) in either intact or castrated athymic nude male mice (55). Para-aortal lymph node metastases develop in all animals orthotopically injected with C4-2 cells, and between 10-25% of mice also develop bone metastases. Cell lines developed from these lesions include the C4-2Ln (lymph node) and C4-2B (bone) series (B2: intact host; B3/B5: castrated hosts; B4: castrated orthotopic tumor) This series of cell lines provide excellent animal models for the elucidation of the cell and molecular biology of targeting of disseminated tumor cells to specific metastatic locations. Selection of the bone metastasis-derived sublines greatly enhance subcutaneous tumor incidence (90-100%) and growth rates in athymic nude mice (56). Injections into other ectopic sites of intact or castrated male athymic nude or SCID male mice also lead to tumor formation and metastasis. Intracardiac injections of C4-2 cells into

either male athymic or SCID mice produce spinal lesions in 20-30% of mice which are associated with slight elevation in PSA levels but are not always accompanied by lymph node metastasis (57). Direct bone inoculation of C4-2 cells also results in tumor formation (between 50-100%), but metastatic tumors are formed only when the cells are injected into the tail vain. These tumors, both primary and metastases, are AR positive, secret PSA and stain positive for cytokeratin 8, validating the prostatic epithelial origin (55, 57, 58). Phenotypically, the osseous lesions resemble human bone metastases, showing primarily osteoblastic reactions with some evidence of osteolytic activities; overall decreases in bone volume and bone mineral density are detected in intratibial xenografts (58). Karyotypic analysis revealed the common eight marker chromosomes shared between C4-2 and its sublines in culture; however, additional chromosomal rearrangements and the consequent production of unique marker chromosomes are also observed separately in the C4-2Ln and C4-2B lines.

Based on the propensity of the C4-2 tumors to develop PSA-secreting bone metastases, it represents an excellent preclinical model to study disease progression and metastasis. It is important to note that only orthotopic C4-2 xenografts accurately mimic the clinical progression of prostate cancer in that cancer cells first invade the surrounding lymph nodes from the primary tumors before establishing bone metastases. This linear temporal relationship is not recapitulated using other injection strategies, although the latency period can be shortened in other models. Recently, it has been shown that the latency period for bone metastasis to occur via intracardiac injection of C4-2 cells is significantly shortened through manipulation of human parathyroid hormone levels (59). This suggests that the differences between human and murine bone biology, particularly the bone turnover/remodeling rates, may have significant impact on metastatic colonization in the bones, and may affect metastatic progression. This highlights the need to take

the bone microenvironment and hormonal milieu into account when modeling this aspect of metastatic progression in prostate cancer.

b. PC346 Derived Cell Lines:

The PC346-derived cell lines have been painstakingly developed over the last 15-20 years in the Department of Urology, Erasmus Medical Center in Rotterdam, Netherlands. The original PC346 cell line was derived from a primary tumor of 68-year-old Caucasian male diagnosed with bladder cancer and stage IV prostate adenocarcinoma (Gleason score 9) without bone and lymph node metastasis (T4N0M0) (60). While the initial report stated that the patient had not undergone any treatment prior to prostatectomy, a subsequent report from the same group indicates that the patient was given cyproterone acetate for four weeks in a neoadjuvant setting prior to transurethral resection of the prostate (61). Treatment with this partial androgen antagonist may have influenced the biology of the surviving tumor cells, although the treatment time was relatively short. Small pieces of the tumor were subcutaneously implanted into male athymic nude mice and were serially propagated in intact male nude mice, generating the PC346P and PC346B xenografts (60, 62). These xenograft tumors demonstrate poorly differentiated tumor morphology lacking glandular architectures, similar to the original tumor. PC346 cells are cytokeratin 8 and 18 positive and express AR, PSA, and prostatic acid phosphatase (PAP) (48). PC346 tumors are relatively fast growing in intact male athymic mice with an average doubling-time of 10 days, reaching a size of 100 mm^3 by 1 to 2 months after transplantation. Due to the heterogeneity of the initial tumor sample, the two PC346 lines respond to androgen ablation with different sensitivity. PC346P tumors are sensitive to androgen

ablation after which tumors exhibit delayed tumor growth, and approximately 30% show evidence of regression. Similar to clinical cases, PC346P tumors eventually relapse after castration and continue to grow. In comparison, PC346B tumors are not significantly responsive to androgen ablation. However, both PC346 lines are considered androgen-responsive as tumors rarely develop in castrated male or female mice and tumors developed in these mice cannot be propagated in females or castrated males.

The PC346C cell line, which was derived *in vitro* from the PC346P tumors, also expresses PCA3, and does not express neuroendocrine markers (48). SKY analysis reveals two subclones of the PC346C cell line that can be distinguished by the absence or presence of Y chromosome with mostly hyperdiploid and near-tetraploid cells, respectively (63). A gain of chromosomes 1, 5, 7, 18 and 20, and loss of chromosome 13 are also found in the PC346C line. No mutations have been identified in the AR and TP53 genes, but an R130X mutation has been identified in PTEN, resulting in the synthesis of an inactive truncated protein without the catalytic domain (64).

To develop androgen-independent models with PC346 xenografts, two different strategies have been employed. PC346I and PC346BI were derived respectively from the parental lines, PC346P and PC346B. These tumors were initially transplanted in testosterone-supplemented female mice, followed by the removal of steroid-containing silastic implants for AI selection. In comparison, the PC346SIcas xenograft was established from PC346P tumors implanted in female mice without androgen supplementation. All resulting tumors are able to grow equally well in male and female mice and are not responsive to castration, so are classified as androgen-independent models. The AI sublines are positive for AR and PSA expression, with generally higher PSA levels compared to the parental lines, although PC346SIcas has relatively

low AR expression. PC346I has acquired a T877A mutation in the steroid-binding domain of the AR, the same mutation seen in the LNCaP cell line, and a frequent mutation identified in hormone-refractory prostate cancer. This mutation is known to widen the ligand specificity of AR and the growth of PC346I tumors can actually be stimulated by estrogens (62). All of the xenografts, except PC346B and PC346BI, have corresponding *in vitro* models which exhibit similar molecular characteristics and androgen-responsiveness.

Orthotopic xenografts of PC346C cells have been successfully established (65) widening the spectrum of PC346 lines that can be used to model prostate cancer. PC346C cells suspended in Matrigel™ greatly enhanced tumor growth rate after injection into the prostate of testosterone-supplemented athymic nude male mice and the resulting tumors reach sizes of approximately 1.0 gram at 6 weeks after injection (Lee, unpublished data). The orthotopic tumors are organ-confined, well vascularized and exhibit characteristics similar to the parental PC346 xenografts with poorly differentiated morphology and sensitivity to the anti-androgen, bicalutamide. These primary tumors display metastatic progression to the lymph nodes and epididymis but not to the bone. Furthermore, heterotypic xenografts of PC346C and PS1cells (rat prostate smooth muscle cells) at a 1:1 ratio suspended in Matrigel™ significantly increase tumor growth, providing a unique model system to investigate stromal-epithelial interactions in prostate cancer. The heterotypic xenografts remain poorly differentiated and lack well-differentiated luminal structures, contrary to other stromal-epithelial models (66).

Other *in vitro* derivatives of PC346C cells have been developed including androgen-independent (PC346DCC) and flutamide-resistant (PC346Flu1 and PC346Flu2) sublines which display common modifications to the AR identified in clinical cases (67, 68). Taken together, the PC346 model, encompassing five xenografts and six *in vitro* cell lines, presents a unique and

powerful orthotopic system that models prostate cancer from early stage, organ confined disease to late stage, androgen-independent and hormone-refractory cancers.

c. LAPC Derived Cell Lines

The LAPC-4 (Los Angeles Prostate Cancer-4) line was derived from a lymph node metastasis of a patient diagnosed with stage D prostate adenocarcinoma. The patient had been treated with androgen deprivation therapy, but showed progressive disease at the time of surgery. Biopsy tissue suspended in Matrigel™ was implanted subcutaneously into intact SCID male mice and tumor formation was observed 1 to 3 months after implantation with a doubling rate of 2-3 weeks (69). In castrated male hosts and females the tumor growth was much slower, but was stimulated by implantation of sustained-release testosterone pellets. Analogous to human prostate cancer, androgen withdrawal in LAPC-4 tumor-bearing mice results in tumor regression that is reflected by decreases in serum PSA levels. Tumor growth resumes 3 to 8 weeks after castration accompanied by over-expression of Her-2/neu and Bcl-2 (69, 70). Micro-metastases, detected by measurement of PSA mRNA expression, are detectable in bone marrow, lung and spleen and the incidence rate is higher in females and castrated hosts than intact males. This demonstrates that LAPC-4 line is androgen-responsive, but can grow in an androgen independent manner. Orthotopic implantation of LAPC-4 cells into the dorsal lobe of the prostate leads to regional lymph node metastases and lung lesions while intratibial injection of LAPC-4 cells results in osteoblastic tumor formation. LAPC-4 tumors contain a preponderance of anaplastic cells with morphology similar to the original patient tumor sample, and stain positive for PSA. Both molecular and cytogenetic characterization of LAPC-4 line reveals a heterogeneous cell

population. The luminal cell marker cytokeratins 8 and 18 are expressed in LAPC-4 cells, however, a small subpopulation of LAPC-4 cells also expresses cytokeratin 5. The majority of cytokeratin 5 positive cells are negative for AR expression, although co-expression of AR and cytokeratin 8 and 18 has not been rigorously evaluated (48). The cells express wild type AR and are positive for PSA, PCA3, PSCA (prostate stem cell antigen), PSMA (prostate-specific membrane antigen), STEAP (six-transmembrane epithelial antigen of the prostate) and KLK2 (glandular kallikrein) expression (71). In addition, LAPC-4 cells express wild type PTEN, but two mutations (P72R and R175H) have been reported in the p53 protein (33, 72). Cytogenetic analyses by different groups of both the xenografts and the corresponding *in vitro* cell line have been inconsistent and revealed either near-triploid (range 62-83) or hypotetraploid (range 79-92; MN 89) cell populations (63, 69, 73). Common structural abnormalities such as deletion of 12p12 and partial loss of the X chromosome have been reported, however the loss of Y chromosome and gain of 8p23 in the LAPC-4 xenografts are not detected *in vitro*, suggesting that there is a clonal selection of specific cell subtypes during serial propagation of the xenografts and the subsequent tissue culture adaptation of LAPC-4 tumors. The loss of chromosome 12p12 has recently been associated with metastatic prostate carcinoma and several investigators have attempted to identify possible tumor suppressors within the region that may contribute to the progression of prostate cancer (74, 75).

A bone-selected LAPC-4 line has been established by intramuscular inoculation of LAPC-4 cells in close proximity to human cancellous bone implanted in the hind limb of irradiated SCID mice (76). The resulting line, designated as LAPC-4^2 (LAPC-4 squared) is more aggressive than the parental line and forms large tumors more readily in male mice with a shorter lag period (5 weeks) compared to LAPC-4 tumors (12-13 weeks). LAPC-4^2 form tumors in

female mice, with a tumor take rate ranging from 20-75% depending on the site of inoculation and the cell line is considered to be androgen-independent (71). LAPC-4^2 cells retain the molecular signatures of the parental cell line, but also express bone sialoprotein, and the bone specific cytokines, osteocalcin and osteopontin. This may contribute to the ability of LAPC-4^2 to migrate and invade human bone implants in SCID mice after orthotopic injection.

LAPC-9 is derived from a femoral metastasis of a patient with progressive disease after hormonal therapy (77). This line expresses wild type AR, produces PSA and PSCA, but has lost PTEN expression and thus represents a late-stage, androgen-responsive model system. In comparison to LAPC-4 xenografts, subcutaneous injection of LAPC-9 cells requires longer lag period for tumor establishment in males (intact and castrated), but can still form tumors in females at lower frequency. In response to androgen deprivation, there is a significant decrease in serum PSA levels without a concomitant reduction in tumor volume. This suggests that the LAPC-9 tumors enter a dormant, androgen-responsive state that may last more than 6 months after androgen ablation. Resumption of tumor growth is accompanied by significantly elevated IGF-1 and IGF-1R mRNA levels, suggesting that dysregulation of IGF signaling and other tyrosine kinase pathways may drive aggressive, hormone-refractory disease (78). Similar to the LAPC-4 line, orthotopic LAPC-9 tumors form distal metastasis at the lung while intratibial injection leads to pure osteoblastic tumors that are positive for PSA, osteoprotegerin and BMP 2, 4 and 6 productions (79, 80). Therefore, LAPC-9 is useful for modeling prostate cancer bone metastasis with pure osteoblastic reaction while the C4-2 line is better to model prostate cancer bone lesions with mixed phenotypes.

d. LuCaP Derived Xenograft Lines

To study metastatic prostate cancer, researchers in the Department of Urology at University of Washington in Seattle have developed the LuCaP lines. LuCaP 23.1, 23.8 and 23.12 lines were established from two different lymph node metastases and from a liver lesion of a 63-year-old Caucasian male with stage D_1 prostate adenocarcinoma with a combined Gleason score of 8 (81). The patient had previously failed both radiation and androgen ablation therapies (bicalutamide and bilateral orchiectomy) before developing hormone-refractory disease, which was then treated with chemotherapy (adriamycin and carboplatinum). Serum PSA levels reached 8000 ng/mL at the time of death with several metastatic lesions in the bones, liver and retroperitoneal lymph nodes. Tumor tissues obtained at autopsy were implanted subcutaneously into athymic nude mice and serially passaged to establish the three xenograft lines. No corresponding *in vitro* lines have been established. Serum PSA levels are detectable 2 to 3 weeks after implantation and correlate with tumor volume in all three lines, even after castration. Though wild type PTEN mRNA is expressed, the protein level has not been assayed (72). Tumor histology shows pseudo-glandular organization, scattered neuroendocrine cells, dysplastic luminal cells with atypic nuclei and minimal stromal compartment, resembling Gleason grade 3 to 4 tumors. Karyotype analysis reveals a heterogeneous cell population with chromosome numbers ranging from 62 to 112 and a modal number of 78. All three lines are AR positive and respond to androgens with doubling times ranging from 2 to 3 weeks in intact males; tumor take and growth rates are significantly lower in castrated males. Androgen depletion in tumor bearing mice for all three lines results in slowed tumor growth along with decreased PSA levels which reach a nadir in 1 to 2 weeks following castration. In all three xenograft lines, many of the tumors subsequently relapse with short or intermediate latent phases. These tumors have been

designated as minimal or intermediate responders and are considered hormone-refractory. However in all three xenograft lines a significant fraction of tumors do not relapse following castration. The biology of these tumors may provide valuable insights into the molecular events that trigger relapse and androgen independence. Using a similar strategy, the progression of prostate cancer from androgen-responsive to androgen-independent disease has been investigated in the LuCaP 23.1 line. AR overexpression and elevated NSE (neuron specific enolase, a neuroendocrine marker) and Bcl-2 levels are common in recurrent tumors (82, 83). A C238Y mutation has been identified in the DNA binding region of TP53 in the LuCaP 23.1 AI line, as well as an R509Q mutation in FZD6, a member of the Wnt signaling pathway (84), suggesting that these mutations may play a role in more rapid relapse. Intratibial injection of LuCaP 23.1 cells into intact SCID male mice results in pronounced tumor growth with a high take rate of 86% (85). These tumors are PSA producing, semi-responsive to castration and exhibit an osteoblastic phenotype, which resembles clinical bone metastasis and therapeutic response of prostate cancer patients.

Orthotopic implantation of LuCaP 23.8 tumor tissues into the anterior prostate (coagulating gland) of SCID mice results in metastases to the lymph nodes and lung while removal of the primary tumors prompts metastasis to additional sites, including liver, diaphragm, testicular fat and adrenal gland (86). Though bone metastases are not observed using this method, measurable PSA levels in bone marrow samples imply possible micrometastases to the bone. Taken together, LuCaP 23 lines provide a model system to study metastatic progression of prostate cancer after castration that can be monitored via PSA evaluation.

The LuCaP 35 model was established from an inguinal lymph node metastasis of a 66-year-old Caucasian male, 3 years after diagnosis with T4 (Stage C) prostate cancer (87). The

patient had undergone surgery and various forms of androgen ablation therapy and presented with metastases in the bladder, bone and lymph nodes. Tumor take rates of LuCaP 35 via subcutaneous implantation into athymic nude mice are higher in intact than castrated males, however, tumor doubling times are equivalent. Histologically, tumors lack glandular differentiation with cells exhibiting morphology reminiscent of epithelial cells in prostate adenocarcinoma. Serum PSA levels are detectable and generally increase in concordance with tumor growth. The LuCaP 35 line expresses wild type AR and is hormone-sensitive; however, FISH analysis has revealed a high-level amplification of the AR gene and a C1863T mutation has also been reported in the AR promoter region, though the functional implication is not known (88, 89). After castration, tumors regress and PSA levels decrease, reaching a nadir by day 7 and remain low for 50 to 60 days. This change is also marked by altered subcellular localization of AR from the nucleus to the cytoplasm with few cells showing low levels of nuclear AR. Recurrent and androgen-independent tumors, preceded by elevated PSA levels, are observed approximately 100 days post-castration and have been reported to have elevated intratumoral androgen levels similar to those seen in prostate tumors from intact men (90). Karyotyping analysis reveals a deletion of distal 8p from one of the chromosome 8 homologues which represents a common genetic aberration identified in prostate cancer and other tumors. No deletions of the PTEN gene have been detected, however, no mRNA or protein is detectable in LuCaP 35 tumors (72). Unlike LuCaP 23, LuCaP 35 can be cultured *in vitro* short term, providing a useful tool for parallel analyses (72, 87). Orthotopic implantation of LuCaP 35 in SCID males resulted in metastatic lesions predominantly in lymph nodes (100%) and lung (90%). Liver, pancreas, diaphragm and peri-vertebral metastases are also observed, but only in prostatectomized SCID males (87). Direct injection of LuCaP 35 cells into the tibia of SCID

males yields PSA positive osteolytic lesions and thickening of the trabeculae within 5 weeks after injection (85).

An androgen-independent LuCaP 35V cell line has been derived via subcutaneous implantation of recurrent tumors from completely regressed post-castration LuCaP 35 xenografts, into new castrated SCID males. These tumors have been maintained in castrated SCID mice only. No substantial differences in tumor morphology or AR status have been noted between 35 and 35V lines however an R83H mutation in WNT6 of the Wnt signaling pathway may confer androgen-independent growth of LuCaP 35 (84, 87). No other prostate cancer markers or cytogenetic analysis have been reported for the LuCaP 35 lines, somewhat hindering complete interpretation of the xenografts in prostate cancer biology.

e. CWR22 Derived Cell Lines

The CWR cell lines were established by investigators in the Institute of Pathology at Case Western Reserve University, Cleveland, OH. CWR22 was established in testosterone-supplemented nude mice from primary tumor tissues of a patient diagnosed with Gleason score 9, Stage D prostate adenocarcinoma with osseous metastases (91). Additional patient information and clinical history have not been reported. Palpable CWR22 tumors develop only in intact or testosterone-supplemented athymic nude mice while only microscopic tumors are observable in castrated mice and no tumor growth has been noted in females (92, 93). Androgen withdrawal (castration and/or removal of exogenous androgen) leads to a decrease in AR levels (94) with concomitant decline in serum PSA levels, which correlates to a decrease in tumor volume. Cytogenetic analysis of the CWR22 line shows an aneuploid cell population with karyotype

49XY; loss of chromosome 2; gain of chromosomes 7, 8, and 12; and an additional isochromosome 1q, which contains a derivative chromosome 4 resulting from the translocation of 2p21 and 4q33 (95). Tumor histology shows highly proliferative tumors (marked by abundant mitotic figures) and occasional glandular structures with little stroma in intact or androgen-supplemented males (92). Sequencing analysis reveals an H874Y mutation in the ligand-binding domain of AR, which widens its ligand specificity to include adrenal androgens (dehydroepiandrosterone), hydroxyflutamide, estradiol and progesterone *in vitro* (96). However, unlike testosterone, equivalent levels of estradiol, progesterone or flutamide do not support tumor growth in castrated athymic nude mice (92), suggesting that the agonist activities seen *in vitro* may not be related to tumor growth or progression *in vivo*.

Similar to the clinical progression of prostate cancer, some CWR22 tumors relapse following castration (often as long as 2 years after castration). This relapse is preceded by elevated PSA levels and correlates with an increase in the proportion of tumor-associated neuroendocrine cells. These tumors have been passaged as the CWR22R, androgen-independent xenograft (97, 98). Initially, four independent relapsed tumor xenografts with distinctive cytogenetic signatures were developed (95). Only one line, CWR22R-2152, has a corresponding *in vitro* model (CWR22Rv1) while the CWR-R1 cell line is derived separately (99). Nonetheless, the CWR22R lines generally have restored nuclear AR expression, show little or no response to androgen in soft agar assay, form tumors in female nude mice and have a slower growth rate compared to CWR22 (94, 98). Molecular characterization of the 22Rv1 and CWR-R1 lines shows positive staining of cytokeratin 8 and 18, loss of PSA protein expression, and heterozygous mutations R273H (CWR-R1 only) and Q331R in the p53 protein (48). Despite the loss of PSA protein expression in culture, serum PSA levels are elevated when 22Rv1 cells are

re-established as tumor xenografts in nude mice (100). Sequence analysis demonstrated an in-frame tandem duplication of exon 3 in the AR gene in 22Rv1 cells and CWR22R-2152 tumors, leading to the generation of approximately 114 kDa and 75-80 kDa AR proteins that support androgen-independent proliferation (101). In comparison, CWR-R1 cells harbor an intragenic deletion in AR intron 1 and produce the AR-V7 variant, which promotes androgen-independent growth and is associated with CRPC metastases and poor prognosis (102, 103). As noted previously, the presence of replication competent XMRV in the 22Rv1 cell line limits its usefulness in animal studies.

Recently, a tissue culture line of CWR22 has been established, designated as CWR22Pc that may serve as a useful replacement for the 22Rv1 line. Similar to the parental line, CWR22Pc is an AR positive, androgen-sensitive and PSA producing cell line. Subcutaneous injection of CWR22Pc cells also yields large tumor development in testosterone-supplemented athymic nude mice, and shows similar responses to androgen ablation with tumor regrowth occurring within two months after castration (104).

Collectively, CWR22 and its sublines model prostate cancer progression from an androgen-dependent to androgen-independent state, which can be recapitulated in cell culture. However, no spontaneous metastases have been reported to date with CWR22 and its sublines when implanted subcutaneously in athymic nude mice. The parental CWR22 cells do not develop tumors when injected directly into the bone; however, 22Rv1 cells do form predominately osteosclerotic lesions with a few osteolytic lesions in immunocompromised Sprague Dawley nude rats with intratibial injection (105). This model provides a way to model the interactions between metastatic prostate cancer and the bone microenvironment. However the

C4-2 orthotopic model probably offers a more complete system for analyzing the molecular events surrounding metastatic progression.

f. The VCaP cell line

The VCaP (Vertebral Cancer of the Prostate) cell line was derived from a vertebral column metastasis of a 59-year-old Caucasian with hormone-refractory disease showing massive osseous metastasis. The patient had failed androgen ablation therapies (goserelin acetate and flutamide) and three different cytotoxic chemotherapies (9-amino-camptothecin, paclitaxel/estramustine/etoposide and cyclophosphamide/prednisone) prior to tissue extraction at autopsy (106). Xenografts were established by subcutaneous transplantation of Matrigel™-coated tumor tissues into the dorsal-lumbar region of SCID mice. The resulting tumors are sensitive to androgen-stimulated proliferation, with a rapid doubling time of 10 days, and histologically resemble undifferentiated, prostate adenocarcinoma. In castrated male and female mice, tumors adapt to grow androgen-independently with a slower doubling rate ranging from 13 to 23 days, respectively. Despite the clinical history of the patient, VCaP xenografts are responsive to the anti-androgen bicalutamide, showing decreases in tumor burden, which is enhanced by dual treatment with dutasteride, a 5α-reductase inhibitor (107). Molecular characterization shows that VCaP cells express wild type AR, PSA, PAP, PCA3 and PTEN protein (48, 108). Interestingly, recent RNA-seq analysis, followed by western blot validation, detected elevated levels of the AR-V7 variant in VCaP xenografts after castration (109). Prostate epithelial markers, cytokeratin 8 and 18, are expressed while neuroendocrine makers are not detected. VCaP cells harbor a p53 mutation (R248W) in the DNA binding domain, which

compromises its conformation and DNA-binding activity. Cytogenetic studies demonstrated the heterogeneity of the near-triploid VCaP cells with thirty structural abnormalities, including translocations, insertions/deletions, duplications and rearrangements. In addition, a significant subpopulation of VCaP cells appears to have lost the Y chromosome, though this was not reported in the comprehensive SKY analyses of prostate cancer cell lines (63, 106). An androgen-independent subline of VCaP has also been generated by subcutaneous propagation of VCaP tumors in castrated SCID males (108). The androgen-independent tumors exhibit similar molecular features as the parental line with elevated expression of PCA3, however, they are insensitive to androgen-stimulated growth despite expression of AR mRNA. Histologically, VCaP androgen-independent tumors have increased neovascularization compared to the parental line. Intratibial inoculation of VCaP cells in intact SCID males results in the development of osteolytic and osteoblastic lesions that are positive for PAP, but do not express PSA, similar to clinical metastases (110, 111). One of the most important features of the VCaP tumor is the presence of the TMPRSS2-ERG fusion gene (112), which has been shown to stimulate growth of VCaP orthotopic xenografts (113). This makes the VCaP xenograft model a useful tool to examine the effect of TMPRSS2-ERG on prostate cancer biology. Since the VCaP xenografts also express wild type TMPRSS2 and ERG genes and contain a copy number gain of 21q, they also provide a very valuable model for examining the role of the fusion protein in the upregulation of wild type ERG in the context of metastatic bone disease, even though the gain of 21q is not common in clinical cases of prostate cancer (114). The panel of prostate cancer cell lines developed by the Rotterdam group, including PC-EW, PC82, PC295 and PC310, as well as NCI-H660 may be used as alternatives to examine the function of TMPRSS2:ERG fusion product (114, 115).

g. Models of Androgen-independent Prostate Cancer

Before the derivation of various cell lines and xenografts to model prostate adenocarcinoma at different stages with varying genetic aberrations and phenotypes, prostate cancer research was restricted to the three 'classical' models: the LNCaP cell line, which was used as the androgen-dependent model system; and the PC3 and DU145 cell lines, which were used as models for androgen-independent prostate cancer. Neither PC3 nor DU145 exhibit essential characteristics of prostate adenocarcinoma, even though they both form primary tumors in mice and develop distal metastases readily and more efficiently than LNCaP xenografts (53). PC3 cells, derived from a vertebral metastatic lesion of a 62-year-old Caucasian, are highly aggressive both *in vitro* and *in vivo* and cannot be stimulated by growth factors, such as epidermal growth factor and fibroblast growth factor, a characteristic common to other prostate cancer model systems (116). PC3 cells have been reported to express cytokeratin 8 and 18, as well as cytokeratin 5 and NSE, but not chromogranin A (48). However, other studies have reported that PC3 xenografts strongly express both NSE and chromogranin A, while a weak and focal staining pattern is observed for cytokeratin 8 (117). PC3 tumors lack AR or PSA expression, but express high levels of CD44 and produce predominantly osteolytic lesions in bone metastases. The molecular characteristics and aggressive nature of the xenografts suggest that PC3 cells may be a model for small-cell neuroendocrine carcinoma of prostate (SCNCP) (85, 117-119), a rare form of prostate cancer that accounts for less than 2% of all prostate cancer cases (American Cancer Society).

DU145 cells are derived from a CNS metastasis of a 69-year-old Caucasian diagnosed with lymphocytic leukemia and advanced prostate carcinoma with widespread metastasis (120). The cells were initially reported to express cytokeratin 7, 8, 18 and 19, but were negative for the

basal markers cytokeratin 5 and 14 (121, 122). However, they have more recently been reported to express cytokeratin 5 (48). Although DU145-derived subcutaneous tumors resemble the brain metastasis of the patient, both in morphology and genotype, the tumors do not model clinical bone metastasis appropriately. Direct bone injections of DU145 cells into SCID mice have demonstrated osteolytic lesions rather than the osteoblastic phenotype commonly observed in clinical cases of prostate cancer (118).

Both PC3 and DU145 cells have been used extensively to model hormone-refractory and aggressive prostate cancer. However, the lack of AR renders them insensitive to androgen or castration; neither secretes measureable levels of PSA, and they are not reflective of the clinical characteristics of CRPC. Inconsistent molecular profiling of both PC3 and DU145 cells also suggests that long term culturing of these two lines may have selected specific cell subtypes that are not clinically relevant. In this regard, the LuCaP 49 xenograft model is a much better characterized model to study SCNCP. Given the number of better model systems outlined above these cell lines are not appropriate models for CRPC, particularly since they lack many of the hallmarks of prostate adenocarcinoma.

3. The LOBUND-Wistar Rat Model of Prostate Cancer

The LOBUND-Wistar autochthonous prostate cancer model was identified in the Laboratory of Bacteriology at the University of Notre Dame (123). Between 25-30% of male Wistar rats in the germ-free colony develop adenocarcinomas in the urogenital system by 2 years of age. The proportion of animals developing tumors can be increased to 75-80% and the time for tumor development decreased to 1 year by administration of methylnitrosourea (MNU) and

testosterone (124). This latter system has been used extensively to examine the effects of dietary manipulation on tumor initiation and progression (125-128). However, careful examination of the histological origin of these tumors in both the MNU/testosterone-stimulated model, and the spontaneous autochthonous models has established that the vast majority of the tumors originate in the seminal vesicles, not the prostate (129-131). Furthermore while dietary intervention may delay the initiation of tumor growth, once tumors are initiated they grow very rapidly, and do not model the natural history of the human disease (129). As a consequence, the LOBUND-Wistar rat is not a useful animal model of human prostate cancer.

4. Transgenic Models of Prostate Cancer

There are several major anatomical differences between the human and mouse prostate that are important when developing and analyzing murine transgenic or knockout models of prostate cancer. The anatomies of the human and rodent prostate are quite distinct. The human prostate consists of an encapsulated, dense fibromuscular stroma and a glandular epithelium containing luminal secretory, basal, and neuroendocrine cells surrounding the proximal urethra. It is organized into three anatomically distinct regions – the central, transitional and peripheral zone. Prostatic adenocarcinoma arises from the secretory epithelium located predominantly in the peripheral zone of the gland. The earliest lesions, low grade PIN (LGPIN) are characterized by an increase in both proliferative and apoptotic activity associated with a loss of basal cells in the peripheral zone. In contrast, the murine prostate is a multi-lobular structure with an anterior (coagulating gland), dorsal, lateral and ventral lobes enclosed by a thin fibromuscular sheath. In the mouse the urethra does not pass through the gland, and in consequence there is no zonal demarcation related to the proximity to the urethra. The secretory epithelium of the mouse is

associated with a significantly less dense stroma which consists predominantly of basal epithelial cells, smooth muscle cells and loose connective tissue. These anatomical differences complicate the modeling of invasion and metastatic progression in the mouse (132). In addition, the mouse is not inherently prone to prostate cancer. Murine models utilize the similarity of the dorsolateral prostate in mouse to the human prostate peripheral zone since the dorsolateral prostate is the origin of hyperproliferation in the mouse (133). Ideally murine models should recapitulate the natural history of the human disease outlined in Figure 1, including metastatic spread to distant sites including bone, brain, lung and liver. This should occur through the manipulation of clinically relevant genes, in a compressed time frame compatible with the shorter lifespan of the mouse. Several strategies have been used to accomplish these goals, including the manipulation of signaling pathways through viral oncogenes and deletion or overexpression of endogenous genes.

a. Probasin -SV40 T Antigen Based Transgenic Models

The earliest transgenic models of prostate cancer were developed through the long standing collaborative efforts between the Baylor College of Medicine, University of Manitoba and Vanderbilt University. These models utilize the rat probasin promoter to drive the prostate specific expression of SV-40 viral large T and small T antigens. Archival tissues samples from the TRAMP (Transgenic adenocarcinoma of the mouse prostate) mouse are available through Roswell Park Cancer Institute, Buffalo, NY.

Probasin was originally identified as an androgen-dependent secretory product restricted to the rat dorsolateral prostate (134, 135). Transcription of the probasin gene is regulated by two

androgen response elements in the proximal promoter of the gene, one located between -236 bp and -223 bp and the other between -140 bp and -117 bp upstream of the transcription start site (136), that direct co-operative binding of the androgen receptor for activity (137). A minimal rat probasin promoter construct, rPB, consisting of –426 to +28 of the probasin promoter is sufficient to drive the prostate-specific transgene expression (138, 139). However the expression of the transgene is not restricted to the dorsolateral prostate, but is also seen in the ventral lobe. There is no detectable expression in other tissues including the anterior prostate and seminal vesicles. In the TRAMP model, the SV40 large T and small t antigen are expressed as male mice begin testicular androgen synthesis at puberty between 2 and 7 weeks of age. Large T antigen (Tag) binds to, and disrupts the function of, p53 and Rb (140, 141), resulting in cell cycle dysregulation, spontaneous genomic instability and decreased apoptosis. Small t antigen inactivates protein phosphatase 2A (PP2A) and leads to constitutive mitogen activated kinase (MAPK) signaling (142). Expression of these two viral proteins disrupts the development processes in the mouse prostate, initiating prostate tumor formation. TRAMP mice develop LGPIN as early as 4-6 weeks and progress through high grade PIN (HGPIN) (6-10 weeks) to well-differentiated adenocarcinoma (10-16 weeks) in the dorsolateral prostate, but not in the ventral or anterior prostate (138, 143). The primary tumors are heterogeneous and multifocal; the tumors metastasize predominantly to peri-aortic lymph nodes and lungs, and occasionally to the kidney and adrenal gland, starting as early as 18 weeks, (143-145). Castration of the TRAMP mouse at 12 weeks results in initial tumor regression, but 80% of mice develop androgen-independent disease, that is associated with poorly differentiated primary tumors and a higher incidence of lymph node metastasis compared to intact controls animals. Moreover, examination of the AR sequence shows that recurrent tumors acquire somatic mutations in the transactivation

domain, and the AR variants have increased activities in the absence of ligand, and in response to androgen and estradiol (146). These aspects of the TRAMP mouse accurately reflects human disease progression (147). However, advanced and poorly differentiated tumors display a distinct neuroendocrine phenotype (145), and the neuroendocrine marker synaptophysin is expressed in all of the primary tumors and 67% of metastases in castrated animals.

A second issue with this transgenic model system, common to most of the prostate transgenic overexpression systems, relates to the expression of the transgene after castration. Since the transgene expression is driven by an androgen-dependent promoter, the pathobiology of post-castration tumor regression, particularly as it relates to cell cycle and apoptosis, may be related to loss of transgene expression as opposed to loss of cellular androgen signaling, making interpretation of androgen ablation studies difficult. Castration of TRAMP mice at 12 weeks of age (at which point these animals exhibit PIN or adenocarcinoma) does not result in the immediate loss of SV40 T antigen expression or cessation of tumor growth, indicating that in this model, after tumorigenesis is initiated, progression does not depend on androgens but is sustained by high levels of oncogenic large T and small t antigens (147).

The studies described above utilized C57BL/6 mice. The F1 generation of these mice crossed onto the FVB background shows increased vascularization, and has a shorter survival span (less than 33 weeks, compared to C57BL/6-TRAMP which survive 52 weeks) and the pattern of metastasis also shows strain dependent differences, with at least one C57BL/6xFVB mouse demonstrating spinal metastasis which models human disease progression (143, 144). This illustrates the effect of different strain backgrounds may have on prostate cancer initiation and metastatic progression.

The minimal probasin promoter does not always achieve consistently high transgene expression. To improve transgene expression, a transgenic mouse expressing only large T antigen under the control of a large probasin promoter (-11.5 kb/+28 bp) was developed (LPB-Tag/LADY). The large probasin promoter (LPB) drives zinc and androgen-regulated expression of the chloramphenicol acetyltransferase (CAT) to the dorsolateral and ventral lobes in transgenic mice with highest level of expression at puberty (approximately 7 weeks of age) (148). LPB-Tag mice develop dorsolateral prostatic hyperplasia by 10 weeks of age and progress through the histological stages similar to human prostate cancer including LGPIN and HGPIN. Multifocal tumors with reactive stroma form between 12 to 20 weeks of age, and display androgen-dependent growth (149). However, while these mice show local invasion only one of seven LPB-Tag mice lines (12T-10) develops metastatic prostate cancer by 6 months of age (149, 150). Primary tumors and metastases which develop in the lymph nodes, liver and lung by 6 months of age display neuroendocrine characteristics (150).

While there are a number of advantages to the LADY and TRAMP models of prostate cancer, including the reproducible, highly penetrant progression to adenocarcinoma, they have several important drawbacks. First, the rapid progression in these models does not adequately recapitulate the relatively slow progression normally seen in human prostate cancer. Large primary tumors often require that mice be euthanized (due to quality-of-life concerns) before metastatic progression can be evaluated. This does not preclude studies using compound mutants. For example, to determine if the vitamin D axis has an inhibitory effect on prostate cancer progression, LPB-Tag mice have been crossed with vitamin D receptor knockout mice (VDRKO) or their WT littermates respectively. VDRWT;LPB-Tag and VDRKO;LPB-Tag mice developed prostate tumors in the dorsolateral lobe at 7 weeks of age, more rapidly than seen in

the LBP-Tag parental strain, a difference that probably reflects strain-specificity of tumor development. However, using a mouse modified Gleason score as a measure of progression, it is clear that tumor progression in VDRKO;LPB-Tag mice is more rapid than VDRWT;LPB-Tag, suggesting that the vitamin D axis plays a role in tumor progression (151). However, due to the very rapid growth of the primary tumors, the effect of the VDRKO knock out on metastatic progression cannot be evaluated (151). Serum testosterone is also very low in a significant proportion of the compound mutant mice resulting in variable transgene expression. Synthetic replacement of testosterone increases tumor growth, abrogating the effects of vitamin D on Gleason score. Whether this relates to direct effects of testosterone on the vitamin D axis or on the expression of the SV40 transgene remains to be definitively elucidated.

Both of these probasin-based transgenic models develop neuroendocrine tumors rather than adenocarcinomas. Extensive neuroendocrine differentiation is seen in less than 10% of human prostate cancers and is associated with tumor progression and poor prognosis (152-156). Thus, neither the TRAMP nor the LPB-Tag models of prostate cancer accurately recapitulate the natural history of prostatic adenocarcinoma in the early stages, but may be valuable models for the rarer neuroendocrine carcinoma of the prostate.

b. PSP94-SV40 T Antigen Based Transgenic Models

To circumvent the issues related to the TRAMP mouse, an alternative mouse model using large T antigen to drive tumorigenesis was developed at the University of Western Ontario, London ON, using the PSP94 promoter. PSP94 is an androgen-responsive glycoprotein, also known as β-microseminoprotein or β-inhibin (157) that is expressed very specifically in the

lateral or dorsolateral lobes of the mouse prostate (158, 159), and is significantly less sensitive to androgen ablation than probasin (160). A fragment of the PSP94 promoter (-3.84 kb to +16 bp) was used to drive the expression of the SV40 large T antigen in the dorsolateral prostate of transgenic animals (161). This transgenic strain (TGMAP) displays many of the characteristics of prostate cancer progression: the mice develop prostatic hyperplasia at 10 weeks of age, PIN between 12-16 weeks of age, and well differentiated and moderately differentiated carcinoma between 16-19 weeks. Metastasis to the peri-nephric lymph nodes was also seen in a significant number of the mice by 20 weeks of age. While castration at 12 weeks of age led to involution and atrophic changes in the tumor, the development of castration resistant disease was not evaluated. At first glance this model appears to be an attractive alternative to the probasin driven SV40 transgenic mouse. However, the usefulness of the model is significantly reduced by the high copy number (100-500 copies) of the transgenes in the TGMAP founder lines, which leads to very significant genomic and phenotype variability and potential for some extra-prostatic expression of the transgene. In addition there is a high degree of neuroendocrine differentiation in the TGMAP tumors (162, 163).

To eliminate the founder line copy number variability, the SV40 large T antigen was knocked into the PSP94 locus (163). These mice, known as KIMAP, express a single copy of the transgene. They reproducibly develop PIN after puberty (8 weeks of age) and well-differentiated slowly progressing multi-focal, heterogeneous prostate cancer starting at 10-12 weeks of age. These tumors express common androgen-dependent markers including hepsin and PSP94 (162). By 52 weeks of age, all mice develop adenocarcinomas. Neuroendocrine differentiation of the KIMAP tumors is a rare event and occurs only in a few late stage carcinomas. By 70 weeks of age, in addition to metastasis to the pelvic lymph nodes, distant spread to liver and lung can be

detected in significant proportion of KIMAP mice (163). The tumors also show marked regression eight weeks after castration, at which time most of the animals display near-normal prostate glands (163), however the animals were not analyzed for tumor relapse and progression to castration-resistant disease.

The KIMAP transgenic model appears to be the most appropriate, currently available transgenic model of prostate cancer. However there is a final caveat regarding all three of these transgenic models of prostate cancer: each of the models initiates tumor progression through the disruption of p53 and/or Rb function, however loss of function of either p53 or Rb is usually a late stage event in human prostate cancer progression. Thus, while the KIMAP model in particular recapitulates the histological natural history of prostate cancer, the molecular mechanisms underlying the histological alterations may not fully reflect the molecular processes involved in the progression of the human disease. The differences in the pathobiology of the different transgenic models - particularly the difference in neuroendocrine differentiation - may be determined by the relative levels of T-antigen expression, however there are likely to be other effects of the long term disruption of p53 and Rb activity that are not immediately obvious. These may complicate interpretation of dietary intervention studies or the evaluation of new chemotherapeutics.

In addition to artificial manipulation of p53 and Rb a number of transgenic technologies have been used to overexpress genes implicated in prostate tumor initiation and progression.

c. Androgen Receptor

Dysregulation of the ligand-binding activation of the AR appears to play a role in the development and progression of prostate cancer, and AR mutations, predominantly in the ligand binding domain have been implicated in the development of CRPC after androgen ablation. To investigate the role of the AR, a transgenic mouse model in which the wild type murine AR is driven by the minimal probasin promoter (PB-mAR) was developed (164). These transgenic mice develop focal HGPIN at one year of age, but do not subsequently develop adenocarcinoma (164). This suggests that activation of the wild type AR plays a role in the development of PIN, but indicates that other molecular events are necessary for advanced progression. In transgenic mice with targeted knockout of the AR in the prostatic epithelium (pes-ARKO; ARR_2PB-Cre:AR^{flox}), there is an increased rate of epithelial proliferation and decreased differentiation. This is accompanied by a decrease in the expression of probasin, PSP94 and Nkx3.1, demonstrating that the wild type AR suppresses proliferation in the mature epithelium and modulates the expression of at least one tumor suppressor (Nkx3.1) that has been implicated in the progression from PIN to adenocarcinoma. Crossing pes-ARKO mice to transgenic mice overexpressing the T857A AR mutation essentially blocks these effects (165). Knockout of the androgen receptor in ARR_2PB-Cre:AR^{flox};TRAMP mice results in apoptosis of luminal epithelial cells and proliferation of basal epithelial cells, leading to more aggressive tumors with higher metastatic potential, specifically to the liver (166). The pes-ARKO system provides a valuable tool for investigating the significance of decreased serum testosterone in older men, and the importance of ligand-activated AR signaling in the initiation and progression of prostate cancer. Crossing these strains to mice with different mutations in the ligand binding domain of the AR will also shed light on the importance of AR mutations in the development of metastatic disease and CRPC.

d. Myc

Increased myc gene copy number has been associated with prostate cancer initiation and progression (167, 168) and mouse models overexpressing c-myc have been developed. To mimic low and high myc expression respectively, myc was placed downstream of the minimal probasin (Lo-Myc) or ARR_2PB (Hi-Myc) promoters (169). Both Hi-Myc and Lo-Myc mice develop PIN and locally invasive adenocarcinoma with high penetrance. While the histology of the tumors appears to be independent of Myc dosage, the rate of progression is dosage-dependent. Castration after development of PIN leads to complete regression of PIN; castration after tumors have developed results in quiescent residual tumors persisting for at least 5 months. It is not clear whether these tumors eventually relapse to hormone-refractory prostate cancer. Critically, these tumors do not express the neuroendocrine differentiation marker, synaptophysin, and this is one of the few single gene overexpression systems models that progresses to adenocarcinoma. In addition the tumors lose Nkx3.1 expression as they transition from PIN to invasive cancer (169). The importance of the interaction of Myc and Nkx3.1 in the progression of prostate cancer has been explored by crossing ARR_2PB-Cre:Z-myc mice with $Nkx3.1^{flox/flox}$ mice (170). In this model, the Cre recombinase is not only responsible for the knockout of Nkx3.1 but also activates latent Z-myc, whose constitutive expression is controlled by the CMV enhancer/actin promoter. Focal, prostate-specific c-myc expression in ARR_2PB-Cre:Z-myc mice results in low grade PIN by two years of age without evidence of further progression, while ARR_2PB-Cre:$Nkx3.1^{flox/flox}$ mice show prostatic dysplasia (170, 171). Simultaneous loss of Nkx3.1 expression coupled with Myc overexpression leads to HGPIN that shows evidence of micro-invasive cancer (170). c-myc expression also cooperates with Pten loss to drive tumorigenesis in ARR_2PB-Cre:Z-

myc:Pten$^{flox/+}$ mice. These mice develop HGPIN and cancerous lesions while single mutant mice do not (172).

e. TMPRSS2 Fusion Proteins

To identify the role of the TMPRSS2-ERG fusion gene in prostate cancer, a transgenic model overexpressing TMPRSS2-ERG under the control of the ARR_2PB promoter was developed; however these mice do not show carcinogenic lesions indicating that TMPRSS2-ERG is not sufficient to initiate tumorigenesis (173).

4. Knockout Models of Prostate Cancer

In a concerted effort to recapitulate the natural history of prostate cancer several groups have knocked out a number of the endogenous genes implicated in human prostatic adenocarcinoma highlighted in Figure 1 using the Cre-loxP system. Prostate-specific expression of the Cre recombinase has been achieved using several prostate specific promoters including the prostate-specific antigen (PSA) promoter, the Nkx3.1 promoter and variants of the probasin promoter, including the small compact probasin promoter, ARR_2PB, which contains the two AR-binding sites ARBS-1 (-236 to -223) and ARBS-2 (-140 to -117) and responds to androgens and glucocorticoids (174).

a. Knockout of Nkx3.1

PSA-Cre:Nkx3.1$^{flox/+}$ and PSA-Cre:Nkx3.1$^{flox/flox}$ mice develop lesions resembling human PIN with low penetrance (<10%) at 15-35 or 21-25 weeks, respectively (175). In Nkx3.1 knockout mice these PIN lesions show evidence of increased oxidative damage, suggesting that antioxidant gene expression is dysregulated (176). Nkx3.1 loss recapitulates the early stages of prostate tumorigenesis, however there is a long latency period and the PIN lesions do not progress to adenocarcinoma (177, 178). This model may mimic early stages of prostate cancer development; however it is clear that Nkx3.1 loss alone is not sufficient to drive formation of adenocarcinoma.

b. PTEN Conditional Knockouts

While the whole-body homozygous PTEN knockout is embryonic lethal, heterozygotes are susceptible to tumorigenesis in various organs, including the prostate (179-181). In mice 6-22 weeks of age, these lesions do not progress further than prostatic intraepithelial neoplasia (179, 181). When TRAMP mice are crossed with PTEN$^{+/-}$ mice, tumor progression is accelerated with a corresponding decrease in median survival time (182). Prostate specific Pten deletion using the ARR$_2$PB composite probasin promoter, results in formation of PIN with progression to invasive adenocarcinoma and metastatic lesions in the lungs, starting at 9 and 12 weeks, respectively. Latency of PIN formation is shorter in homozygous ARR$_2$PB-Cre:PTEN$^{flox/flox}$ mice compared to heterozygous ARR$_2$PB-Cre:PTEN$^{flox/+}$ animals (8-10 months compared to 1.5 months) (183). After castration at 16 weeks, PTEN$^{-/-}$ and PTEN$^{-/+}$ prostate tumors show increased apoptosis and tumor regression; however 2-3 months after castration, the prostate glands of Pten knockout mice remain significantly larger than WT mice (183), indicating that there is either incomplete

regression or androgen-independent growth. When the PSA promoter is used to drive the Cre-recombinase, PSA-Cre:PTEN$^{flox/flox}$ homozygous mice develop PIN at 4 to 5 months and progress to invasive prostate carcinoma at 10 to 14 months with occasional lymph node metastases (184). This suggests that the choice of promoter may significantly influence the natural history of the disease driven. Nevertheless both of these homozygous Pten knockout models recapitulate the progression of prostate cancer from PIN to well-differentiated carcinoma and lymph node metastases, and may also model some aspects of the biology of CRPC. They represent the first clinically relevant mouse model of prostate cancer in which deletion of one endogenous gene initiates the disease and promotes progression to lymphatic and lung metastases.

Nkx3.1$^{+/-}$;PTEN$^{+/-}$ compound mutant mice develop lesions resembling HGPIN that progresses to invasive adenocarcinoma with lymph node metastases by 52 weeks (171, 185). These tumors also progress to androgen-independent disease after androgen ablation (185). Critically, Nkx3.1 was recently found to be expressed in a rare population of luminal epithelial stem cells after castration (castration-resistant Nkx3.1-expressing cells (CARNs)), which may represent prostate tumor initiating cells (TICs). Using a tamoxifen-inducible Cre recombinase under the control of the Nkx3.1 promoter to generate Nkx3.1 heterozygous Pten nullizygous (Nkx3.1$^{CreERT2/+}$:Pten$^{flox/flox}$) CARNS, it has been shown that mice develop carcinomas with evidence of micro-invasion after androgen supplementation (186). This is a very interesting strategy and the double knockout model appears to be an excellent mouse model to study the activation of TICs in the prostate

c. Conditional Knockout of p53 and/or Rb

While mutations in p53 and Rb are rare, prostate specific conditional knockouts for each gene have been created using the composite probasin promoter (ARR_2PB) to drive the expression of the Cre recombinase (187). Individual deletion of p53 or Rb leads to PIN-like lesions after 600 days of age, indicating that mutation of either gene alone is not sufficient for progression to carcinoma. However, mice with inactivation of both Rb and p53 develop rapidly progressing, androgen-independent tumors with neuroendocrine differentiation, which produce metastases to the regional lymph nodes, liver, lungs and adrenal glands, reminiscent of the TRAMP transgenic model (187).

d. Knockout of Wnt Signaling

Disruption of Wnt signaling has been implicated in prostate cancer progression, and loss of heterozygosity at the Apc (adenomatous polyposis coli) locus as well as promoter hypermethylation have been identified in human prostate cancers (188-190). ARR_2PB-Cre:$Apc^{flox/flox}$ mice have been generated to investigate the role of Wnt signaling in prostate cancer. Prostate specific knockout of Apc results in elevated β-catenin levels and progression from very early hyperplasia at 4-5 weeks of age to adenocarcinoma by 7 months, without any evidence of subsequent metastases even after 15 months. Castration of mice with large advanced tumors results in only partial regression of tumors two months after castration, indicating the potential for androgen-independent growth (191). These data demonstrate the potential importance of Wnt signaling in tumor progression and, given the clinical relevance of this model,

this appears to be a good model for studying the role of other components of the Wnt pathway in prostate cancer progression.

These examples highlight the fact that, with the exception of PTEN and possibly Apc, a single gene knockout is not sufficient to drive prostate tumorigenesis. On the other hand double and triple knockouts may be able to fully recapitulate the natural history of prostate cancer tumor progression in the future. Single conditional knockout mouse models will continue to provide insight into the molecular events that can give rise to hyperplasia and PIN.

6. Transgenic Models of the Tumor Micro-environment

All of the transgenic and knockout models described above focus on the epithelial component of prostate cancer. However, interactions between epithelial cells and the tumor micro-environment are also critical for tumorigenesis. Tumor-associated reactive stroma is characterized by phenotype-switching to myofibroblasts, matrix remodeling, elevated angiogenesis and tumor associated macrophage (TAM) infiltration, all of which promote prostate cancer progression (192). This is accompanied by remodeling of the extracellular matrix, accompanying changes in glycoprotein and proteoglycan synthesis, reduced expression of desmin and smooth muscle α-actin, and alterations in extracellular matrix protease expression (192, 193). Molecular pathology studies have also indicated a strong association between prostatic inflammation and prostate cancer. Prostatic inflammation, characterized by infiltration of lymphocytes, macrophages and neutrophils, leads to proliferative inflammatory atrophy (PIA), which is thought to stimulate PIN as a result of genetic instability and proliferation of luminal epithelial cells (194).

There are also major changes in the synthesis and secretion of numerous cytokines, including TGFβ-1, FGF-2, and changes in cell surface receptors ERBB2, TGFβRII, and endothelin receptors (192, 195, 196).

a. Models of Prostatic Inflammation

The POET (probasin ovalbumin expressing transgene) mouse has provided the first opportunity to evaluate the importance of inflammation in the initiation of prostate cancer. The ARR_2PB promoter drives the expression of mouse ovalbumin (mOVA), resulting in increased expression of mOVA in the ventral and dorsolateral lobes of the prostate starting 4-6 weeks of age (197). Subsequent adoptive transfer of mOVA-specific $CD8^+$ T cells (OT-I) induces acute prostatitis (197), leading to an increase in epithelial proliferation (day 7-80) after induction of inflammation (198). Since this effect lasts well after OT-I cells lose their functional ability (16 days post transfer (197)), this suggests that inflammation induces changes in the epithelium are not reversed after the loss of stimulus. POET-3/Luc/ARR_2PB-Cre:$Pten^{+/flox}$ mice develop hyperplastic acini 30 days after OT-I cell transfer and slowly develop PIN, but do not progress to prostate cancer (198). Because of the clinical relevance and slow progression of PIN, this mouse model has great potential to study the role of inflammation in early tumorigenesis. The induction of $\alpha_v\beta_6$ integrin in the POET mouse model suggests that there may be a relationship between prostatic inflammation and adenocarcinoma that can be explored mechanistically in this model (199).

b. Overexpression of Cytokines

Overexpression of TGFβ has been implicated as a key regulator of reactive stroma in human prostate cancer (200, 201). To delineate the role of TGFβ in prostate tumor initiation and progression, a transgenic mouse expressing HA-tagged TGFβ1 driven by the ARR_2PB promoter was developed (202). At one year of age, the basal lamina of the prostate shows focal discontinuity and irregularities in the epithelial acini walls, inflammation primarily associated with neurovascular bundles and local ganglia, and regional stromal fibroplasia that is characterized by collagen deposition (202). However, even extended overexpression of TGFβ1 does not result in progression to carcinoma.

In addition to TGFβ, other cytokines have been associated with reactive stroma, including IL-8, which has also been shown to be overexpressed in reactive stroma (203). Overexpression of the mouse IL-8 paralog keratinocyte-derived chemokine (KC) in the prostate of transgenic mice (ARR_2PB-Intron-KC-V5) produces ventral prostatic hyperplasia associated with an increased epithelial/stromal proliferation index ratio (204). These transgenic animals do not appear to develop prostate cancer.

c. Serine Proteases and Inhibitors

Prostate specific overexpression of hepsin in transgenic mice does not result in increased proliferation, PIN or cancerous lesions; however the structure of the basement membrane is disrupted by one year of age (205). Crossing ARR_2PB-hepsin mice with LPB-Tag mice (line 12T-7f, which develop PIN-like lesions and foci of prostate cancer, but show no evidence of

metastases), results in approximately 50% of the double transgenic mice developing metastases to the liver and lung by 21 weeks of age (205). Remarkably, nearly 40% of the animals developing metastases to the liver or lung also develop bone metastases. However, like the LBP-Tag parental line, the double transgenic mice display neuroendocrine differentiation (205), which may limit the general applicability of the findings. Nevertheless, the ARR_2PB-hepsin;LPB-Tag double transgenic model provides valuable insights into the mechanisms underlying metastatic invasion and the role of hepsin in this process.

Maspin, a serine protease inhibitor (serpin) has been associated with prostate cancer. The tumor suppressor has been implicated in inhibition of invasion, motility, tumor growth and angiogenesis (206, 207). Mapsin heterozygous ($Mp^{+/-}$) mice develop prostatic stromal hyperplasia, a consequence of smooth muscle cell and epithelial hyperproliferation. The composition of the extracellular matrix associated with the hypoproliferative foci is altered resulting in the loss of epithelial polarity, although mapsin haploinsufficiency does not lead to adenocarcinoma within the first year (208). This highlights an important role for mapsin in tumor initiation, but also suggests that additional genetic events are required for tumor progression. It is important to note that manipulation of the prostate microenvironment is not sufficient to drive tumorigenesis. Combination of these models with clinically relevant models of prostate cancer, including those of prostate-specific Pten deletion should clarify the role of the microenvironment in tumorigenesis and progression.

d. Growth Factors

An ingenious transgenic model system using mice carrying the ARR_2PB-KBPA-iFGFR1 (JOCK-1) transgene has been developed to study the effect of enhanced growth factor signaling on prostate tumor progression. Activation of FGFR-mediated signaling is achieved in the model by replacing the extracellular ligand-binding domain of the receptor with a cytoplasmic localized drug-binding domain. This Chemical Inducer of Dimerization (CID) methodology makes use of a lipid-permeable dimeric drug (AP20187) that induces FGFR dimerization and activation (209). These mice develop LGPIN three months after induction, and HGPIN within six months (209). Prolonged activation of FGFR1 signaling (42 weeks) leads to epithelial-mesenchymal transition and formation of adenocarcinoma with no evidence of neuroendocrine differentiation. This model system recapitulates many of the stages of the natural history of prostate cancer. However at later time points transitional sarcomatoid-carcinoma and sarcoma also develop, and distant metastases are only detected in mice with sarcomas, possibly limiting the utility of the model for mechanistic studies focused on metastatic progression (210). This model has been used to identify "points of no return" in the natural history of the disease. Abrogation of FGFR1 signaling (by removal of AP20187) at four weeks, before extensive neovascularization has occurred, results in reversion of hyperplasia. However, once vascularization has occurred hyperplasia is not reversible (209). Increases in vascular volume are detectable as early as one week after activation of FGFR1 signaling, however FGFR1 signaling is not required for vessel maintenance even though further progression requires continual FGFR1 signaling (211). After the development of adenocarcinoma, abrogation of FGFR1 signaling does not lead to regression but may slow progression in continuously treated mice (210).

The CID technology makes this a versatile model to determine at which stages of tumor initiation and progression the FGFR transgene is necessary. It has the added advantage that the

activation or inactivation of the transgene can be repeated several times during the progression of the disease, something that is not possible in other transgenic models. Furthermore, the technology can be adapted to examine the role of other dimeric receptor proteins in prostate tumor progression.

References Cited

1. Altekruse SF, Huang L, Cucinelli JE, et al. Spatial patterns of localized-stage prostate cancer incidence among white and black men in the southeastern United States, 1999-2001. *Cancer Epidemiol Biomarkers Prev* 2010; **19**: 1460-7.

2. Vis AN, Schroder FH. Key targets of hormonal treatment of prostate cancer. Part 1: the androgen receptor and steroidogenic pathways. *BJU Int* 2009; **104**: 438-48.

3. McNeal JE. Regional morphology and pathology of the prostate. *Am J Clin Pathol* 1968; **49**: 347-57.

4. McNeal JE. The zonal anatomy of the prostate. *Prostate* 1981; **2**: 35-49.

5. Garnis C, Buys TP, Lam WL. Genetic alteration and gene expression modulation during cancer progression. *Mol Cancer* 2004; **3**: 9.

6. Saramaki O, Visakorpi T. Chromosomal aberrations in prostate cancer. *Front Biosci* 2007; **12**: 3287-301.

7. He WW, Sciavolino PJ, Wing J, et al. A novel human prostate-specific, androgen-regulated homeobox gene (NKX3.1) that maps to 8p21, a region frequently deleted in prostate cancer. *Genomics* 1997; **43**: 69-77.

8. Bowen C, Bubendorf L, Voeller HJ, et al. Loss of NKX3.1 expression in human prostate cancers correlates with tumor progression. *Cancer Res* 2000; **60**: 6111-5.

9. Li DM, Sun H. TEP1, encoded by a candidate tumor suppressor locus, is a novel protein tyrosine phosphatase regulated by transforming growth factor beta. *Cancer Res* 1997; **57**: 2124-9.

10. Steck PA, Pershouse MA, Jasser SA, et al. Identification of a candidate tumour suppressor gene, MMAC1, at chromosome 10q23.3 that is mutated in multiple advanced cancers. *Nat Genet* 1997; **15**: 356-62.

11. Li J, Yen C, Liaw D, et al. PTEN, a putative protein tyrosine phosphatase gene mutated in human brain, breast, and prostate cancer. *Science* 1997; **275**: 1943-7.

12. McMenamin ME, Soung P, Perera S, et al. Loss of PTEN expression in paraffin-embedded primary prostate cancer correlates with high Gleason score and advanced stage. *Cancer Res* 1999; **59**: 4291-6.

13. Suzuki H, Freije D, Nusskern DR, et al. Interfocal heterogeneity of PTEN/MMAC1 gene alterations in multiple metastatic prostate cancer tissues. *Cancer Res* 1998; **58**: 204-9.

14. Niraula S, Chi K, Joshua AM. Beyond castration-defining future directions in the hormonal treatment of prostate cancer. *Horm Cancer* 2012; **3**: 3-13.

15. Gottlieb B, Beitel LK, Nadarajah A, et al. The androgen receptor gene mutations database: 2012 update. *Hum Mutat* 2012; **33**: 887-94.

16. Gaddipati JP, McLeod DG, Heidenberg HB, et al. Frequent detection of codon 877 mutation in the androgen receptor gene in advanced prostate cancers. *Cancer Res* 1994; **54**: 2861-4.

17. Taplin ME, Bubley GJ, Ko YJ, et al. Selection for androgen receptor mutations in prostate cancers treated with androgen antagonist. *Cancer Res* 1999; **59**: 2511-5.

18. Bussemakers MJ, van Bokhoven A, Verhaegh GW, et al. DD3: a new prostate-specific gene, highly overexpressed in prostate cancer. *Cancer Res* 1999; **59**: 5975-9.

19. Liss MA, Santos R, Osann K, et al. PCA3 molecular urine assay for prostate cancer: association with pathologic features and impact of collection protocols. *World J Urol* 2011; **29**: 683-8.

20. Dhanasekaran SM, Barrette TR, Ghosh D, et al. Delineation of prognostic biomarkers in prostate cancer. *Nature* 2001; **412**: 822-6.

21. Rhodes DR, Barrette TR, Rubin M, et al. Meta-analysis of microarrays: interstudy validation of gene expression profiles reveals pathway dysregulation in prostate cancer. *Cancer Res* 2002; **62**: 4427-33.

22. Chen Z, Fan Z, McNeal JE, et al. Hepsin and maspin are inversely expressed in laser capture microdissectioned prostate cancer. *J Urol* 2003; **169**: 1316-9.

23. Stephan C, Yousef GM, Scorilas A, et al. Hepsin is highly over expressed in and a new candidate for a prognostic indicator in prostate cancer. *J Urol* 2004; **171**: 187-91.

24. Pace G, Pomante R, Vicentini C. Hepsin in the diagnosis of prostate cancer. *Minerva Urol Nefrol* 2012; **64**: 143-8.

25. Goel MM, Agrawal D, Natu SM, et al. Hepsin immunohistochemical expression in prostate cancer in relation to Gleason's grade and serum prostate specific antigen. *Indian J Pathol Microbiol* 2011; **54**: 476-81.

26. Scheble VJ, Scharf G, Braun M, et al. ERG rearrangement in local recurrences compared to distant metastases of castration-resistant prostate cancer. *Virchows Arch* 2012.

27. Tomlins S, Rhodes DR, Perner S, et al. Recurrent fusion of TMPRSS2 and ETS transcription factor genes in prostate cancer. *Science* 2005; **310**: 644-8.

28. Pettersson A, Graff RE, Bauer SR, et al. The TMPRSS2:ERG Rearrangement, ERG Expression, and Prostate Cancer Outcomes: a Cohort Study and Meta-analysis. *Cancer Epidemiol Biomarkers Prev* 2012.

29. Salagierski M, Schalken JA. Molecular diagnosis of prostate cancer: PCA3 and TMPRSS2:ERG gene fusion. *J Urol* 2012; **187**: 795-801.

30. Kwabi-Addo B, Ozen M, Ittmann M. The role of fibroblast growth factors and their receptors in prostate cancer. *Endocr Relat Cancer* 2004; **11**: 709-24.

31. Rebar RW, Morandini IC, Petze JE, et al. Hormonal basis of reproductive defects in athymic mice: reduced gonadotropins and testosterone in males. *Biol Reprod* 1982; **27**: 1267-76.

32. Claus S, Aumuller G, Tunn S, et al. Influence of hormone application by subcutaneous injections or steroid-containing silastic implants on human benign hyperplastic prostate tissue transplanted into male nude mice. *Prostate* 1993; **22**: 199-215.

33. van Bokhoven A, Varella-Garcia M, Korch C, et al. Widely used prostate carcinoma cell lines share common origins. *Prostate* 2001; **47**: 36-51.

34. Kang DE, Lee MC, Das GJ, et al. XMRV Discovery and Prostate Cancer-Related Research. *Adv Virol* 2011; **2011**: 432837.

35. Paprotka T, Delviks-Frankenberry KA, Cingoz O, et al. Recombinant origin of the retrovirus XMRV. *Science* 2011; **333**: 97-101.

36. Das GJ, Luk KC, Tang N, et al. Absence of XMRV and closely related viruses in primary prostate cancer tissues used to derive the XMRV-infected cell line 22Rv1. *PLoS One* 2012; **7**: e36072.

37. Sfanos KS, Aloia AL, Hicks JL, et al. Identification of replication competent murine gammaretroviruses in commonly used prostate cancer cell lines. *PLoS One* 2011; **6**: e20874.

38. Horoszewicz JS, Leong SS, Chu TM, et al. The LNCaP cell line--a new model for studies on human prostatic carcinoma. *Prog Clin Biol Res* 1980; **37**: 115-32.

39. Horoszewicz JS, Leong SS, Kawinski E, et al. LNCaP model of human prostatic carcinoma. *Cancer Res* 1983; **43**: 1809-18.

40. Pettaway CA, Pathak S, Greene G, et al. Selection of highly metastatic variants of different human prostatic carcinomas using orthotopic implantation in nude mice. *Clin Cancer Res* 1996; **2**: 1627-36.

41. Rembrink K, Romijn JC, van der Kwast TH, et al. Orthotopic implantation of human prostate cancer cell lines: a clinically relevant animal model for metastatic prostate cancer. *Prostate* 1997; **31**: 168-74.

42. Sato N, Gleave ME, Bruchovsky N, et al. A metastatic and androgen-sensitive human prostate cancer model using intraprostatic inoculation of LNCaP cells in SCID mice. *Cancer Res* 1997; **57**: 1584-9.

43. Cui L, Chen P, Tan Z, et al. Hemostatic gelatin sponge is a superior matrix to matrigel for establishment of LNCaP human prostate cancer in nude mice. *Prostate* 2012.

44. Pretlow TG, Delmoro CM, Dilley GG, et al. Transplantation of human prostatic carcinoma into nude mice in Matrigel. *Cancer Res* 1991; **51**: 3814-7.

45. Wang X, An Z, Geller J, et al. High-malignancy orthotopic nude mouse model of human prostate cancer LNCaP. *Prostate* 1999; **39**: 182-6.

46. Williams SS, Alosco TR, Croy BA, et al. The study of human neoplastic disease in severe combined immunodeficient mice. *Lab Anim Sci* 1993; **43**: 139-46.

47. Sato N, Gleave ME, Bruchovsky N, et al. Intermittent androgen suppression delays progression to androgen-independent regulation of prostate-specific antigen gene in the LNCaP prostate tumour model. *J Steroid Biochem Mol Biol* 1996; **58**: 139-46.

48. van Bokhoven A, Varella-Garcia M, Korch C, et al. Molecular characterization of human prostate carcinoma cell lines. *Prostate* 2003; **57**: 205-25.

49. Veldscholte J, Ris-Stalpers C, Kuiper GG, et al. A mutation in the ligand binding domain of the androgen receptor of human LNCaP cells affects steroid binding characteristics and response to anti-androgens. *Biochem Biophys Res Commun* 1990; **173**: 534-40.

50. Veldscholte J, Voorhorst-Ogink MM, Bolt-de Vries J, et al. Unusual specificity of the androgen receptor in the human prostate tumor cell line LNCaP: high affinity for progestagenic and estrogenic steroids. *Biochim Biophys Acta* 1990; **1052**: 187-94.

51. Tomlins SA, Laxman B, Dhanasekaran SM, et al. Distinct classes of chromosomal rearrangements create oncogenic ETS gene fusions in prostate cancer. *Nature* 2007; **448**: 595-9.

52. Ishikura N, Kawata H, Nishimoto A, et al. Establishment and characterization of an androgen receptor-dependent, androgen-independent human prostate cancer cell line, LNCaP-CS10. *Prostate* 2010; **70**: 457-66.

53. Sobel RE, Sadar MD. Cell lines used in prostate cancer research: a compendium of old and new lines--part 1. *J Urol* 2005; **173**: 342-59.

54. Wu HC, Hsieh JT, Gleave ME, et al. Derivation of androgen-independent human LNCaP prostatic cancer cell sublines: role of bone stromal cells. *Int J Cancer* 1994; **57**: 406-12.

55. Thalmann GN, Anezinis PE, Chang SM, et al. Androgen-independent cancer progression and bone metastasis in the LNCaP model of human prostate cancer. *Cancer Res* 1994; **54**: 2577-81.

56. Thalmann GN, Sikes RA, Wu TT, et al. LNCaP progression model of human prostate cancer: androgen-independence and osseous metastasis. *Prostate* 2000; **44**: 91-103.

57. Wu TT, Sikes RA, Cui Q, et al. Establishing human prostate cancer cell xenografts in bone: induction of osteoblastic reaction by prostate-specific antigen-producing tumors in athymic and SCID/bg mice using LNCaP and lineage-derived metastatic sublines. *Int J Cancer* 1998; **77**: 887-94.

58. Pfitzenmaier J, Quinn JE, Odman AM, et al. Characterization of C4-2 prostate cancer bone metastases and their response to castration. *J Bone Miner Res* 2003; **18**: 1882-8.

59. Gomes RR, Jr., Buttke P, Paul EM, et al. Osteosclerotic prostate cancer metastasis to murine bone are enhanced with increased bone formation. *Clin Exp Metastasis* 2009; **26**: 641-51.

60. van Weerden WM, de Ridder CM, Verdaasdonk CL, et al. Development of seven new human prostate tumor xenograft models and their histopathological characterization. *Am J Pathol* 1996; **149**: 1055-62.

61. Marques RB, van Weerden WM, Erkens-Schulze S, et al. The human PC346 xenograft and cell line panel: a model system for prostate cancer progression. *Eur Urol* 2006; **49**: 245-57.

62. van Weerden WM, Romijn JC. Use of nude mouse xenograft models in prostate cancer research. *Prostate* 2000; **43**: 263-71.

63. van Bokhoven A, Caires A, Maria MD, et al. Spectral karyotype (SKY) analysis of human prostate carcinoma cell lines. *Prostate* 2003; **57**: 226-44.

64. Vlietstra RJ, van Alewijk DC, Hermans KG, et al. Frequent inactivation of PTEN in prostate cancer cell lines and xenografts. *Cancer Res* 1998; **58**: 2720-3.

65. Kraaij R, van Weerden WM, de Ridder CM, et al. Validation of transrectal ultrasonographic volumetry for orthotopic prostate tumours in mice. *Lab Anim* 2002; **36**: 165-72.

66. Hayward SW, Haughney PC, Lopes ES, et al. The rat prostatic epithelial cell line NRP-152 can differentiate in vivo in response to its stromal environment. *Prostate* 1999; **39**: 205-12.

67. Marques RB, Erkens-Schulze S, de Ridder CM, et al. Androgen receptor modifications in prostate cancer cells upon long-termandrogen ablation and antiandrogen treatment. *Int J Cancer* 2005; **117**: 221-9.

68. Marques RB, Dits NF, Erkens-Schulze S, et al. Modulation of androgen receptor signaling in hormonal therapy-resistant prostate cancer cell lines. *PLoS One* 2011; **6**: e23144.

69. Klein KA, Reiter RE, Redula J, et al. Progression of metastatic human prostate cancer to androgen independence in immunodeficient SCID mice. *Nat Med* 1997; **3**: 402-8.

70. Craft N, Shostak Y, Carey M, et al. A mechanism for hormone-independent prostate cancer through modulation of androgen receptor signaling by the HER-2/neu tyrosine kinase. *Nat Med* 1999; **5**: 280-5.

71. Davies MR, Lee YP, Lee C, et al. Use of a SCID mouse model to select for a more aggressive strain of prostate cancer. *Anticancer Res* 2003; **23**: 2245-52.

72. Whang YE, Wu X, Suzuki H, et al. Inactivation of the tumor suppressor PTEN/MMAC1 in advanced human prostate cancer through loss of expression. *Proc Natl Acad Sci U S A* 1998; **95**: 5246-50.

73. Laitinen S, Karhu R, Sawyers CL, et al. Chromosomal aberrations in prostate cancer xenografts detected by comparative genomic hybridization. *Genes Chromosomes Cancer* 2002; **35**: 66-73.

74. Kibel AS, Faith DA, Bova GS, et al. Loss of heterozygosity at 12P12-13 in primary and metastatic prostate adenocarcinoma. *J Urol* 2000; **164**: 192-6.

75. Kibel AS, Huagen J, Guo C, et al. Expression mapping at 12p12-13 in advanced prostate carcinoma. *Int J Cancer* 2004; **109**: 668-72.

76. Tsingotjidou AS, Zotalis G, Jackson KR, et al. Development of an animal model for prostate cancer cell metastasis to adult human bone. *Anticancer Res* 2001; **21**: 971-8.

77. Craft N, Chhor C, Tran C, et al. Evidence for clonal outgrowth of androgen-independent prostate cancer cells from androgen-dependent tumors through a two-step process. *Cancer Res* 1999; **59**: 5030-6.

78. Nickerson T, Chang F, Lorimer D, et al. In vivo progression of LAPC-9 and LNCaP prostate cancer models to androgen independence is associated with increased expression of insulin-like growth factor I (IGF-I) and IGF-I receptor (IGF-IR). *Cancer Res* 2001; **61**: 6276-80.

79. Lee Y, Schwarz E, Davies M, et al. Differences in the cytokine profiles associated with prostate cancer cell induced osteoblastic and osteolytic lesions in bone. *J Orthop Res* 2003; **21**: 62-72.

80. Saffran DC, Raitano AB, Hubert RS, et al. Anti-PSCA mAbs inhibit tumor growth and metastasis formation and prolong the survival of mice bearing human prostate cancer xenografts. *Proc Natl Acad Sci U S A* 2001; **98**: 2658-63.

81. Ellis WJ, Vessella RL, Buhler KR, et al. Characterization of a novel androgen-sensitive, prostate-specific antigen-producing prostatic carcinoma xenograft: LuCaP 23. *Clin Cancer Res* 1996; **2**: 1039-48.

82. Liu AY, Corey E, Bladou F, et al. Prostatic cell lineage markers: emergence of BCL2+ cells of human prostate cancer xenograft LuCaP 23 following castration. *Int J Cancer* 1996; **65**: 85-9.

83. Rocchi P, Muracciole X, Fina F, et al. Molecular analysis integrating different pathways associated with androgen-independent progression in LuCaP 23.1 xenograft. *Oncogene* 2004; **23**: 9111-9.

84. Kumar A, White TA, MacKenzie AP, et al. Exome sequencing identifies a spectrum of mutation frequencies in advanced and lethal prostate cancers. *Proc Natl Acad Sci U S A* 2011; **108**: 17087-92.

85. Corey E, Quinn JE, Bladou F, et al. Establishment and characterization of osseous prostate cancer models: intra-tibial injection of human prostate cancer cells. *Prostate* 2002; **52**: 20-33.

86. Corey E, Quinn JE, Vessella RL. A novel method of generating prostate cancer metastases from orthotopic implants. *Prostate* 2003; **56**: 110-4.

87. Corey E, Quinn JE, Buhler KR, et al. LuCaP 35: a new model of prostate cancer progression to androgen independence. *Prostate* 2003; **55**: 239-46.

88. Linja MJ, Savinainen KJ, Saramaki OR, et al. Amplification and overexpression of androgen receptor gene in hormone-refractory prostate cancer. *Cancer Res* 2001; **61**: 3550-5.

89. Waltering KK, Wallen MJ, Tammela TL, et al. Mutation screening of the androgen receptor promoter and untranslated regions in prostate cancer. *Prostate* 2006; **66**: 1585-91.

90. Montgomery B, Nelson PS, Vessella R, et al. Estradiol suppresses tissue androgens and prostate cancer growth in castration resistant prostate cancer. *BMC Cancer* 2010; **10**: 244.

91. Pretlow TG, Wolman SR, Micale MA, et al. Xenografts of primary human prostatic carcinoma. *J Natl Cancer Inst* 1993; **85**: 394-8.

92. Shao TC, Li H, Eid W, et al. In vivo preservation of steroid specificity in CWR22 xenografts having a mutated androgen receptor. *Prostate* 2003; **57**: 1-7.

93. Wainstein MA, He F, Robinson D, et al. CWR22: androgen-dependent xenograft model derived from a primary human prostatic carcinoma. *Cancer Res* 1994; **54**: 6049-52.

94. Gregory CW, Hamil KG, Kim D, et al. Androgen receptor expression in androgen-independent prostate cancer is associated with increased expression of androgen-regulated genes. *Cancer Res* 1998; **58**: 5718-24.

95. Kochera M, Depinet TW, Pretlow TP, et al. Molecular cytogenetic studies of a serially transplanted primary prostatic carcinoma xenograft (CWR22) and four relapsed tumors. *Prostate* 1999; **41**: 7-11.

96. Tan J, Sharief Y, Hamil KG, et al. Dehydroepiandrosterone activates mutant androgen receptors expressed in the androgen-dependent human prostate cancer xenograft CWR22 and LNCaP cells. *Mol Endocrinol* 1997; **11**: 450-9.

97. Huss WJ, Gregory CW, Smith GJ. Neuroendocrine cell differentiation in the CWR22 human prostate cancer xenograft: association with tumor cell proliferation prior to recurrence. *Prostate* 2004; **60**: 91-7.

98. Nagabhushan M, Miller CM, Pretlow TP, et al. CWR22: the first human prostate cancer xenograft with strongly androgen-dependent and relapsed strains both in vivo and in soft agar. *Cancer Res* 1996; **56**: 3042-6.

99. Gregory CW, Johnson RT, Jr., Mohler JL, et al. Androgen receptor stabilization in recurrent prostate cancer is associated with hypersensitivity to low androgen. *Cancer Res* 2001; **61**: 2892-8.

100. Sramkoski RM, Pretlow TG, Giaconia JM, et al. A new human prostate carcinoma cell line, 22Rv1. *In Vitro Cell Dev Biol Anim* 1999; **35**: 403-9.

101. Tepper CG, Boucher DL, Ryan PE, et al. Characterization of a novel androgen receptor mutation in a relapsed CWR22 prostate cancer xenograft and cell line. *Cancer Res* 2002; **62**: 6606-14.

102. Hu R, Dunn TA, Wei S, et al. Ligand-independent androgen receptor variants derived from splicing of cryptic exons signify hormone-refractory prostate cancer. *Cancer Res* 2009; **69**: 16-22.

103. Li Y, Hwang TH, Oseth LA, et al. AR intragenic deletions linked to androgen receptor splice variant expression and activity in models of prostate cancer progression. *Oncogene* 2012; doi: 10.1038/onc.2011.637.

104. Dagvadorj A, Tan SH, Liao Z, et al. Androgen-regulated and highly tumorigenic human prostate cancer cell line established from a transplantable primary CWR22 tumor. *Clin Cancer Res* 2008; **14**: 6062-72.

105. Andersen C, Bagi CM, Adams SW. Intra-tibial injection of human prostate cancer cell line CWR22 elicits osteoblastic response in immunodeficient rats. *J Musculoskelet Neuronal Interact* 2003; **3**: 148-55.

106. Korenchuk S, Lehr JE, MClean L, et al. VCaP, a cell-based model system of human prostate cancer. *In Vivo* 2001; **15**: 163-8.

107. Ateeq B, Vellaichamy A, Tomlins SA, et al. Role of dutasteride in pre-clinical ETS fusion-positive prostate cancer models. *Prostate* 2012.

108. Loberg RD, St John LN, Day LL, et al. Development of the VCaP androgen-independent model of prostate cancer. *Urol Oncol* 2006; **24**: 161-8.

109. Watson PA, Chen YF, Balbas MD, et al. Constitutively active androgen receptor splice variants expressed in castration-resistant prostate cancer require full-length androgen receptor. *Proc Natl Acad Sci U S A* 2010; **107**: 16759-65.

110. Kirschenbaum A, Liu XH, Yao S, et al. Prostatic acid phosphatase is expressed in human prostate cancer bone metastases and promotes osteoblast differentiation. *Ann N Y Acad Sci* 2011; **1237**: 64-70.

111. Li X, Loberg R, Liao J, et al. A destructive cascade mediated by CCL2 facilitates prostate cancer growth in bone. *Cancer Res* 2009; **69**: 1685-92.

112. Demichelis F, Fall K, Perner S, et al. TMPRSS2:ERG gene fusion associated with lethal prostate cancer in a watchful waiting cohort. *Oncogene* 2007; **26**: 4596-9.

113. Wang J, Cai Y, Yu W, et al. Pleiotropic biological activities of alternatively spliced TMPRSS2/ERG fusion gene transcripts. *Cancer Res* 2008; **68**: 8516-24.

114. Mertz KD, Setlur SR, Dhanasekaran SM, et al. Molecular characterization of TMPRSS2-ERG gene fusion in the NCI-H660 prostate cancer cell line: a new perspective for an old model. *Neoplasia* 2007; **9**: 200-6.

115. Hermans KG, van Marion R, van Dekken H, et al. TMPRSS2:ERG fusion by translocation or interstitial deletion is highly relevant in androgen-dependent prostate cancer, but is bypassed in late-stage androgen receptor-negative prostate cancer. *Cancer Res* 2006; **66**: 10658-63.

116. Kaighn ME, Narayan KS, Ohnuki Y, et al. Establishment and characterization of a human prostatic carcinoma cell line (PC-3). *Invest Urol* 1979; **17**: 16-23.

117. Tai S, Sun Y, Squires JM, et al. PC3 is a cell line characteristic of prostatic small cell carcinoma. *Prostate* 2011; **71**: 1668-79.

118. Nemeth JA, Harb JF, Barroso U, Jr., et al. Severe combined immunodeficient-hu model of human prostate cancer metastasis to human bone. *Cancer Res* 1999; **59**: 1987-93.

119. Papandreou CN, Daliani DD, Thall PF, et al. Results of a phase II study with doxorubicin, etoposide, and cisplatin in patients with fully characterized small-cell carcinoma of the prostate. *J Clin Oncol* 2002; **20**: 3072-80.

120. Stone KR, Mickey DD, Wunderli H, et al. Isolation of a human prostate carcinoma cell line (DU 145). *Int J Cancer* 1978; **21**: 274-81.

121. Billstrom A, Lecander I, Dagnaes-Hansen F, et al. Differential expression of uPA in an aggressive (DU 145) and a nonaggressive (1013L) human prostate cancer xenograft. *Prostate* 1995; **26**: 94-104.

122. Sherwood ER, Berg LA, Mitchell NJ, et al. Differential cytokeratin expression in normal, hyperplastic and malignant epithelial cells from human prostate. *J Urol* 1990; **143**: 167-71.

123. Pollard M, Luckert PH. Transplantable metastasizing prostate adenocarcinomas in rats. *J Natl Cancer Inst* 1975; **54**: 643-9.

124. Pollard M, Luckert PH. Autochthonous prostate adenocarcinomas in Lobund-Wistar rats: a model system. *Prostate* 1987; **11**: 219-27.

125. Oades GM, Dredge K, Kirby RS, et al. Vitamin D receptor-dependent antitumour effects of 1,25-dihydroxyvitamin D3 and two synthetic analogues in three in vivo models of prostate cancer. *BJU Int* 2002; **90**: 607-16.

126. Pollard M, Wolter W. Prevention of spontaneous prostate-related cancer in Lobund-Wistar rats by a soy protein isolate/isoflavone diet. *Prostate* 2000; **45**: 101-5.

127. Schleicher RL, Lamartiniere CA, Zheng M, et al. The inhibitory effect of genistein on the growth and metastasis of a transplantable rat accessory sex gland carcinoma. *Cancer Lett* 1999; **136**: 195-201.

128. Wilson MJ, Lindgren BR, Sinha AA. The effect of dietary supplementation with limonene or myo-inositol on the induction of neoplasia and matrix metalloproteinase and plasminogen activator activities in accessory sex organs of male Lobund-Wistar rats. *Exp Mol Pathol* 2008; **85**: 83-9.

129. O'Sullivan J, Sheridan J, Mulcahy H, et al. The effect of green tea on oxidative damage and tumour formation in Lobund-Wistar rats. *Eur J Cancer Prev* 2008; **17**: 489-501.

130. Slayter MV, Anzano MA, Kadomatsu K, et al. Histogenesis of induced prostate and seminal vesicle carcinoma in Lobund-Wistar rats: a system for histological scoring and grading. *Cancer Res* 1994; **54**: 1440-5.

131. Tamano S, Rehm S, Waalkes MP, et al. High incidence and histogenesis of seminal vesicle adenocarcinoma and lower incidence of prostate carcinomas in the Lobund-Wistar prostate cancer rat model using N-nitrosomethylurea and testosterone. *Vet Pathol* 1996; **33**: 557-67.

132. Roy-Burman P, Wu H, Powell WC, et al. Genetically defined mouse models that mimic natural aspects of human prostate cancer development. *Endocr Relat Cancer* 2004; **11**: 225-54.

133. Xue L, Yang K, Newmark H, et al. Induced hyperproliferation in epithelial cells of mouse prostate by a Western-style diet. *Carcinogenesis* 1997; **18**: 995-9.

134. Wilson EM, French FS. Biochemical homology between rat dorsal prostate and coagulating gland. Purification of a major androgen-induced protein. *J Biol Chem* 1980; **255**: 10946-53.

135. Matuo Y, Adams PS, Nishi N, et al. The androgen-dependent rat prostate protein, probasin, is a heparin-binding protein that co-purifies with heparin-binding growth factor-1. *In Vitro Cell Dev Biol* 1989; **25**: 581-4.

136. Rennie PS, Bruchovsky N, Leco KJ, et al. Characterization of two cis-acting DNA elements involved in the androgen regulation of the probasin gene. *Mol Endocrinol* 1993; **7**: 23-36.

137. Kasper S, Rennie PS, Bruchovsky N, et al. Cooperative binding of androgen receptors to two DNA sequences is required for androgen induction of the probasin gene. *J Biol Chem* 1994; **269**: 31763-9.

138. Greenberg NM, DeMayo F, Finegold MJ, et al. Prostate cancer in a transgenic mouse. *Proc Natl Acad Sci U S A* 1995; **92**: 3439-43.

139. Greenberg NM, DeMayo FJ, Sheppard PC, et al. The rat probasin gene promoter directs hormonally and developmentally regulated expression of a heterologous gene specifically to the prostate in transgenic mice. *Mol Endocrinol* 1994; **8**: 230-9.

140. DeCaprio JA, Ludlow JW, Figge J, et al. SV40 large tumor antigen forms a specific complex with the product of the retinoblastoma susceptibility gene. *Cell* 1988; **54**: 275-83.

141. Linzer DIH, Levine AJ. Characterization of a 54K Dalton cellular SV40 tumor antigen present in SV40-transformed cells and uninfected embryonal carcinoma cells. *Cell* 1979; **17**: 43-52.

142. Pallas DC, Shahrik LK, Martin BL, et al. Polyoma small and middle T antigens and SV40 small t antigen form stable complexes with protein phosphatase 2A. *Cell* 1990; **60**: 167-76.

143. Gingrich JR, Barrios RJ, Foster BA, et al. Pathologic progression of autochthonous prostate cancer in the TRAMP model. *Prostate Cancer Prostatic Dis* 1999; **2**: 70-5.

144. Gingrich JR, Barrios RJ, Morton RA, et al. Metastatic prostate cancer in a transgenic mouse. *Cancer Res* 1996; **56**: 4096-102.

145. Kaplan-Lefko PJ, Chen TM, Ittmann MM, et al. Pathobiology of autochthonous prostate cancer in a pre-clinical transgenic mouse model. *Prostate* 2003; **55**: 219-37.

146. Han G, Foster B, Mistry S, et al. Hormone status selects for spontaneous somatic androgen receptor variants that demonstrate specific ligand and cofactor dependent activities in autochthonous prostate cancer. *J Biol Chem* 2001; **276**: 11204-13.

147. Gingrich JR, Barrios RJ, Kattan MW, et al. Androgen-independent prostate cancer progression in the TRAMP model. *Cancer Res* 1997; **57**: 4687-91.

148. Yan Y, Sheppard PC, Kasper S, et al. Large fragment of the probasin promoter targets high levels of transgene expression to the prostate of transgenic mice. *Prostate* 1997; **32**: 129-39.

149. Kasper S, Sheppard PC, Yan Y, et al. Development, progression, and androgen-dependence of prostate tumors in probasin-large T antigen transgenic mice: a model for prostate cancer. *Lab Invest* 1998; **78**: 319-33.

150. Masumori N, Thomas TZ, Chaurand P, et al. A probasin-large T antigen transgenic mouse line develops prostate adenocarcinoma and neuroendocrine carcinoma with metastatic potential. *Cancer Res* 2001; **61**: 2239-49.

151. Mordan-McCombs S, Brown T, Wang WLW, et al. Tumor progression in the LPB-Tag transgenic model of prostate cancer is altered by vitamin D receptor and serum testosterone status. *J Steroid Biochem Mol Biol* 2010; **121**: 368-71.

152. Bollito E, Berruti A, Bellina M, et al. Relationship between neuroendocrine features and prognostic parameters in human prostate adenocarcinoma. *Ann Oncol* 2001; **12** Suppl 2: S159-S164.

153. Bonkhoff H. Neuroendocrine differentiation in human prostate cancer. Morphogenesis, proliferation and androgen receptor status. *Ann Oncol* 2001; **12** Suppl 2: S141-S144.

154. di Sant'Agnese P. Neuroendocrine differentiation in carcinoma of the prostate. Diagnostic, prognostic, and therapeutic implications. *Cancer* 1992; **70**: 254-68.

155. Segawa N, Mori I, Utsunomiya H, et al. Prognostic significance of neuroendocrine differentiation, proliferation activity and androgen receptor expression in prostate cancer. *Pathol Int* 2001; **51**: 452-9.

156. Sun Y, Niu J, Huang J. Neuroendocrine differentiation in prostate cancer. *Am J Transl Res* 2009; **1**: 148-62.

157. Dube JY, Pelletier G, Gagnon P, et al. Immunohistochemical localization of a prostatic secretory protein of 94 amino acids in normal prostatic tissue, in primary prostatic tumors and in their metastases. *J Urol* 1987; **138**: 883-7.

158. Kwong J, Xuan JW, Chan PS, et al. A comparative study of hormonal regulation of three secretory proteins (prostatic secretory protein-PSP94, probasin, and seminal vesicle secretion II) in rat lateral prostate. *Endocrinology* 2000; **141**: 4543-51.

159. Kwong J, Xuan JW, Choi HL, et al. PSP94 (or beta-microseminoprotein) is a secretory protein specifically expressed and synthesized in the lateral lobe of the rat prostate. *Prostate* 2000; **42**: 219-29.

160. Imasato Y, Onita T, Moussa M, et al. Rodent PSP94 gene expression is more specific to the dorsolateral prostate and less sensitive to androgen ablation than probasin. *Endocrinology* 2001; **142**: 2138-46.

161. Gabril MY, Onita T, Ji PG, et al. Prostate targeting: PSP94 gene promoter/enhancer region directed prostate tissue-specific expression in a transgenic mouse prostate cancer model. *Gene Ther* 2002; **9**: 1589-99.

162. Gabril MY, Duan W, Wu G, et al. A novel knock-in prostate cancer model demonstrates biology similar to that of human prostate cancer and suitable for preclinical studies. *Mol Ther* 2005; **11**: 348-62.

163. Duan W, Gabril MY, Moussa M, et al. Knockin of SV40 Tag oncogene in a mouse adenocarcinoma of the prostate model demonstrates advantageous features over the transgenic model. *Oncogene* 2005; **24**: 1510-24.

164. Stanbrough M, Leav I, Kwan PW, et al. Prostatic intraepithelial neoplasia in mice expressing an androgen receptor transgene in prostate epithelium. *Proc Natl Acad Sci U S A* 2001; **98**: 10823-8.

165. Wu CT, Altuwaijri S, Ricke W, et al. Increased prostate cell proliferation and loss of cell differentiation in mice lacking prostate epithelial androgen receptor. *Proc Natl Acad Sci U S A* 2007; **104**: 12679-84.

166. Niu Y, Altuwaijri S, Lai KP, et al. Androgen receptor is a tumor suppressor and proliferator in prostate cancer. *Proc Natl Acad Sci U S A* 2008; **105**: 12182-7.

167. Jenkins RB, Qian J, Lieber MM, et al. Detection of c-myc oncogene amplification and chromosomal anomalies in metastatic prostatic carcinoma by fluorescence in situ hybridization. *Cancer Res* 1997; **57**: 524-31.

168. Qian J, Jenkins RB, Bostwick DG. Detection of chromosomal anomalies and c-myc gene amplification in the cribriform pattern of prostatic intraepithelial neoplasia and carcinoma by fluorescence in situ hybridization. *Mod Pathol* 1997; **10**: 1113-9.

169. Ellwood-Yen K, Graeber TG, Wongvipat J, et al. Myc-driven murine prostate cancer shares molecular features with human prostate tumors. *Cancer cell* 2003; **4**: 223-38.

170. Anderson PD, McKissic SA, Logan M, et al. Nkx3.1 and Myc crossregulate shared target genes in mouse and human prostate tumorigenesis. *J Clin Invest* 2012; **122**: 1907-19.

171. Kim MJ, Cardiff RD, Desai N, et al. Cooperativity of Nkx3.1 and Pten loss of function in a mouse model of prostate carcinogenesis. *Proc Natl Acad Sci U S A* 2002; **99**: 2884-9.

172. Kim J, Eltoum IE, Roh M, et al. Interactions between cells with distinct mutations in c-MYC and Pten in prostate cancer. *PLoS Genet* 2009; **5**: e1000542.

173. King JC, Xu J, Wongvipat J, et al. Cooperativity of TMPRSS2-ERG with PI3-kinase pathway activation in prostate oncogenesis. *Nat Genet* 2009; **41**: 524-6.

174. Zhang J, Thomas TZ, Kasper S, et al. A small composite probasin promoter confers high levels of prostate-specific gene expression through regulation by androgens and glucocorticoids in vitro and in vivo. *Endocrinology* 2000; **141**: 4698-710.

175. Abdulkadir SA, Magee JA, Peters TJ, et al. Conditional loss of Nkx3.1 in adult mice induces prostatic intraepithelial neoplasia. *Mol Cell Biol* 2002; **22**: 1495-503.

176. Ouyang X, DeWeese TL, Nelson WG, et al. Loss-of-function of Nkx3.1 promotes increased oxidative damage in prostate carcinogenesis. *Cancer Res* 2005; **65**: 6773-9.

177. Kim MJ, Bhatia-Gaur R, Banach-Petrosky WA, et al. Nkx3.1 mutant mice recapitulate early stages of prostate carcinogenesis. *Cancer Res* 2002; **62**: 2999-3004.

178. Bhatia-Gaur R, Donjacour AA, Sciavolino PJ, et al. Roles for Nkx3.1 in prostate development and cancer. *Genes Dev* 1999; **13**: 966-77.

179. Di Cristofano A, Pesce B, Cordon-Cardo C, et al. Pten is essential for embryonic development and tumour suppression. *Nat Genet* 1998; **19**: 348-55.

180. Suzuki A, de la Pompa JL, Stambolic V, et al. High cancer susceptibility and embryonic lethality associated with mutation of the PTEN tumor suppressor gene in mice. *Curr Biol* 1998; **8**: 1169-78.

181. Podsypanina K, Ellenson LH, Nemes a, et al. Mutation of Pten/Mmac1 in mice causes neoplasia in multiple organ systems. *Proc Natl Acad Sci U S A* 1999; **96**: 1563-8.

182. Kwabi-Addo B, Giri D, Schmidt K, et al. Haploinsufficiency of the Pten tumor suppressor gene promotes prostate cancer progression. *Proc Natl Acad Sci U S A* 2001; **98**: 11563-8.

183. Wang S, Gao J, Lei Q, et al. Prostate-specific deletion of the murine Pten tumor suppressor gene leads to metastatic prostate cancer. *Cancer cell* 2003; **4**: 209-21.

184. Ma X, Ziel-van der Made A, Autar B, et al. Targeted biallelic inactivation of Pten in the mouse prostate leads to prostate cancer accompanied by increased epithelial cell proliferation but not by reduced apoptosis. *Cancer Res* 2005; **65**: 5730-9.

185. Abate-Shen C, Banach-Petrosky W, Sun X, et al. Nkx3.1; Pten mutant mice develop invasive prostate adenocarcinoma and lymph node metastases. *Cancer Res* 2003; **63**: 3886-90.

186. Wang X, Kruithof-de Julio M, Economides KD, et al. A luminal epithelial stem cell that is a cell of origin for prostate cancer. *Nature* 2009; **461**: 495-500.

187. Zhou Z, Flesken-Nikitin A, Corney DC, et al. Synergy of p53 and Rb deficiency in a conditional mouse model for metastatic prostate cancer. *Cancer Res* 2006; **66**: 7889-98.

188. Brewster SF, Browne S, Brown KW. Somatic allelic loss at the DCC, APC, nm23-H1 and p53 tumor suppressor gene loci in human prostatic carcinoma. *J Urol* 1994; **151**: 1073-7.

189. Jeronimo C, Henrique R, Hoque MO, et al. A quantitative promoter methylation profile of prostate cancer. *Clin Cancer Res* 2004; **10**: 8472-8.

190. Phillips SM, Morton DG, Lee SJ, et al. Loss of heterozygosity of the retinoblastoma and adenomatous polyposis susceptibility gene loci and in chromosomes 10p, 10q and 16q in human prostate cancer. *Br J Urol* 1994; **73**: 390-5.

191. Bruxvoort KJ, Charbonneau HM, Giambernardi T, et al. Inactivation of Apc in the mouse prostate causes prostate carcinoma. *Cancer Res* 2007; **67**: 2490-6.

192. Tuxhorn JA, Ayala GE, Rowley DR. Reactive stroma in prostate cancer progression. *J Urol* 2001; **166**: 2472-83.

193. Ayala G, Tuxhorn JA, Wheeler TM, et al. Reactive stroma as a predictor of biochemical-free recurrence in prostate cancer. *Clin Cancer Res* 2003; **9**: 4792-801.

194. De Marzo AM, Platz EA, Sutcliffe S, et al. Inflammation in prostate carcinogenesis. *Nat Rev Cancer* 2007; **7**: 256-69.

195. Dakhova O, Ozen M, Creighton CJ, et al. Global gene expression analysis of reactive stroma in prostate cancer. *Clin Cancer Res* 2009; **15**: 3979-89.

196. Tuxhorn J, Ayala GE, Smith MJ, et al. Reactive stroma in human prostate cancer: induction of myofibroblast phenotype and extracellular matrix remodeling. *Clin Cancer Res* 2002; **8**: 2912-23.

197. Lees JR, Charbonneau B, Swanson AK, et al. Deletion is neither sufficient nor necessary for the induction of peripheral tolerance in mature CD8+ T cells. *Immunology* 2006; **117**: 248-61.

198. Haverkamp JM, Charbonneau B, Crist S, et al. An inducible model of abacterial prostatitis induces antigen specific inflammatory and proliferative changes in the murine prostate. *Prostate* 2011; **71**: 1139-50.

199. Garlick DS, Li J, Sansoucy B, et al. alpha(V)beta(6) integrin expression is induced in the POET and Pten(pc-/-) mouse models of prostatic inflammation and prostatic adenocarcinoma. *Am J Transl Res* 2012; **4**: 165-74.

200. Gann PH, Klein KG, Chatterton RT, et al. Growth factors in expressed prostatic fluid from men with prostate cancer, BPH, and clinically normal prostates. *Prostate* 1999; **40**: 248-55.

201. Rowley DR. Reactive Stroma and Evolution of Tumors: Integration of Transforming Growth Factor-beta, Connective Tissue Growth Factor, and Fibroblast Growth Factor-2 Activities. In: Jakowlew SB, editor. Transforming Growth Factor-beta in Cancer Therapy. Totowa, NJ: Humana Press; 2008. pp. 475-505.

202. Barron DA, Strand DW, Ressler SJ, et al. TGF-beta1 induces an age-dependent inflammation of nerve ganglia and fibroplasia in the prostate gland stroma of a novel transgenic mouse. *PLoS One* 2010; **5**: e13751.

203. Schauer IG, Ressler SJ, Tuxhorn JA, et al. Elevated epithelial expression of interleukin-8 correlates with myofibroblast reactive stroma in benign prostatic hyperplasia. *Urology* 2008; **72**: 205-13.

204. Schauer IG, Ressler SJ, Rowley DR. Keratinocyte-derived chemokine induces prostate epithelial hyperplasia and reactive stroma in a novel transgenic mouse model. *Prostate* 2009; **69**: 373-84.

205. Klezovitch O, Chevillet J, Mirosevich J, et al. Hepsin promotes prostate cancer progression and metastasis. *Cancer cell* 2004; **6**: 185-95.

206. Cher ML, Biliran HR, Jr., Bhagat S, et al. Maspin expression inhibits osteolysis, tumor growth, and angiogenesis in a model of prostate cancer bone metastasis. *Proc Natl Acad Sci U S A* 2003; **100**: 7847-52.

207. Sheng S, Carey J, Seftor E, et al. Maspin acts at the cell membrane to inhibit invasion and motility of mammary and prostatic cancer cells. *Proc Natl Acad Sci U S A* 1996; **93**: 11669-74.

208. Shao Lj, Shi HY, Ayala G, et al. Haploinsufficiency of the maspin tumor suppressor gene leads to hyperplastic lesions in prostate. *Cancer Res* 2008; **68**: 5143-51.

209. Freeman KW, Welm BE, Gangula RD, et al. Inducible prostate intraepithelial neoplasia with reversible hyperplasia in conditional FGFR1-expressing mice. *Cancer Res* 2003; **63**: 8256-63.

210. Acevedo VD, Gangula RD, Freeman KW, et al. Inducible FGFR-1 activation leads to irreversible prostate adenocarcinoma and an epithelial-to-mesenchymal transition. *Cancer cell* 2007; **12**: 559-71.

211. Winter SF, Acevedo VD, Gangula RD, et al. Conditional activation of FGFR1 in the prostate epithelium induces angiogenesis with concomitant differential regulation of Ang-1 and Ang-2. *Oncogene* 2007; **26**: 4897-907.

Figure Legend:

Figure 1: Model of human prostate cancer progression from normal to advanced stages. The severity of disease is illustrated with increased red intensity with concomitant genetic changes chromosomal alterations. Overexpression of a gene is denoted as ↑ while downregulation is indicated as ↓. Other alterations, including deletion/loss of expression, silencing, rearrangements and mutations are also indicated. Genetic changes that are discussed in this chapter are bolded.